CONTRACT 950137

RANGER TV SUBSYSTEM (BLOCK III) FINAL REPORT

VOLUME 5: EVALUATION

Prepared For:

JET PROPULSION LABORATORY
CALIFORNIA INSTITUTE OF TECHNOLOGY
PASADENA, CALIFORNIA

By The:

ASTRO-ELECTRONICS DIVISION
DEFENSE ELECTRONIC PRODUCTS
RADIO CORPORATION OF AMERICA
PRINCETON, NEW JERSEY

AED R-2620

Issued: JULY 22, 1965

Preface

This report summarizes the Ranger TV Subsystem program. This work was performed by the Radio Corporation of America, under JPL Contract No. 950137, for the Jet Propulsion Laboratory of the California Institute of Technology, Pasadena, California. The period covered by this, the Final Report on the program, extends from July, 1961 through July, 1965. The report is submitted in five volumes:

Volume 1	Summary
Volume 2	Subsystem Analysis
Volume 3	TV Subsystem Design
Volume 4	Manufacturing, Product Assurance, and Test
Volume 5	Evaluation

This volume, Volume 5, contains an analysis of the performance of the Ranger TV Subsystem equipment.

Table of Contents

Table of Contents (Continued)

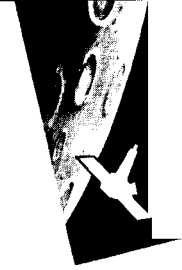

Table of Contents (Continued)

List of Illustrations

List of Illustrations (Continued)

List of Illustrations (Continued)

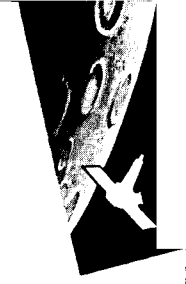

List of Illustrations (Continued)

List of Illustrations (Continued)

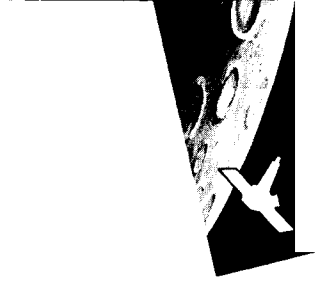

List of Illustrations (Continued)

List of Tables

List of Tables (Continued)

List of Tables (Continued)

Section I

Introduction

The mission of the Ranger Spacecraft was to obtain high-resolution close-up pictures of the lunar surface during the terminal phase of a lunar impacting trajectory. The TV Subsystem was to be the imaging transducer operating from a spacecraft-based observation platform. It was also intended that the TV Subsystem process the video signal and provide the power for the subsequent transmission of the lunar pictures to Earth.

Any evaluation of equipment designed and built for space application can only be based upon the successful operation of this equipment in the performance of its assigned mission. This is also true of the program which led to the design and manufacture of the equipment. The evaluation of the Ranger VI, VII, VIII, and IX missions are presented herein. These evaluations are the basis for the conclusions reached regarding the success of the Ranger TV Subsystem Project.

Section II

Ranger VI Mission Evaluation

A. SUMMARY OF RANGER VI MISSION

Ranger VI, consisting of the JPL Ranger Spacecraft and the Flight Model III-1 of the RCA Ranger TV Subsystem, was launched from Cape Kennedy, AMR, on an Atlas-D/ Agena-B vehicle. Liftoff occurred at 15:49:00 GMT, January 30, 1964. Impact on the Moon occurred 70-3/4 hours after launch. The primary objective of the Ranger VI mission was not fulfilled since the spacecraft did not return television pictures of the lunar surface.

The first nonstandard event occurred when the TV Subsystem Channel-8 telemetry inadvertently turned on at 15:51:30.0 GMT and transmitted data until 15:52:36.5 GMT, at which time the transmission ceased. Normal turn-on of the Channel-8 telemetry occurred at a time corresponding to 17 minutes after separation of the Ranger system from the Agena (16:36:34 GMT). Except for a brief period during the midcourse maneuver when the JPL telemetry was switched to Mode II operation, reception of the Channel-8 data continued to be normal until impact.

The first timing pulse from the TV Subsystem clock was received, via the Channel-8 telemetry, on schedule at 16 hours after separation (08:19:50 GMT, January 31, 1964). Subsequent pulses were received as anticipated at separation plus 32 hours, 48 hours, and 64 hours.

Because of the near-perfect trajectory and orientation of the spacecraft as it approached the Moon, it was decided that a terminal maneuver would not be employed. Considering the temperatures and voltages of the Subsystem components, as determined by reducing the 15-point telemetry, it was further decided to allow the Subsystem Clock to time out and to initiate warm-up of the F-Channel of the Subsystem at Impact minus 19 minutes. An RTC-7 command would be sent four minutes later to initiate warm-up of the P-Channel. Each channel was to be activated into full power when the 5-minute accumulators for each channel completed timing. Because the terminal maneuver was not performed, the warm-up command and backup full-power command from the JPL Central Computer and Sequencer (CC&S) were not used.

The warm-up command to the F-Channel of the TV Subsystem was initiated by the TV Subsystem Clock at separation plus 64-3/4 hours (09:05:42 GMT, February 2, 1964). At this time, a drop in the Channel-8 telemetry point monitoring the F-battery indicated that a warm-up load had been placed on the F-Battery. The first RTC-7 command was initiated at 09:08:00 GMT and verified by telemetry from the Spacecraft Bus. The state of the P-Channel warm-up was confirmed by both a drop in the P-Channel battery voltage and the presence of the 30-second accumulator pulse on the Channel-8 telemetry. No indications of full power were received from either the F- or the P-Channels after five minutes of warm-up, and no video was received at the Goldstone DSIF ground station. A second RTC-7 command was initiated at 09:15:29 GMT and verified; however, emergency telemetry was not received. The third RTC-7 command was initiated at 09:19:20 GMT and verified. Impact occurred at 09:24:33 GMT. No video, 225-kc telemetry, or emergency telemetry was received from the TV Subsystem.

Subsequent playback of the magnetic tape records obtained at the Goldstone ground station through narrow band-pass filters and processed through a computerized autocorrelation program failed to produce evidence of data transmission from the TV Subsystem.

Table 1, below, presents in chronological order essentially all of the discrete events pertaining to the Ranger VI Spacecraft, from the time of power turn-on for the countdown until the spacecraft impacted on the Moon. Some of the data contained in the sequence were extracted from spacecraft telemetry recorded by DSIF and ETR tracking stations and reduced at JPL.

B. ANALYSIS OF THE POSSIBLE CAUSES OF FAILURE

1. General

Immediately following the impact of the Ranger VI Spacecraft on the Moon, an evaluation team made up of RCA and JPL personnel initiated an analysis to determine why the Ranger VI system failed to return expected photographic information of the lunar surface. This joint investigation was carried out at JPL through February 14, 1964, following which time, the analysis was continued at AED by the RCA personnel.

The initial investigation at JPL centered on a single failure mode that could have occurred during the terminal phase of the mission and could be correlated with the telemetry information obtained. As part of this investigation, a thorough search of the tapes recorded during the terminal phase of the mission was performed, using special techniques of spectrum analysis and correlation detection. These techniques would have enabled the detection of the presence of any signal emanating from the TV Subsystem Transmitters, including that normally obtained during Subsystem warm-up, or even the spike that could be expected during a transmitter-chain failure. Since the tapes were completely devoid of any signal for either channel, it became clearly apparent that the failure occurred prior to the terminal phase of the Ranger VI mission.

The Channel-8 telemetry received indicated that the TV Subsystem operated as expected from Agena-separation plus 17 (S+17) minutes until the turn-on of the F-Channel by Clock command. There was no significant drain on either the P- or F-Channel battery; the temperatures of the batteries stabilized after S+10 hours at +20 degrees C above nominal, but well within the design limits of the Subsystem. Any failure occurring during the cruise mode, which could have caused the loss of both transmission channels, would most probably have been detected on the combined RCA and JPL telemetry.

With the limited information available for evaluation, the analysis was concentrated on the period of booster-engine separation, at which time four inadvertent frames of Channel-8 telemetry were received. The analysis first attempted to determine the most probable failure mode that could have occurred during this period, and then sought to isolate the mechanism that could have caused this failure mode.

2. Failure-Mode Analysis

Each group of assemblies within the TV Subsystem was analyzed to determine whether a single failure within that group and isolated within that group could have caused the Subsystem to fail. These investigations indicated that the two most probable failure modes had to occur early in the Ranger VI mission.

One potential area of failure was a loss of a connection between the Four-Port Hybrid Ring on the TV Subsystem and Case 2 on the JPL Bus. This failure would satisfactorily explain the complete loss of RF. However, studies at JPL indicated that a break in the connection would have caused a change in the level of the JPL signal. For such a signal change to occur and not be noticed would require that it occur very early in the mission. If the connection was made correctly at the Explosive-Safe Area (ESA), the environment required to cause a complete loss of RF would have had to be more severe than that apparently encountered during the Ranger VI mission. It should also be noted that this failure mode could not, of

TABLE 1
DISCRETE EVENTS PERTAINING TO THE RA-6 MISSION

Mission Time	GMT	Subsystem	Event
	Jan 30 (030)		
T-210m	10:22:00	OSE	Turn on S/C external power (transponder, data encoder, CC&S, gyros on)
T-175m	11:00:00	D/E	Mode 2
		RAD	Transfer to high gain antenna
T-160m	11:22:23	D/E	Commutator fast stepping
	11:22:58	D/E	Commutator stopped
T-130m		D/E	Commutator running, Mode 1
T-128m	12:17:01	TV	Ch-8 telemetry on (starts on segment 15)
T-126m	12:19:02	TV	Ch-8 telemetry off (stops between segments 2 and 3)
T125m		OSE	Transmit two RTC-0's and one RTC-2
	12:23:39	CMD	RTC monitor blip (B-20)
		A/C	Antenna hinge preset to 135 deg
T-113m	12:35:26	CCS	Clear relay check event (B-2-1 blip)
T-100m	12:48:11	OSE	Transmitter off (begin RF frequency checks)
		RAD	S/C receiver out of lock
	12:57:00	OSE	Transmitter on
		RAD	S/C receiver in lock
	13:09:20	PWR	S/C to internal power (battery voltage checks)
	13:15:50	PWR	S/C to external power

TABLE 1
DISCRETE EVENTS PERTAINING TO THE RA-6 MISSION (Continued)

Mission Time	GMT	Subsystem	Event
T-55m	14:07:05	OSE	Transmitter off (RF frequency checks)
		RAD	S/C receiver out of lock
	14:11:50	OSE	Transmitter on
		RAD	S/C receiver in lock
T-42m	14:19:40	OSE	Transmitter off
		RAD	S/C receiver out of lock
			A) 960.028599 Mc D) 960.051951 Mc
			B) 890.047290 Mc E) -.0078 volts
			C) 960.051034 Mc F) 76 deg F
	14:19:54	RAD	Transfer from high-gain to omni antenna
	15:15:27	D/E	Rate 4 (H9) sync pulse ends
T-5m	15:43:50	PWR	S/C to internal power
T-2m	15:47:02	CCS	Release inhibit, start launch counter
T-1m	15:48:01.8	CCS	Clear relays event (B-2-1 blip)
T+0	15:49:00 (Approximate)	VEH	Ignition (launch plan 30E, azimuth 95 deg)
L+0	15:49:09.092	VEH	Liftoff (umbilical removed)
		PWR	Monitor voltages increase 5% (OSE load removed)
		D/E	Address 66 frequency drops 2.8 cps (OSE load removed)

TABLE 1
DISCRETE EVENTS PERTAINING TO THE RA-6 MISSION (Continued)

Mission Time	GMT	Subsystem	Event
L+2m		SFA	Squib firing assembly armed by g-switch (no telemetry)
L+137s	15:51:26.16	VEH	Mark 1
L+140s	15:51:29.10	VEH	Mark 2
	15:51:29.26±.05	(DSIF-71)	Rcvr AGC starts sharp drop, loses lock with S/C carrier.
		(ETR-1/Tel II)	Agena carrier and all subcarriers unchanged.
	15:51:29.7±.2	TV	Ch-8 telemetry on; starts between segments 2 and 3; channel noisy
	15:51:30.0	(DSIF-71)	Receiver back in lock (RF returns to previous level)
	15:51:55	D/E	Start of occasional 1-sec frequency shifts (up to 2 cps) on J-deck samples
	15:51:59.0	TV	Ch-8 noise disappears
	15:52:36.5	TV	Ch-8 telemetry off, (stops between segments 9 and 10)
L+288s	15:53:57.27	VEH	Mark 3
L+305s	15:54:13.90	VEH	Mark 4
L+306s	15:54:15.13	VEH	Shroud ejection (Mark 5)
		RAD	Omni-antenna coupler removed, RF drive up 2 db
L+310s	15:54:18.72	VEH	Atlas-Agena separation (Mark 6)
		VEH	Agena 1st ignition (Mark 7) (still over Cape)
		VEH	Agena 1st cutoff (Mark 8) (over Antigua)

TABLE 1
DISCRETE EVENTS PERTAINING TO THE RA-6 MISSION (Continued)

Mission Time	GMT	Subsystem	Event
L+23m	16:12:01.8	CCS	Transmitter power up command (B-2-1) (over Ascension)
		RAD	Plate volts from 150 to 250, omni drive to 35 dbm
		VEH	Agena 2nd ignition (Mark 9) (over YANKEE)
		VEH	Agena 2nd cutoff (injection) (Mark 10) (over YANKEE)
	16:18:33	(DSIF-51)	Transmitter turned on (for possible RTC-7's)
		RAD	S/C receiver in and out of lock for next 26 min
L+30m8s	16:19:17.20	VEH	S/C-Agena electrical disconnect (Mark 11) (over YANKEE) (Remove S/C telemetry from Agena carrier)
L+30m14s	16:19:23.20	VEH	S/C-Agena separation (Mark 12) (over Pretoria YANKEE)
S+0		BYCT	Start BU command timer
		TV	Start Electronic Clock
		CCS	Relays unclamped
	16:20:32	RAD	S/C receiver in lock with DSIF-51 transmitter (MTS T/M in lock)
		D/E	No more noise on J-deck measurements
	16:30:47	RAD	S/C receiver out of lock (10-sec dropout DSIF-59)
	16:35:44	RAD	S/C receiver locked up with DSIF-51 transmitter (after 70-sec ground receiver dropout)

TABLE 1
DISCRETE EVENTS PERTAINING TO THE RA-6 MISSION (Continued)

Mission Time	GMT	Subsystem	Event
S+17m	16:36:34	TV	Ch-8 telemetry on, starts between segments 9 and 10
	16:42:13	RAD	S/C receiver out of lock (followed by 16-sec dropout)
	16:44:01	RAD	Locked up 2-way with DSIF-41 transmitter (after 10-sec dropout)
L+60m	16:49:01.8	CCS	Command solar panel extension (B-2-1)
		SFA	Fire solar panel squibs (B-2, B-2-3)
	16:50:06	S/C	Solar panels extended (B-2-4)
L+63m	16:52:01.3	CCS	Command Sun acquisition (Sun sensor error signal starts)
		A/C	DC power on, extend antenna, start Sun acquisition
	16:52:01.8	D/E	B-2-1 blip readout (delay due to synchronization, B-2 pulses with RTC-2 commutator pulses)
	16:53:50	PWR	Switch to solar panel power
	16:53:30	A/C	Sun acquisition complete (yaw error nulled)
	16:57:13	A/C	Antenna at acquisition angle (135 deg)
L+211m	19:20:02	CCS	Command Earth acquisition
		A/C	E/S power on, start roll search
	19:40:40	A/C	E/S threshold signal
	19:45:00	A/C	Earth acquisition complete
L+270m	20:25:00	DSIF-41	Initiate RTC-0 (command sequence stopped because of marginal ground transmitter power)

TABLE 1
DISCRETE EVENTS PERTAINING TO THE RA-6 MISSION (Continued)

Mission Time	GMT	Subsystem	Event
	21:08:00	DSIF-51	Initiate RTC-0
	21:10:00	DSIF-51	Initiate RTC-0
	21:12:00	DSIF-51	Initiate RTC-3
	21:12:40	CMD	RTC monitor blip (B-20)
		RAD	Switch S/C transmitter from omni to hi-gain antenna, hi-gain drive at normal 25 dbm
	Jan 31 (031)		
M-70m	07:20:00	DSIF-12	Initiate RTC-0
	07:22:00	DSIF-12	Initiate RTC-0
	07:24:00	DSIF-12	Initiate SC-1 (roll turn: 54 sec, neg)
	07:24:40	CMD	Stored command readout: 25-0450-0 (B-20)
	07:24:44	CCS	Capacitor cycling command (B-2-1)
	07:26:00	DSIF-12	Initiate SC-2 (pitch turn: 328 sec, neg)
	07:26:40	CMD	Stored command readout: 35-0372-0
	07:28:00	DSIF-12	Initiate SC-3 (velocity increment: 135.1 fps)
	07:28:40	CMD	Stored command readout: 03-2610-1
S+16 hr	08:19:50	TV	Electronic Clock 16-hr pulse
M-10m	08:20:00	DSIF-12	Initiate RTC-3
		CMD	RTC monitor blip (B-20)
	08:20:40	RAD	Switch S/C transmitter from hi-gain to omni antenna; Low-gain drive at normal 35 dbm
	08:30:00	DSIF-12	Initiate RTC-4

TABLE 1
DISCRETE EVENTS PERTAINING TO THE RA-6 MISSION (Continued)

Mission Time	GMT	Subsystem	Event
M	08:30:39*	CMD	RTC monitor blip (B-20)
		CCS	Start maneuver counter
M+5s	08:30:44*	CCS	Start roll command (B-2-1)
		A/C	E/S power off, start antenna exit, A/P on, start negative roll turn
M+59s	08:31:38*	CCS	Stop roll turn command
		A/C	Stop roll turn after 54 sec
	08:32:37*	A/C	Antenna at exit angle
M+9m30s	08:40:08*	CCS	Command start pitch turn
		A/C	Start negative pitch turn
	08:44:00*	PWR	To power sharing mode (panels and battery)
	08:44	(TPS)	Telemetry out of lock (pitch through omni-antenna null)
M+14m58s	08:45:37*	CCS	Command stop pitch turn, Telemetry mode II (B-2-1)
		A/C	Stop pitch turn after 328 sec
		D/E	Telemetry mode II
M+26m30s	08:57:07*	CCS	Command motor ignition (B-2-1), start shutoff computer countdown.
		SFA	Fire motor ignition squibs (B-2-2, B-2-3)
		PROP	Motor ignition
		A/C	Jetvane control, gate accelerometer pulses to CCS

*These times read from real time SDAT analog record (approximately 1 sec behind DSIF time).

TABLE 1
DISCRETE EVENTS PERTAINING TO THE RA-6 MISSION (Continued)

Mission Time	GMT	Event	Subsystem
	08:57:20*	D/E	Temperature bridges G and D1, measurements to Ch-2 band edge (power supply shorted out)
M+27m37s	08:58:16*	CCS	Command motor cutoff after 1351 accelerometer pulses (B-2-1)
		SFA	Fire motor cutoff squibs (B-2-2, B-2-3)
		PROP	Motor cutoff
M+30m	09:00:38*	CCS	Telemetry mode sun reacquisition, Telemetry mode III
		A/C	A/P off, start Sun reacquisition, start antenna to reacquisition angle
		D/E	Telemetry mode III
	09:01	(TPS)	Telemetry out of lock briefly (turn through null)
	09:01:53*	PWR	Switch to solar panel power
	09:02:49*	A/C	Antenna at reacquisition angle (122 deg)
	09:05	A/C	Sun reacquisition complete
M+58m	09:28:38	CCS	Command Earth reacquisition (B-21)
		A/C	Earth sensor power on, acquisition immediate
	09:44:00*	DSIF-12	Initiate TRC-3
	09:44:39*	RAD	Switch transmitter from omni to hi-gain antenna (B-20) hi-gain drive at normal 25 dbm
S+32 hr	Feb. 1 (032) 00:20:11	TV	Electronic Clock 32-hr pulse

*These times read from real time SDAT analog record (approximately 1 sec behind DSIF time).

TABLE 1
DISCRETE EVENTS PERTAINING TO THE RA-6 MISSION (Continued)

Mission Time	GMT	Subsystem	Event
S+48 hr	16:20:32	TV	Electronic Clock 48-hr pulse
	23:46	RAD	Ground transmitter transfer DSIF-41 to -51
	Feb. 2 (033) 06:00	RAD	2-way with DSIF-12
	08:11:00	DSIF-12	Initiated RTC-0
	08:13:00	DSIF-12	Initiated RTC-9
S+64 hr	08:20:41	TV	Electronic Clock 64-hr pulse
S+64-3/4 hr	09:05:42	TV	Electronic Clock starts F-Channel 5-min accumulator, battery voltage indicates warm-up
	09:08:00	DSIF-12	Initiate RTC-7 (No. 1)
I-15m	09:08:41*	CMD	RTC Monitor blip (B-20)
		TV	Start P-Channel 5-min accumulator
	09:09:20	TV	P-Channel accumulator 30-sec pulse verifies RTC-7 advanced command switch properly
S-64hr50m	09:11	TV	No F-Channel full power video signal
I-10m	09:14	TV	No F- or P-Channel full power video signal
	09:15:29	DSIF-12	Initiate RTC-7 (No. 2)
	09:16:09*	CMD	RTC monitor blip (B-20)
		TV	No indication of emergency mode
	09:19:21	DSIF-12	Initiate RTC-7 (No. 3)
	09:20:02*	CMD	RTC monitor blip (B-20)
		TV	No indication of full-power video signal
I	09:24:33	S/C	Impact

*These times read from real time SDAT analog record (approximately 1 sec behind DSIF time).

itself, cause the anomalous turn-on of the Channel-8 telemetry at booster-engine separation; a second, unrelated failure would have to be advanced to explain this malfunction.

The one failure mode that appears to explain the complete lack of RF during the terminal mode and the anomalous turn-on of Channel-8 telemetry during the launch phase, and is supported by all of the data received, is the inadvertent turn-on of the TV Subsystem during booster-engine separation. If the TV Subsystem went into warm-up or full power at this time, the partial-pressure environment inside the Agena-shroud would produce RF arcing. The probability of arcing in this type of environment is supported by considerable analytical and empirical data and is substantiated by the failure that occurred in June 1962, when the proof test model (PTM) turned on in a partial-pressure environment. The PTM failure is indicative of the extent of damage possible under the conditions prevalent at booster-engine separation. The fact that a partial-pressure condition existed at that time can be substantiated by data received from Lockheed Corporation on the Agena-Shroud pressures.

It could be inferred, therefore, that if turn-on of the TV Subsystem did occur at booster-engine separation, severe arcing would have resulted, causing the destruction of a sufficient number of critical components to prevent the transmission of any RF signal during the terminal mode. The only datum received during the 67-second anomalous turn-on which requires further explanation in support of this hypothesis of an arcing-induced failure is the absence of a pulse which is normally displayed on point 11 of the Channel-8 telemetry about 30 seconds after the warm-up command is initiated. The presence of this pulse, called the P-Channel 5-Minutes Accumulator Pulse. indirectly indicates that the Intermediate and Final Power Amplifiers, and the P-Camera subsystems are in the warm-up mode, and that full power will be applied four minutes and thirty seconds from the appearance of the pulse. The facts indicate that the P-Channel Sequencer was available for producing the point-11 pulse during the anomalous turn-on since this pulse did appear later, during the terminal mode. It must be further hypothesized, then, that the P-Channel Sequencer was temporarily prevented from producing the point-11 pulse during the anomalous turn-on. The postulated high-voltage arcing, in either the camera electronics or the transmitter power supplies, could have prevented this pulse from appearing by causing one of two conditions in the output of the -27.5-volt regulator which supplies the sequencer:

(1) The regulator output was less than -20 volts during the 30 seconds at turn-on, in which case the accumulator could not have started counting.

(2) The regulator output was initially greater than -20 volts, but dropped to less than -5 volts for more than 10 milliseconds before the 30-second period was reached, thereby resetting the accumulator.

The heavy battery drain and telemetry noise lend further credence to the possibility that severe arcing occurred during this turn-on.

The Cameras for each channel are powered by their respective HCVR's through a 3-ampere fuse. The HCVR's reach their short-circuit current of 3.6 amperes when high-voltage arcing occurs. If this arcing occurs simultaneously in either two F-Channel Cameras or in a minimum of two P-Channel Cameras, the 3.6-ampere current from the HCVR would be divided such that only 1.8 amperes will be provided to each of the two Cameras, thus preventing the destruction of the 3-ampere fuse. This current limitation would then cause the Cameras to cease arcing, and the output voltage of the HCVR would rise. When the voltage rises sufficiently, arcing will resume. This constitutes a motor-boating effect, which will continue until the components fail or until the Subsystem is transported beyond the critical-pressure environment. At

the same time, a similar effect is produced in the Transmitter Power Supplies on the unregulated lines, which are not current-limited. The high-voltage arcing results in a current drain which causes the DC input to the DC converter to stop the converter from oscillating. The loss of the AC component for the high-voltage transformer, as a result of the stoppage of oscillation, causes the arcing to stop. Removal of this shorting effect permits the choppers to resume oscillation, thereby again producing the high-voltage arcing.

The Cameras and Transmitter Power Supplies, as a result of high-voltage arcing, acted as noise generators, drawing current as high as 60 amperes through the ground planes. These currents could be the source of the noise on both the baseline reference and the sampled data points in the Channel-8 telemetry received. The arcing could be the source of the baseline drifts which were observed during the initial 31 seconds of the spurious Channel-8 turn-on. Destruction of components in the Transmitter Power Supplies after the 31 seconds could thus have been the reason for the abrupt reduction of the noise on the telemetry readout.

3. Analysis of Failure Mechanism

The TV Subsystem was analyzed to determine possible occurrences that could inadvertently energize the Subsystem into the warm-up mode of operation and turn on the Channel-8 telemetry at booster-engine separation. A logic diagram of the command and control circuitry is shown in Figure 1. By design, the SCR's in the High-Current Voltage Regulators must be gated-on to supply regulated and unregulated voltages to the Subsystem to put it into the warm-up mode of operation. In the Ranger VI Spacecraft, three separate mechanisms were available to provide SCR turn-on (see Figure 2). These were:

- Energizing of relay K2 in the Distribution Control Unit (DCU);
- Output command from the Electronic Clock; and
- Stepping of the Command Switch to the warm-up position.

The energizing of a relay (K2) in the DCU would cause the SCR's in both the F- and P-Channel HCVR's to fire by tying the SCR's to ground through 220 ohms, thereby putting both channels into the warm-up mode of operation. If the Subsystem were to go into the warm-up mode because of the closure of the K2 relay in the DCU, then telemetry data points 1 and 2 would not have been present in the Channel-8 telemetry received. Points 1 and 2 are the input and output of the Low-Current Voltage Regulator (LCVR) and have no connections whatsoever with the K2 relay and therefore are not affected by its closure.

An inadvertent output command from the Electronic Clock would turn on the F-Channel, but not the P-Channel, into the warm-up mode by tying the gate of the SCR in the F-Channel HCVR to ground through 220 ohms. The P-Channel chain, therefore, would have been available for normal operation during the terminal mode of operation. Since this was not the case, it can be assumed that the inadvertent turn-on of the TV Subsystem was not caused by an incorrect output command from the Electronic Clock.

There is also a possibility that the SCR gates could have been energized directly by an inadvertent shorting-to-ground of pins 36 and 37 of connector A34J2 in the Command Switch. Pins 36 and 37 carry the SCR gates for the F-Channel and P-Channel, respectively. The connector itself is used mainly as a ground bus and has large (two different) solder busses joining the ground pins together. Vibration may have caused the solder busses to have come in contact with pins 36 and 37, thereby producing a short-to-ground and a firing of the SCR's, causing the Subsystem to go into the warm-up mode of operation. Had this possible but improbable situation occurred,

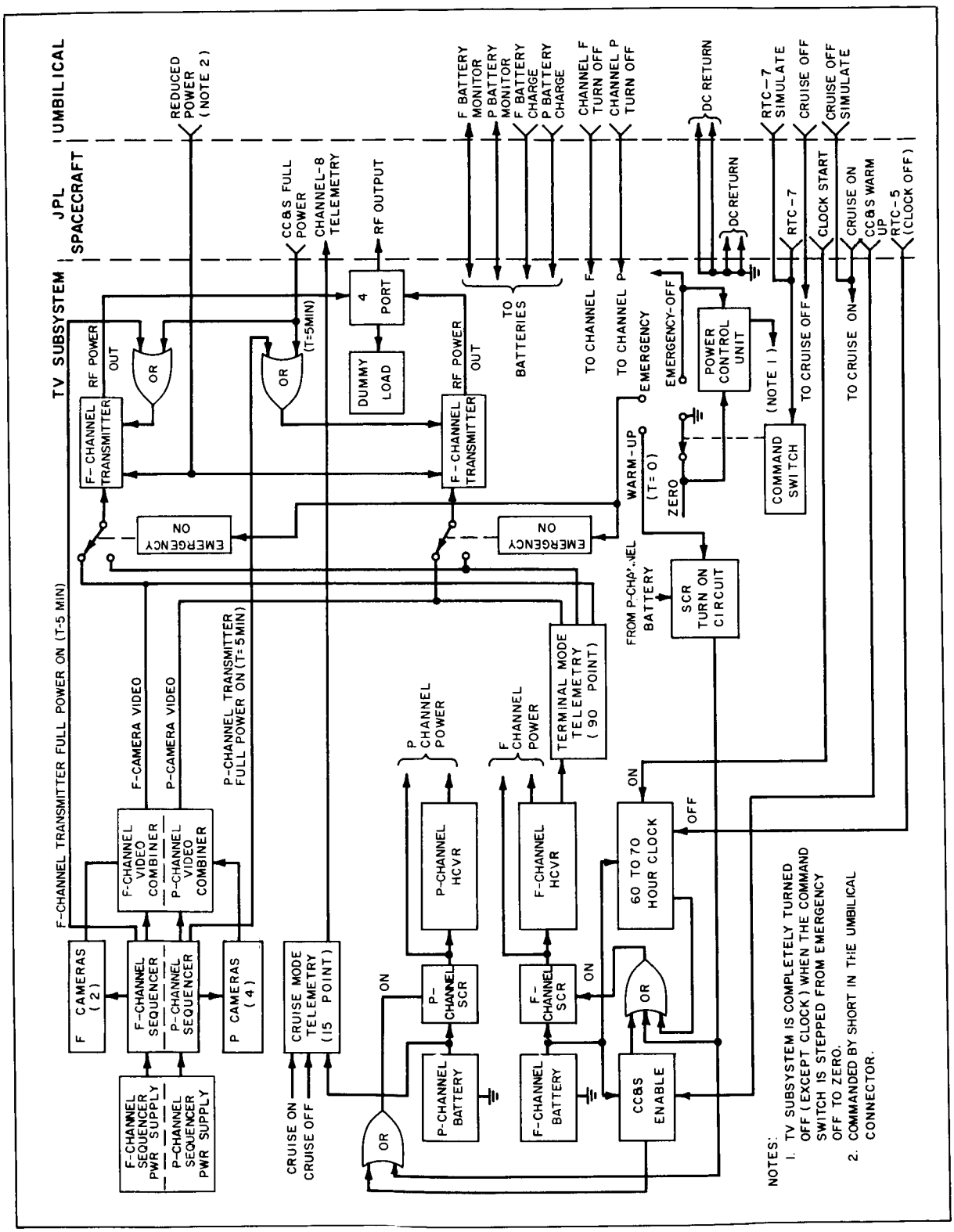

Figure 1. Logic Diagram of Ranger VI Command and Control Circuitry

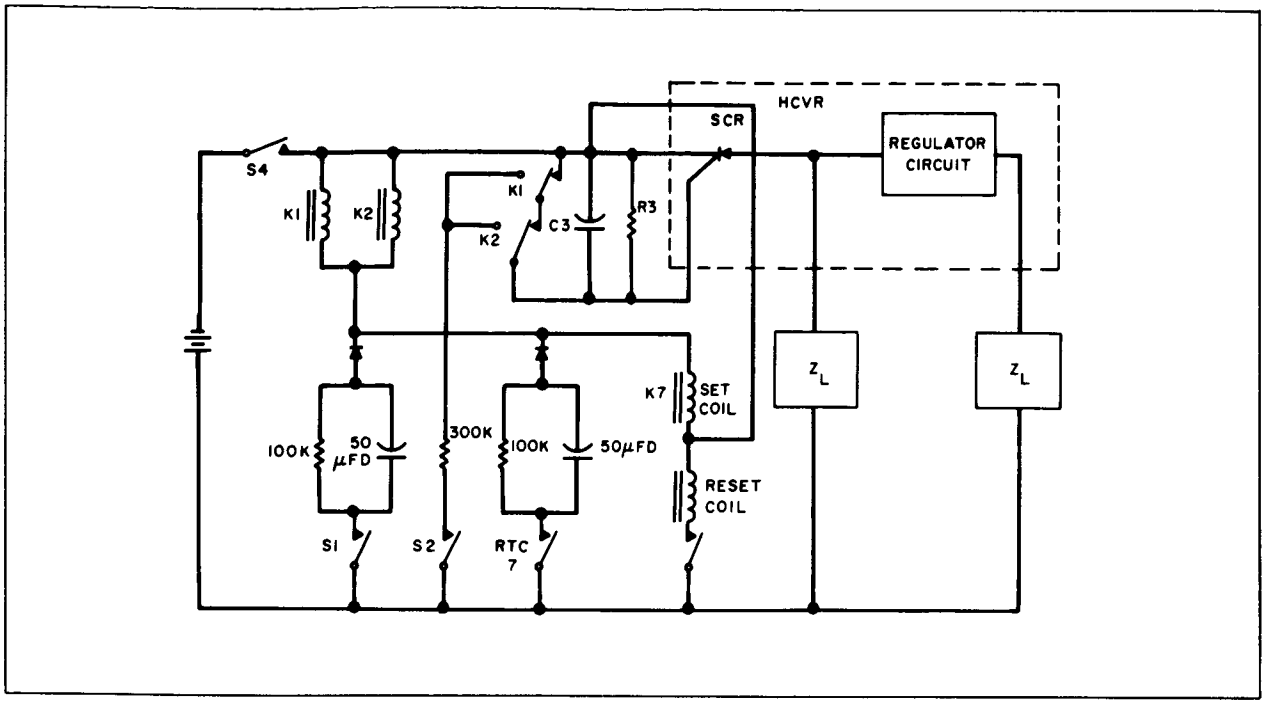

Figure 2. SCR Firing Circuit and Relay Controls

points 1 and 2 of the telemetry received during the inadvertent turn-on of Channel-8 would not have been present, since the LCVR would not be activated by this turn-on.

Another possibility for the inadvertent turn-on of the TV Subsystem would be the gating of the SCR's in the High-Current Voltage Regulators by the presence of transients in the SCR cathode or anode circuits. It has been indicated that SCR's will fire when a change in the cathode-to-anode voltage occurs at a rate of approximately 25 volts per microsecond. In the TV Subsystem, this would require a change in battery voltage from 0 to 35 volts in approximately 1.75 to 2 microseconds. This voltage change across the cathode of the SCR could induce a turn-on mode. To carry this a step further, it has been stated that if the Transmitter Power Supplies were energized in the partial-pressure environment, severe arcing would result. This arcing could induce transients via series inductance on the primary side to back-bias the SCR on the anode side and cause the SCR to turn off by reducing current flow to zero; the values for turn-off transient need be only equal to the voltage drop across the SCR. Thus, a transient spike greater than one volt for 20 microseconds could turn off the SCR, and it would remain off if the blocking voltage were applied at a rate of 11 volts per microsecond or less. The inadvertent turn-on possibility is based on the assumption that the voltage spike has sufficient power to overcome the load currents. If a transient had caused the turn-on of the Subsystem into the warm-up mode, again, points 1 and 2 of the received Channel-8 telemetry would not have been present.

Therefore, the only mechanism which satisfies all of the data received is an inadvertent stepping of the Command Switch. Stepping the Command Switch to the "Warm-Up" position during the critical-pressure environment would cause the SCR's in both HCVR's to fire by grounding their gates through the center

tap of the switch, thereby placing both the P- and F-Channels of the Subsystem into the warm-up mode. This inadvertent stepping would also initiate operation of the LCVR, thereby providing an indication on points 1 and 2 of the Channel-8 telemetry. Subsequent stepping of the Command Switch through "Emergency-On", "Emergency-Off", and back to the "Zero" position would account for the Subsystem turn-off.

Stepping of the Command Switch was accepted as the most probable cause of the inadvertent Subsystem turn-on. The investigation was then concentrated on determining what specifically caused this inadvertent actuation of the Command Switch. The sensitivity of the Command-Switch relay driver is a possible cause of the actuation. A high-impedance short, but less than 30 kilohms, between the "RTC-7" or "RTC-7 Simulate" input leads and ground would cause the switch to step. An increase in the impedance of the short to 130 kilohms would seat the switch and reenable the driver circuit. A subsequent reduction in the impedance to the 40-kilohm level would cause the switch to step again. If this situation was repeated four or a multiple of four times, and then the short cleared itself, the Command Switch would have returned to "Zero", and be in position to accept the actual RTC-7 command. Since this command was sent and received during the terminal phase of the mission and the P-Channel Accumulator pulse was received at the correct time, it must be assumed that the Command Switch was in the zero position and the fault had been cleared when the anomalous Channel-8 telemetry turned off.

Another possible means of actuating of the Command Switch is the actual receipt of a series of RTC-7 commands from the JPL Bus, due, perhaps, to mechanical chatter or electrical short of the RTC-7 relay. Again, it would require four or a multiple of four actuations of this relay to return the Command Switch to the zero position and turn off the HCVR's and the Channel-8 telemetry.

A short circuit to ground on the RTC-7 Simulate Command line anywhere along its route would also step the switch. A short, open, short, situation is again required four times, to step the Command Switch through a complete cycle back to the zero position. RTC-7 Simulate is an extension of the real RTC-7 and goes into the umbilical connector.

One possible means of stepping the Command Switch has been advanced which appears to have a high probability of occurrence; that is that an arc from the cover of the umbilical connector to the RTC-7 simulate command line could cause the command switch to step into warm-up. One hypothesis upon which this failure mechanism is based considers the development of an equipotential charge on the entire surface of the launch vehicle and spacecraft. This static charge may be caused by the passage of the engine fuels through the rocket engine feed lines. As long as nothing disturbs this charge, it will continue to increase while the flow of fuel continues.

During the Ranger mission, however, a change in the configuration of the launch vehicle does take place which could drastically disrupt this equipotential condition. At the time of Booster-Engine separation the booster engine bracket moves into the plume of the sustainer rocket. This plume contains a great number of free electrons and ions which cause the development of a charge on the booster-engine bracket that is very negative in relation to the skin of the missile. By capacitive action, this relatively negative charge causes the base of the vehicle to become positive with respect to the equipotential charge that existed on the entire vehicle prior to booster-engine separation. Since the total charge on that portion of the vehicle that remains intact after booster-engine separation would remain constant during this very short period of time, the upper end of the vehicle would become negative with respect to the original equipotential charge. This configuration is shown diagramatically in Figure 3.

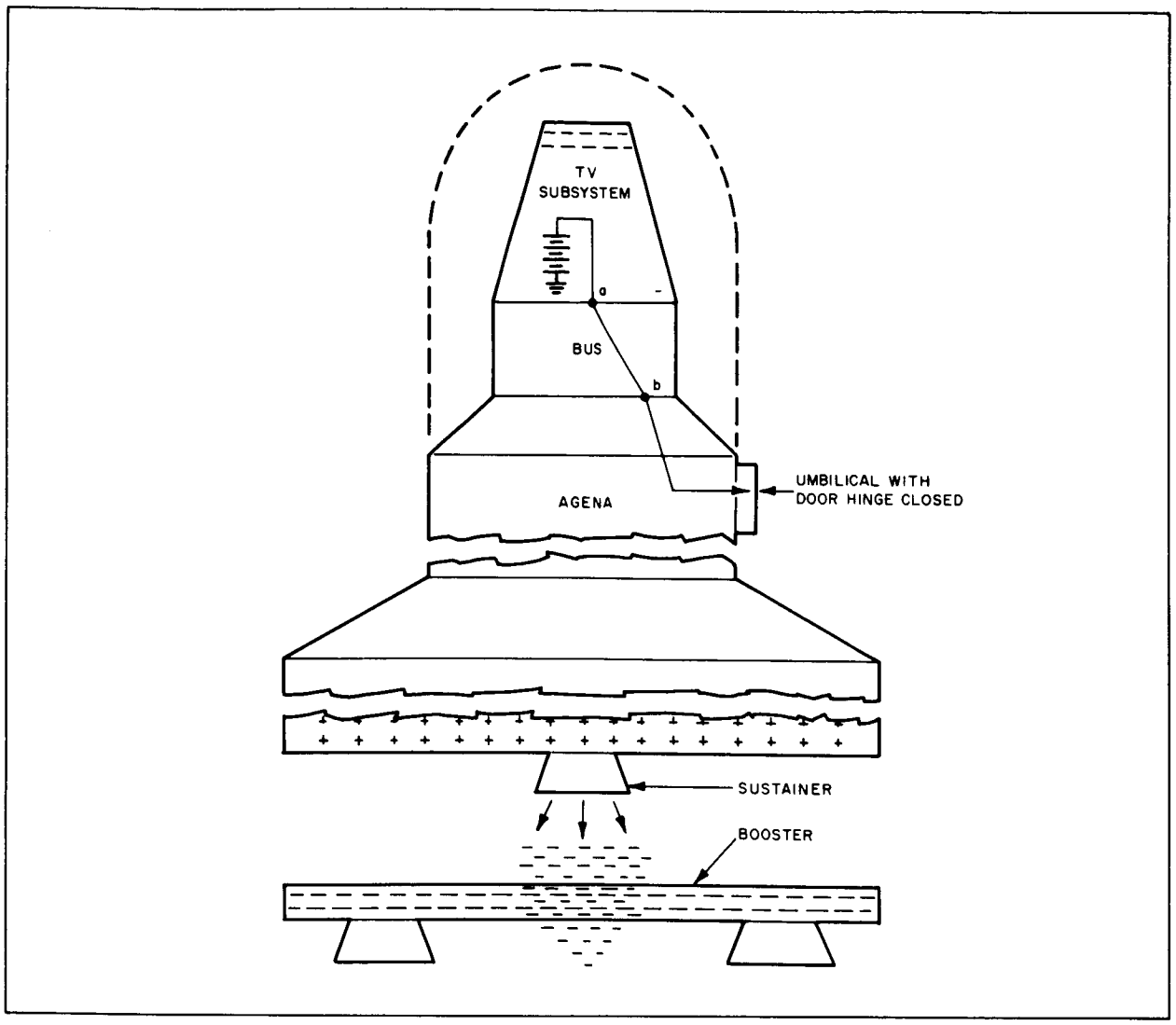

Figure 3. Missile Configuration at Booster Jettison

The redistribution of charge thus described would cause a considerable change in the effective charge at the umbilical connector on the Agena skin. Since there is no intentional electrical connection between the TV Subsystem ground and the case of the umbilical connector, and since the only electrical connection that apparently does exist is through the bolts connecting the TV Subsystem to the Bus, it is possible to hypothesize the existence of a potential difference between the TV Subsystem ground and the case of the umbilical connector. If this potential difference were great enough, and if a partial-pressure condition existed within the umbilical connector, then an arcing condition could exist inside this connector. If this arcing did take place between pin 4X, which was the RTC-7 Simulate line, and the umbilical-connector cover then it is quite possible that a signal would have

been sent to the Command Switch on the TV Subsystem to step into warmup. Figure 4 shows the location of pin 4X in the umbilical connector and the relation between this pin and the latch on the umbilical-connector cover. Considering the fact that the RTC-7 Simulate pin inside this umbilical disconnect plug is in close proximity to the latching mechanism of the door (approximately 6.3 mm) and the connector is male with rounded pins (see Figure 4, b and c), it is feasible that arcing would have existed from this latch to the pin if the difference of potential were approximately 300 volts at an altitude of 130,000 feet (see Figure 5). If this voltage were present to an altitude of 200,000 feet, it is probable that arcing would have continued throughout this altitude change.

At the time of the anomalous receipt of Channel-8 telemetry (GMT 030:15:51:29) the vehicle was at an altitude of 172,000 feet and an approximate pressure of 8×10^{-1} mm of Hg. Experiments were performed in a vacuum jar with a series of potential differences existent between pin 4X and the cover of the umbilical connector. Arcing took place at a potential of +350 volts applied to the cover plate with the Command Switch at zero volts and a pressure of approximately 1 mm of Hg (Equivalent to an altitude of 150,000 feet.) The wafer switch stepped into the warm-up position. This step was caused by an arc between the umbilical connector cover latch and pin 4X (RTC-7 Simulate). The vacuum jar continued to be evacuated until the pressure level reached approximately 1×10^{-1} mm of Hg (equivalent to an altitude of 250,000 feet). Arcing was seen throughout this pressure change and the wafer switch in the Command Switch stepped through "Emergency-On", "Emergency-Off", and back to "Zero" where it stopped.

These tests prove that such a failure mechanism can be duplicated and therefore is highly possible. Since no other method of actuating the Command Switch has been advanced with as high a probability of occurrence, arcing

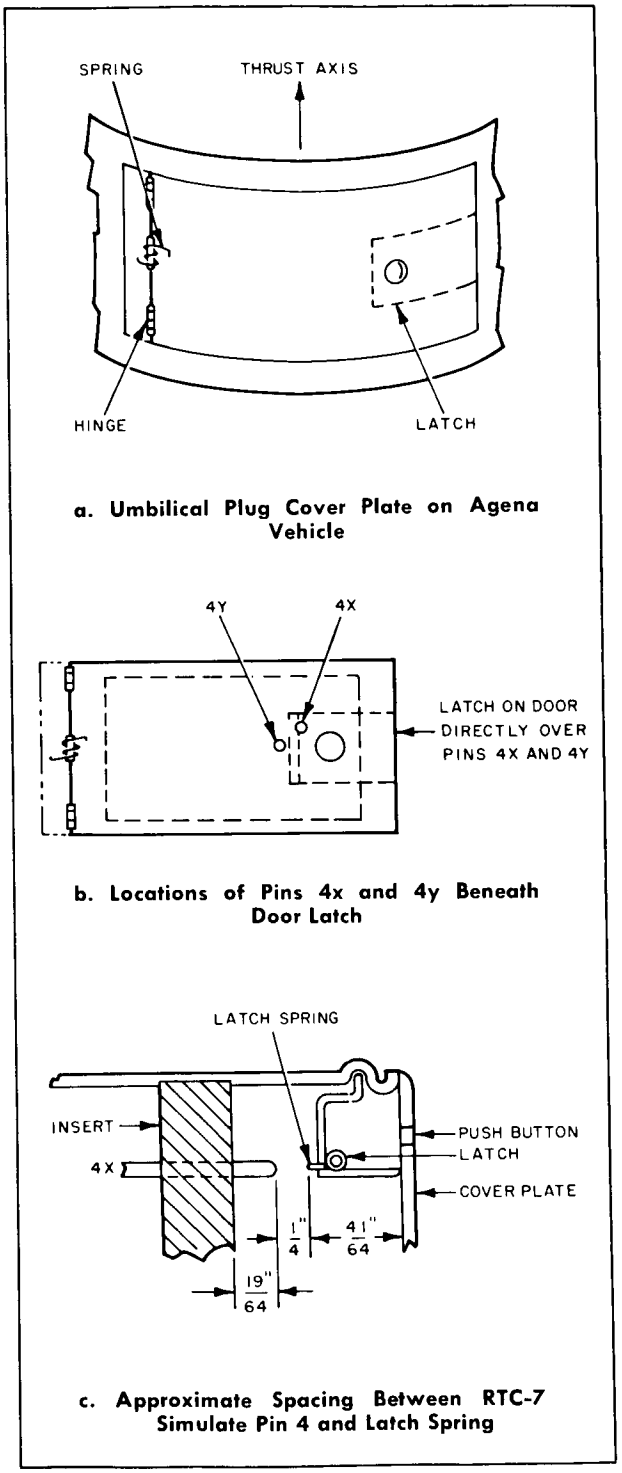

a. Umbilical Plug Cover Plate on Agena Vehicle

b. Locations of Pins 4x and 4y Beneath Door Latch

c. Approximate Spacing Between RTC-7 Simulate Pin 4 and Latch Spring

Figure 4. Details of Umbilical Connector Cover Plate

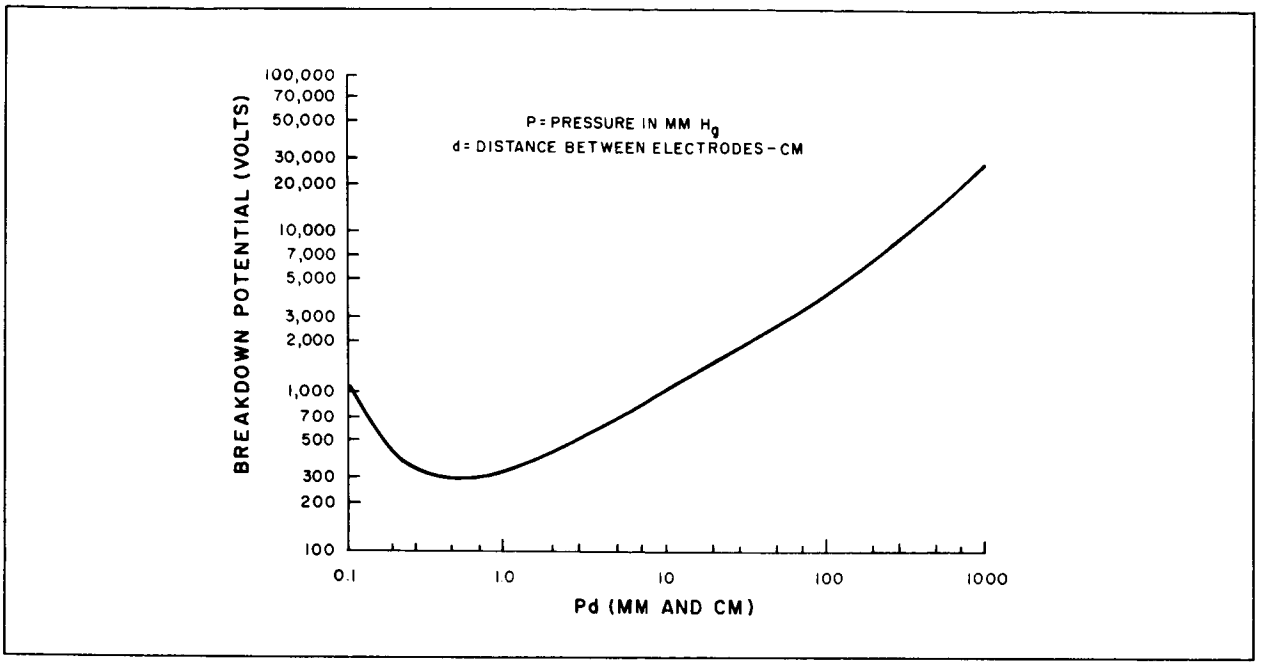

Figure 5. Characteristics of Potential Breakdown

in the umbilical connector was considered as the prime suspect for the cause of the Ranger VI failure.

4. Design Study

Based on a comprehensive design study, several modifications were incorporated into the Ranger TV Subsystem to provide a greatly increased probability of success for the Ranger VII mission. The design study was initiated immediately following the unsuccessful Ranger VI mission and was performed concurrent with and in accordance with the results of the Ranger VI failure investigation. The design study was concentrated on major modifications in two areas of the Subsystem, with some additional portions of the Subsystem considered for design refinements.

The areas in which major design modifications occurred were the Command and Control circuitry and the 15- and 90-point telemetry. Because the inadvertent stepping of the Command Switch was held to be the most probable cause of turn-on of the Ranger VI TV Subsystem into the warm-up mode, it was decided to simplify the entire Command and Control circuitry and provide more reliable methods for turn-on and turn-off of the Subsystem.

Following the analysis of the potential problem areas in the Ranger VI Command and Control circuitry, the command pholosophy and logic were revised in such a manner that potential problem areas were at least minimized if not completely eliminated. Circuits were then developed to meet the new philosophical and logical requirements. These circuits were developed with the following objectives in mind.

- Prevent premature turn-on of the Subsystem;
- Permit immediate Subsystem turn-off, if it became necessary.
- Retain the good features of the former Command and Control circuit; and

- Utilize existing hardware wherever possible.

All of the revised command logic and circuits developed were analyzed for both real- and hypothetical-fault conditions. Each circuit was then analyzed in a worst-case condition to check analytically the choice of component parts.

COMMAND PHILOSOPHY AND LOGIC REVISIONS

The following changes were made in the philosophy and logic of the Command and Control circuitry:

- Circuit effects on the battery SCR were minimized;
- Clock control was revised for single battery dependence;
- Inadvertent command initiation during launch was prevented;
- The continuous latching effect of the CC&S warm-up relays was removed;
- The RTC-7 command system was revised for exclusive turn-on of both channels with complete channel redundancy;
- Clock-output command was retained;
- CC&S full-power command was retained;
- The time for the Sequencer full-power command was changed from 5 minutes to 80 seconds;
- The RTC-5 command was revised to incorporate the added function of turning off the Subsystem;
- The reduced-power command was revised so that it was inhibited during flight;
- All ground checkout commands from the blockhouse were eliminated, with the exception of one, which was used to enable on-board commands. This command was isolated from a single fault mode.

A revised Command and Control circuitry incorporating these logic modifications was developed and employed in Ranger VII.

5. Post Flight Thermal Analysis

a. THERMAL-VACUUM TESTS

Immediately following the flight of the Ranger VI Spacecraft, preparations were made to perform the following thermal-vacuum tests on Flight Model III-4 TV Subsystem at AED:

(a) A test duplicating the real-time flight of the Ranger VI Spacecraft. Temperature curves obtained from the Ranger VI telemetry were used as a guide for inputs to the fin heaters. The fin inputs were known at this point). The fin inputs were adjusted in such a manner as to cause the test-vehicle temperatures to follow the above mentioned curves and at the same time, where possible, maintain the usual ratio of inputs to the fins. This temperature-time duplication is shown in Figure 6. The resulting fin heater input energy for this test is shown in Table 2.

(b) A test establishing "nominal" temperatures on the vehicle using the pre-flight calculations for the fin inputs. This test

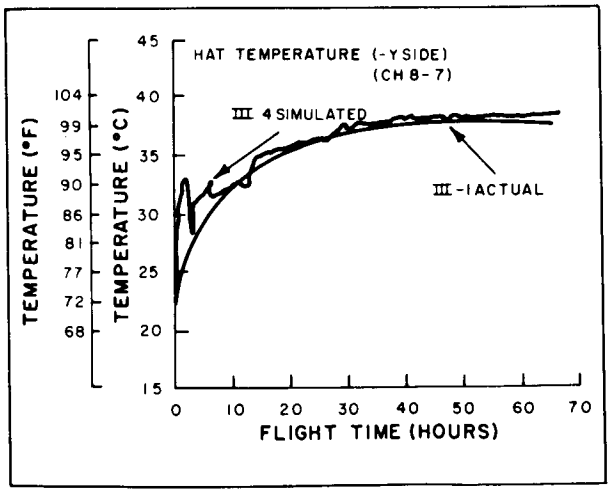

Figure 6. Actual versus Simulated Temperature Profile for Ranger VI Top Hat, Y Axis

verified that the III-4 Subsystem was thermally akin to the Ranger VI Spacecraft. The temperatures obtained were those previously called "nominal". The fin energy input is shown in Table 2.

(c) A test establishing a temperature field on the Subsystem 10 degrees C lower than the temperatures obtained from the flight duplication test. This test was called the revised flight test. Table 2

TABLE 2
THERMAL INPUT ENERGY

		Calculations for Ranger III-1				Calculations for Ranger III-2		
	a	b	c	d	e	f	g	h
Finish Ident.	Proj. Finish Area	α Value	Original Input Calculation S=0.9	Input Without Reflection S=0.93	Input With Reflection S=0.93	α Value	Input Without Reflection S=0.87	Input With Reflection S=0.87
	Inches^2		Watts	Watts	Watts		Watts	Watts
A	58.5	0.65	34.3	35.4	44.7	0.58	29.5	38.9
B*	53.2	0.65	31.1	32.2	45.0	0.58	26.9	43.0
B**	16.4	(0.65) 0.41	9.7	10.0		(0.93) 0.58	13.3	
C	68.4	0.82	50.5	52.2	54.4	0.77	45.8	48.1
D	74.7	0.82	55.1	57.0	58.6	0.77	50.0	51.9
E	45.2	0.41	16.7	17.2	17.2	0.20	7.9	7.9
F	50.1	(0.84) 0.65	37.9	39.1	39.7	(0.81) 0.58	35.3	36.0
Totals	366.5	-	253.3	243.1	259.6	-	208.7	225.8

TABLE 2
THERMAL INPUT ENERGY (Continued)

	Test Data (From III-4 Tests)			Comparisons		
				(m-k)	(m-n)	(e-h)
	k	m	n	p	r	s
Finish Ident.	Nominal Input Test	III-1 Flight Duplication Test	Revised Flight Test	Increase, Nominal to III-1 Flt.	Decrease, III-1 Flt. to Revised	Calculated Decrease, III-1 to III-2
	Watts	Watts	Watts	Watts	Watts	Watts
A	34.4	48.5	37.9	14.1	10.6	5.8
B*	42.0	60.3	56.1	18.3	4.2	2.0
B**						
C	51.4	70.7	66.3	19.3	4.4	6.3
D	55.1	71.0	64.0	15.9	7.0	6.7
E	16.7	19.9	10.1	3.2	9.8	9.3
F	37.8	32.3	32.4	-5.5	-0.1	3.7
Totals	237.4	302.7	266.8	65.3	35.9	33.8

(α) Indicates Effective Absorption Value. S = Solar Constant (watt/in^2)

Corresponding

Component	c	d	e	g	h	k	m	n
Battery	15	18	23	7	14	14	36	26
Near Vidicon Face Plate	16	19	20	6	8	14	28	19
Thermal Shield - Hat (-Y)	27	30	31	16	18	27	39	30
Thermal Shield Below Fin A (-Y)	16	19	25	9	15	16	38	27
Camera Electronics	15	18	23	7	15	14	35	27
	Calculated Temperatures					Measured Test Temperatures		

indicates the fin energy input for this test. Energy loss calculations are presented in Tables 3 through 5. A calculation of the average radiation coupling factor (K) from the Subsystem surface to the chamber wall is given at the bottom of these tables. The agreement in the calculated values of K for the three tests (880, 887, 887, in^2) indicate that good energy balances were achieved.

The key thermal information obtained from these tests can be summarized as:

- Flight Duplication Test–Provided the values of input energy that may represent the energy absorbed during the flight of the Ranger VI Spacecraft.
- Nominal Test - Verified that the Flight Model III-4 was thermally the same as Flight Model III-1 (Ranger VI).
- Revised Flight Test - Indicated the amount of energy input reduction required to reduce the temperatures of the flight duplication test by approximately 10 degrees C.

b. ANALYTICAL CALCULATIONS

The thermal control of the Subsystem during cruise mode is almost entirely dependent upon the external environment; the internal power dissipation is so small as to be an insignificant input during normal cruise operation. However, a large internal power dissipation during the cruise phase would cause a large temperature increase on the Subsystem due to the "semi-insulated" design configuration. One postulation that would explain the higher flight temperatures of the Ranger VI Spacecraft was that there was abnormal internal power during cruise mode. This theory is discounted since the dissipation would have to occur for the entire flight; battery telemetry did not indicate this to be true. Therefore, if unusual internal power dissipation effects are discounted, the higher temperatures must be due to external effects. Another assumption is that the unknown cause of the discrepancy may be isolated to energy inputs, that is the energy-loss parameters (emissivity, surface area) did not change from those determined via thermal-vacuum testing. Many precautions are taken to see that the emissivity of the large polished aluminum skin area does not change from testing to flight, including frequent repolishing to remove oxides and residue and using strip coat as a protective cover.

Thus, the cause of the discrepancy was placed in the area of external energy input. This input is due to the solar energy available at the vehicle surface, the energy composed of two components:

(1) Solar energy arriving at the surface directly.

(2) Solar energy arriving at the surface indirectly, i.e., reflected from other surfaces.

A calculation of total energy absorbed is required. This is a simple task for the case of directly incident solar energy, since the absorbed amount is given by:

$$Q_{D_i} = \left[SA_p \alpha \right]_i$$

where:

Q_{D_i} = direct solar energy absorbed by surface i

S = solar intensity constant

A_p = projected area of surface i to the solar field

α = solar absorptivity of surface i

The energy absorbed for the indirect or reflected solar energy case can be computed by:

$$Q_{R_{ij}} = \left[SA_p(1-\alpha) \right]_i C_{ij}$$

TABLE 3
TEMPERATURE BALANCE AND ENERGY LOSS, FLIGHT DUPLICATION TEST

Item	A Area (In^2)	B Effective (Σ)	AxB (In^2)	Temp T (^0C)	σT^4 ($Watt/In^2$)	Energy Loss (Watts)
Fin F	48.1	0.98	47.14	47	0.383	18.1
Fin E	45.24	0.89	40.26	72	0.518	20.9
Hat Skin	666.	0.05	33.30	38	0.342	11.4
Flange D	33.1	0.88	29.13	40	0.350	10.2
Fin D	149.4	0.89	133	40	0.350	46.6
Skin C – D	491.	0.05	24.6	37	0.337	8.3
Camera Holes	151	0.98	148	37	0.337	49.9
Electronics Shield	67	0.94	63	1	0.206	13.0
Flange C	31.3	0.88	27.54	42	0.360	9.9
Fin C	139.2	0.89	123.9	42	0.360	44.6
Skin B – C	714	0.05	35.7	37	0.337	12.0
Flange B	43.7	0.88	38.46	38	0.342	13.2
Fin B	139.2	0.89	123.9	38	0.342	42.4
Skin A – B	550	0.05	27.5	38	0.342	9.4
Flange A	49.3	0.88	43.38	38	0.342	14.8
Skin Below A	579	0.05	28.9	37	0.337	9.7
Base Ring	160	0.02	3.2	32	0.316	1.0
Legs	129	0.30	38.7	32	0.316	12.2
Fin A	117	0.89	104.1	38	0.342	35.6
			$\Sigma A \times B =$ 1113.7		Total Energy Loss	383.2

$Q_{IN} = 302.7$

$K' = \frac{266.8}{.301} = 887\ in^2$

$(\sigma T^4)_{Avg.} = \frac{334.8}{1113.7} = 0.301$

$T_{Avg.} = 28.2^\circ C$

TABLE 4
TEMPERATURE BALANCE AND ENERGY LOSS, NOMINAL TEST

Item	A Area (In^2)	B Effective (Σ)	AxB (In^2)	Temp T (^oC)	σT^4 ($Watt/In^2$)	Energy Loss (Watts)
Fin F	48.1	0.98	47.14	42	0.360	17.0
Fin E	45.24	0.89	40.26	52	0.407	16.4
Hat Skin	666	0.05	33.30	26	0.292	9.7
Flange D	33.1	0.88	29.13	23	0.280	8.2
Fin D	149.4	0.89	133	23	0.280	37.2
Skin C — D	491	0.05	24.6	18	0.262	6.4
Camera Holes	151	0.98	148	18	0.262	38.8
Electronics Shield	67	0.94	63	-13.5	0.164	10.3
Flange C	31.3	0.88	27.54	20	0.269	7.4
Fin C	139.2	0.89	123.9	20	0.269	33.3
Skin B — C	714	0.05	35.7	17	0.258	9.2
Flange B	43.7	0.88	38.46	17	0.258	9.9
Fin B	139.2	0.89	123.9	17	0.258	32.0
Skin A — B	550	0.05	27.5	16	0.255	7.0
Flange A	49.3	0.88	43.38	16	0.255	11.1
Skin Below A	579	0.05	28.9	15	0.251	7.3
Base Ring	160	0.02	3.2	12	0.241	0.8
Legs	129	0.30	38.7	12	0.241	9.3
Fin A	117	0.89	104.1	16	0.255	26.5
			$\Sigma A \times B =$ 1113.7		Total Energy Loss	297.8

$Q_{IN} = 237.2$

$K = \frac{237.2}{.267} = 887\ in^2$ $\quad (\sigma T^4)_{Avg.} = \frac{297.8}{1113.7} = 0.267$ $\quad T_{Avg.} = 19.4^\circ C$

TABLE 5
TEMPERATURE BALANCE AND ENERGY LOSS, REVISED FLIGHT TEST

Item	A Area (In^2)	B Effective (Σ)	AxB (In^2)	Temp T (^0C)	σT^4 (Watt/In^2)	Energy Loss (Watts)
Fin F	48.1	0.98	47.14	38	0.342	16.1
Fin E	45.24	0.89	40.26	26.5	0.292	11.8
Hat Skin	666	0.05	33.30	29	0.304	10.1
Flange D	33.1	0.88	29.13	32	0.316	9.2
Fin D	149.4	0.89	133	32	0.316	42.0
Skin C — D	491	0.05	24.6	30	0.308	7.6
Camera Holes	151	0.98	148	30	0.308	45.6
Electronics Shield	67	0.94	63	-5	0.188	11.8
Flange C	31.3	0.88	27.54	34	0.324	8.9
Fin C	139.2	0.89	123.9	34	0.324	40.1
Skin B — C	714	0.05	35.7	28	0.300	10.7
Flange B	43.7	0.88	38.46	28	0.300	11.5
Fin B	139.2	0.89	123.9	28	0.300	37.2
Skin A — B	550	0.05	27.5	28	0.300	8.3
Flange A	49.3	0.88	43.38	28	0.300	13.0
Skin Below A	579	0.05	28.9	26	0.292	8.4
Base Ring	160	0.02	3.2	20	0.269	0.9
Legs	129	0.30	38.7	20	0.269	10.4
Fin A	117	0.89	104.1	28	0.300	31.2
			$\Sigma A \times B = 1113.7$		Total Energy Loss	334.8

$Q_{IN} = 266.8$ $\qquad Q_{IN} = K\delta[T^4]$

$K = \frac{266.8}{0.301} = 887\ in^2$ $\qquad (\sigma T^4)_{Avg.} = \frac{334.8}{1113.7} = 0.301$ $\qquad T_{Avg.} = 28.2^{\circ}C$

where:

$Q_{R_{ij}}$ = direct energy reflected by surface i that is absorbed by surface j.

C_{ij} = solar reflection coupling factor.

This expression is no more complex than that written for the direct input if C_{ij} is known. However, obtaining the value of C_{ij} is a complex calculation which requires use of a large computer. This solar reflection coupling factor is a complex function of the absorptivities of the reflecting surfaces, and the configuration factors relating the reflecting surfaces. Values of C_{ij} from computer analysis are given for selected vehicle absorptivity values in Figures 7 through 16.

The configuration factors (ϕ_{ij}) used to obtain these values are shown in Table 6. Table 7 gives computer values for the I.R. coupling factors (K_{ij}) for the vehicle. These factors are used for energy loss calculations and are computed in the same manner as ϕ_{ij} except emissivities are substituted for solar absorptivities.

Computations of the absorbed energy flight were performed for the III-1 vehicle as shown in Table 2. Prelaunch column (b) absorptivity values were verified with the reflectometer at ETR. Column (c) represents the original (before flight) input based upon these α values. For this set of calculations, a nominal solar constant of 0.90 watt/in^2 was used, and reflection inputs were assumed to be minor and neglected. This was done for "safety" reasons since the primary thermal concern was for maintaining the battery temperature above 10° C. The reasoning was that the calculation would indicate a conservative cruise temperature and the reflection input in flight would be additional insurance against a cold battery. Calculations based on this input would yield a battery temperature of 15° C and a vidicon housing temperature of 16° C.

Column (d) of Table 2 indicates the input for Flight Model III-1 for a solar constant of 0.93 watt/in^2 (the actual value for the January launch). The yearly variation in the solar constant is approximately ±3.3%. Column (e) indicates the input for the higher solar constant, and includes the effect of solar reflections. It can be seen that reflections account for 16.5 watts additional input, while the higher solar constant yields about 8 additional watts input. Accounting for the higher solar constant and solar reflections in the input calculation results in predicted battery and camera housing temperatures of 23 and 20° C respectively. Table 8 gives a comparison of the maximum input calculation for Flight Model III-1 and the data obtained from the flight duplication test. A total of 43 watts of energy remain unaccounted for. Possible sources of this differential are indicated in Table 8.

In selecting the thermal finish to be used for Flight Model III-2, a "compromise" design modification was selected as a solution to the problem. Values of solar absorptivity were applied that reduced the energy input only enough to produce a temperature field of approximately 10° C lower than that obtained during the Ranger VI Mission. Table 2, column (f), indicates the approximate values of absorptance used on Flight Model III-2. Note that only two gray paints were required. The calculated energy inputs are shown in columns (g) and (h) for these values. The input of column (g) represents a "worst condition" low-temperature situation (no reflections accounted for), based upon the III-1 flight. Column (h) represents what might be called the lower bound of the nominal temperature range. The values were computed using the same techniques as for Flight Model III-1 computation.

This upper temperature bound was obtained as follows:

- Test data existed on the input required to duplicate the Ranger VI flight.

- Test data existed on the input required to establish a temperature balance at 10° C below the level of Ranger IV flight; and

- The difference in input between the two tests was determined. This difference was related to the amount of reduction in the value of solar absorptivity required on the respective fin surfaces.

Column (r) of Table 2 indicates the difference in input between the two tests to be 36 watts. Column (s) indicates the difference between Flight Models III-1 and III-2 calculated inputs to be 34 watts. Therefore, the upper nominal temperature bound was determined.

At the bottom of Table 2, temperature values are indicated for the components which were monitored on the 15-point telemetry for the Ranger VII flight. These values represent the equilibrium temperatures (achieved after approximately 40 hours of cruise-mode flight).

The values in columns (c) through (h) are calculated while those in columns (k) through (n) are measured test data. The temperature calculations are obtained by utilizing the equations given in Table 9. These equations were obtained by fitting thermal-vacuum test data of Block III vehicles to a straight line approximation using the technique of "least squares". Accuracy of these equations is on the order of ±3° C over the temperature range of 15° C to 35° C.

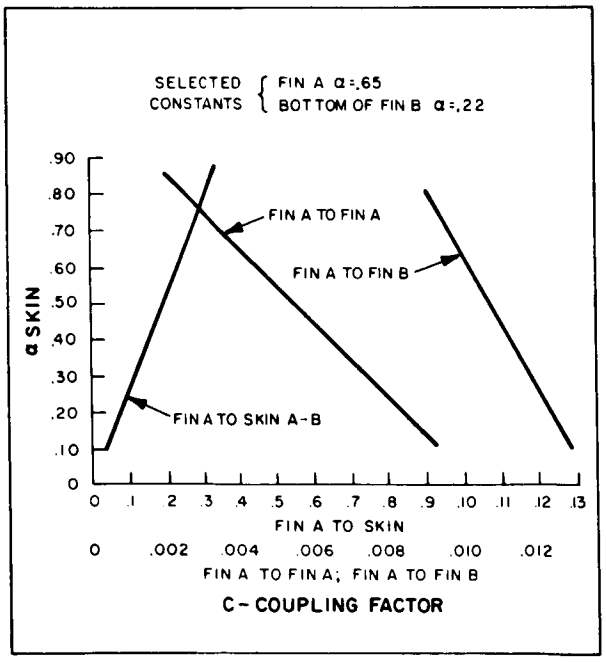

Figure 7. Solar Coupling Factors, Section Between Fin A and Fin B

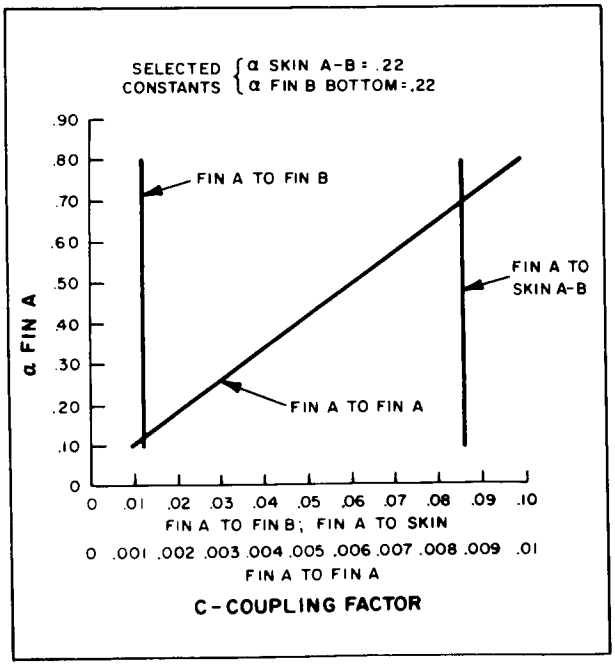

Figure 8. Solar Coupling Factors, Section Between Fin A and Fin B

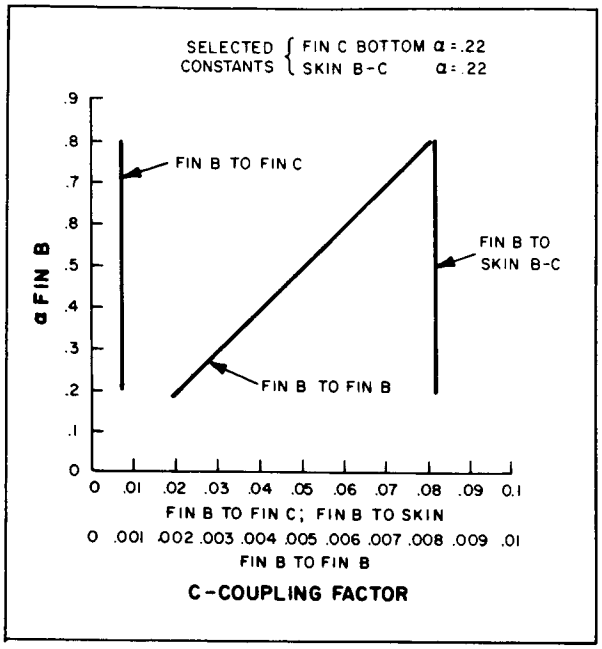

Figure 9. Solar Coupling Factors, Section Between Fin B and Fin C

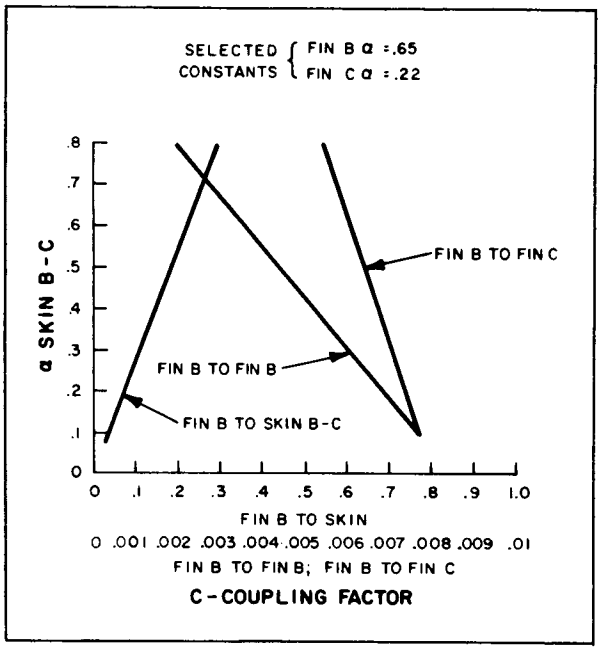

Figure 10. Solar Coupling Factors, Section Between Fin B and Fin C

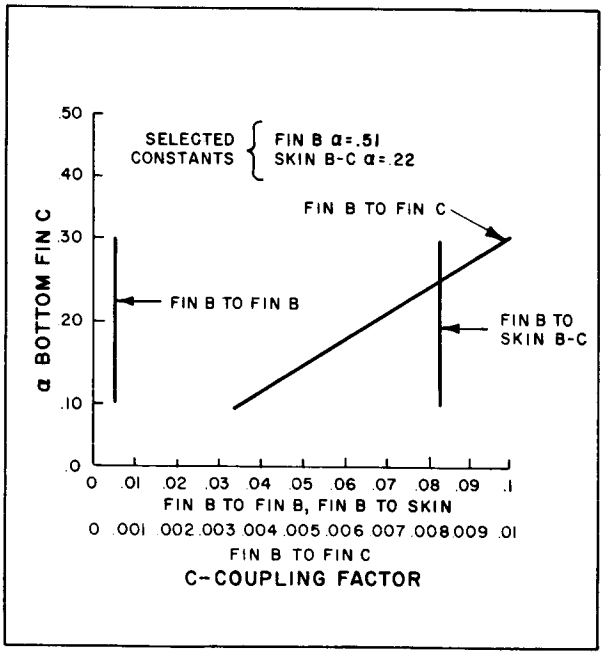

Figure 11. Solar Coupling Factors, Section Between Fin B and Fin C

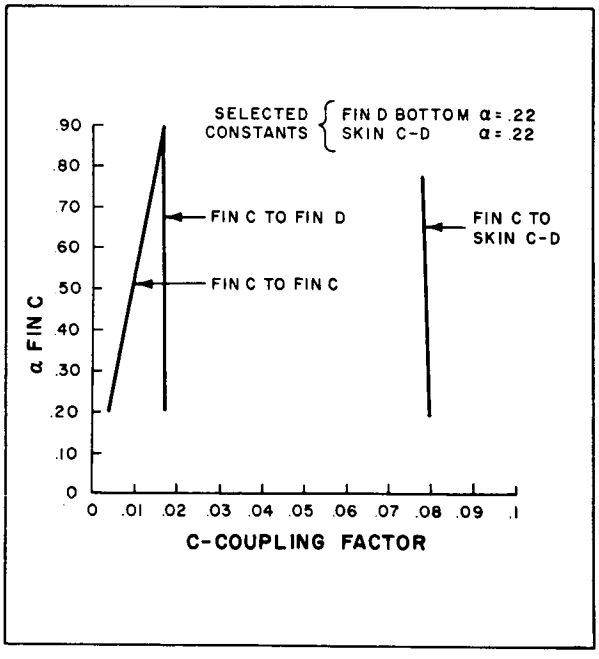

Figure 12. Solar Coupling Factors, Section Between Fin C and Fin D

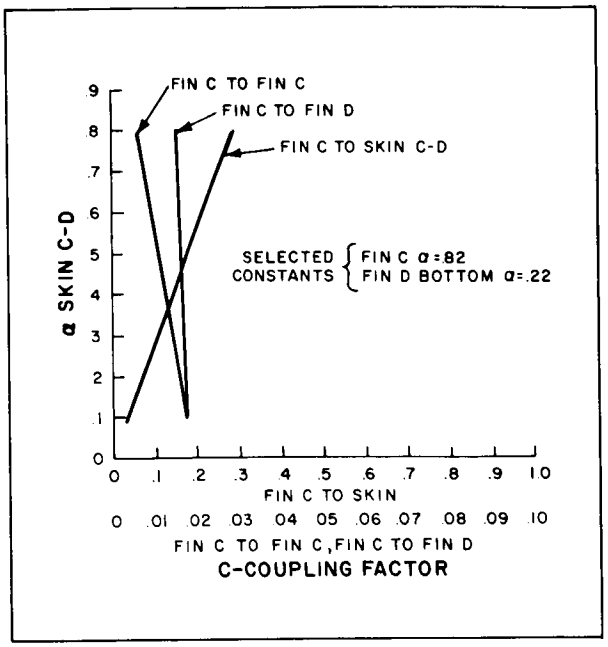

Figure 13. Solar Coupling Factors, Section Between Fin C and Fin D

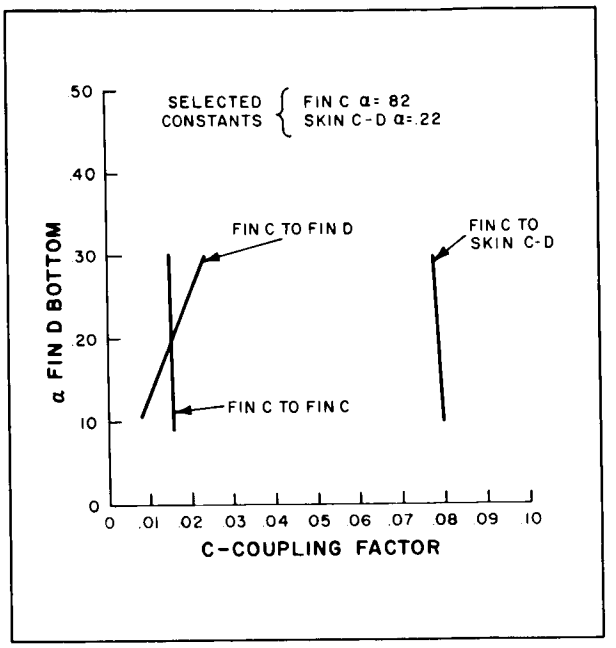

Figure 14. Solar Coupling Factors, Section Between Fin C and Fin D

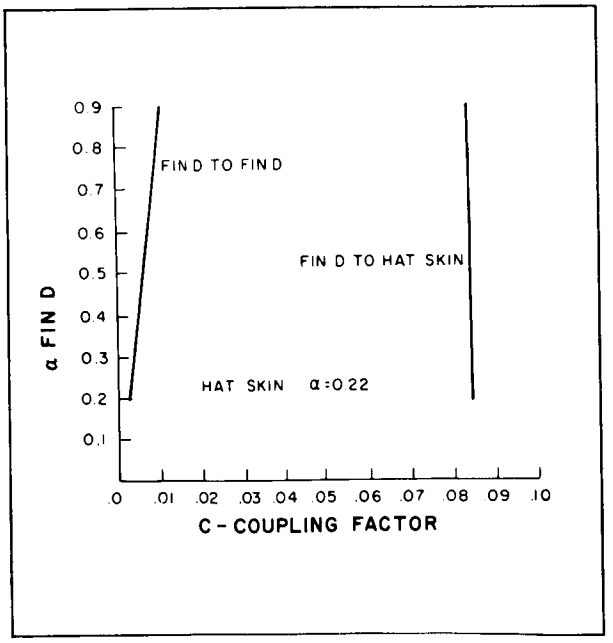

Figure 15. Solar Coupling Factors, Section Between Fin D and Top Hat

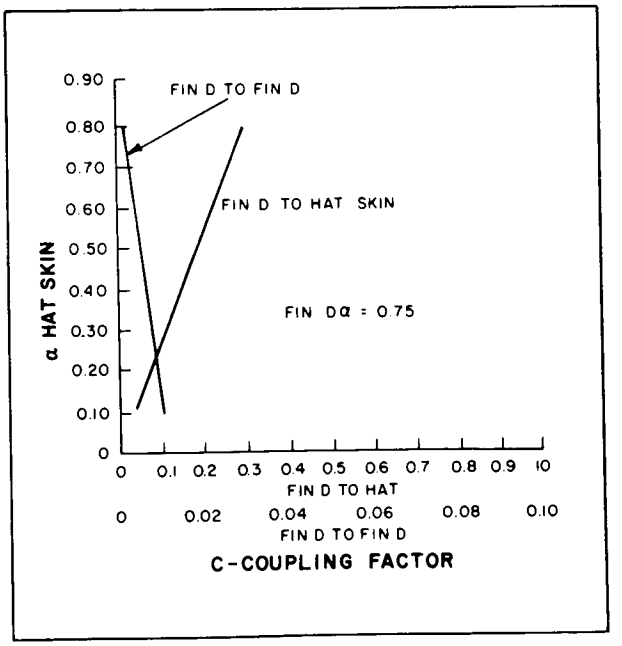

Figure 16. Solar Coupling Factors, Section Between Fin D and Top Hat

TABLE 6
RANGER CONFIGURATION FACTORS ($\varnothing_{ij}$)

From \ To	Fin D Top	Fin Flange C	Hat Skin	Space	
Fin D Top	0	0.250	0.130	0.620	
Flange D	0.565	0	0	0.435	
Hat Skin	0.014	0	0	0.986	

From \ To	Fin C Top	Fin D Bottom	Flange C	Skin C to D	Space
Fin C Top	0	0.060	0.210	0.120	0.610
Fin D Bottom	0.060	0	0	0.430	0.510
Flange C	0.470	0	0	0	0.530
Skin C to D	0.017	0.065	0	0	0.918

From \ To	Fin B Top	Fin C Bottom	Flange B	Skin B to C	Space
Fin B Top	0	0.022	0.260	0.100	0.618
Fin C Bottom	0.022	0	0	0.440	0.538
Flange B	0.415	0	0	0	0.585
Skin B to C	0.010	0.040	0	0	0.950

From \ To	Fin A Top	Fin B Bottom	Flange A	Skin A to B	Space
Fin A Top	0	0.040	0.290	0.080	0.590
Fin B Bottom	0.030	0	0	0.510	0.460
Flange A	0.350	0	0	0	0.650
Skin A to B	0.010	0.065	0	0	0.925

From \ To	Fin A Bottom	Skin Below A	Space		
Fin A Bottom	0	0.480	0.520		
Skin Below A	0.048	0	0.952		

ϕ_{ij} ≡ *Percent of the Thermal Energy leaving surface i that arrives at surface j.*

TABLE 7
IR COUPLING FACTORS (K_{ij}) FOR RANGER

From	Top Fin D	Flange D	Hat Skin	Space	
Fin D Top	~0.012	0.220	0.006	0.762	
Flange D	0.502	~0.014	0	0.484	
Hat Skin	0	0	0	1.000	
From	Top Fin C	Bottom Fin D	Flange C	Skin C to D	Space
Fin C Top	~0.012	0.054	0.194	0.006	0.734
Fin D Bottom	0.021	~0.024	0	0.021	0.934
Flange C	0.394	0	~0.010	0	0.596
Skin C to D	0.015	0.060	0	0	0.925
From	Top Fin B	Bottom Fin C	Flange B	Skin B to C	Space
Fin B Top	~0.012	0.019	0.230	0.005	0.734
Fin C Bottom	0.019	~0.016	0	0.021	0.944
Flange B	0.370	0	~0.010	0	0.620
Skin B to C	0.009	0.036	0	0	0.955
From	Top Fin A	Bottom Fin B	Flange A	Skin A to B	Space
Fin A Top	~0.012	0.037	0.258	0.004	0.689
Fin B Bottom	0.027	~0.030	0	0.026	0.917
Flange A	0.310	0	~0.010	0	0.780
Skin A to B	0.008	0.058	0	0	0.930
From	Bottom Fin A	Skin Below A	Space		
Fin A Bottom	~0.019	0.023	0.960		
Skin Below A	0.043	0	0.960		

Where: K_{ij} = Percentage of the energy radiated by body i that is absorbed by body i

Energy from i absorbed by i (net) = $q_{ij} = A_i \, \Sigma_i \, K_{ij} \left[T_i^4 - T_i^4 \right]$

Values of emissivity used to calculate these factors:

Σ top of fins = 0.89 Σ flanges = 0.88

Σ bottom of fins = 0.90 Σ skin = 0.05

TABLE 8
INPUT ENERGY NOT ACCOUNTED FOR ON FLIGHT MODEL III-1

Fin Identification	Actual Energy Input for III-1 (from Test Data)	Maximum Input Calculation for III-1	Input Energy Not Accounted For
	Watts	Watts	Watts
A	48.5	44.7	3.8
B	60.3	45.0	15.3
C	70.7	54.4	16.3
D	71.0	58.6	12.4
E	19.9	17.2	2.7
F	32.3	39.7	-7.4
Totals	302.7	259.6	43.1

Possible Cause of Discrepancy	Comment
Incorrect solar absorptivity values	Measurement error can be ±5% however good agreement on values between RCA/JPL/STL.
Oscillation of capsule about z-axis	Variation ≈ 0.2° per JPL. Thus not significant.
Solar reflections from bus, solar panels, and fin surfaces	Accounted for in part but values could be higher due to the large areas of polished aluminum on capsule.
Yearly variation in solar constant	Accounted for in above calculation (normal variation ±3.3%).
I. R. inputs from bus and solar panels	Accounted for in thermal-vacuum testing.
Errors in measurement of temperature during T/V testing	Not significant since error ≈ 1° to 2° C.
1/2° sun angle decollimation	Not significant since intensity is low in decollimated areas.
Solar panels not locked in 90° position	Would cause solar reflections to capsule - but did not occur per JPL.
Incorrect temperature telemetry	Estimate max. error ±5° C.
Equipment operating during cruise inside capsule	Theoretically would cause higher temperatures — however battery telemetry discounts this source.
Solar constant much higher than stated by literature	Not true since bus and solar panel temperatures normal.
Errors in values of emissivity of fins or polished skin	Little effect as long as the values do not change after the thermal-vacuum verification test. Every effort made to protect the surfaces via strip coat and covers.

TABLE 9
EQUATIONS TO CALCULATE TEMPERATURES OF SELECTED COMPONENTS FOR RANGER

Component	Equation
BATTERY	$\sigma T^4 = (1.1025 \times 10^{-3})\, X + (-0.1208 \times 10^{-3})\, Y \left(\frac{watts}{in^2}\right)$
VIDICON HOUSING (F_a)	$\sigma T^4 = (0.9697 \times 10^{-3})\, X + (0.4767 \times 10^{-3})\, Y$
CAMERA ELECTRONICS (-Y)	$\sigma T^4 = (1.107 \times 10^{-3})\, X + (-0.157 \times 10^{-3})\, Y$
THERMAL SHIELD, HAT (-Y)	$\sigma T^4 = (1.106 \times 10^{-3})\, X + (0.662 \times 10^{-3})\, Y$
THERMAL SHIELD, BELOW FIN A (-Y)	$\sigma T^4 = (1.1286 \times 10^{-3})\, X + (-0.1638 \times 10^{-3})\, Y$

Where:

$X = Q_A + Q_B + Q_C + Q_D + Q_E + Q_F$ *(Total heat input via fins) watts*

$Y = -2Q_A - Q_B + Q_D + 2\left[Q_E + Q_F\right]$ *watts*

Q_i = *Energy absorbed by fin i* *(watts)*

T = *Temperature in °K*

σ = *Stefan-Boltzmann's constant* $= 3.657 \times 10^{-11} \frac{watts}{in^2 \circ K^4}$

NOTE: Above equations obtained from applying least squares method to thermal vacuum test data. The equations represent an approximation of the true solution.

Section III

Ranger VII Mission Evaluation

A. SUMMARY OF RANGER VII MISSION

1. Prelaunch

The prelaunch countdown began during the early morning of July 28, 1964. Approximately 3 hours before launch, the Television Subsystem was turned on in the reduced-power mode for a final system check. Telemetry and video indications were normal at this time. The countdown continued, and at launch minus 25 minutes, cruise-mode telemetry was turned on. The telemetry data, evaluated by both the ETR launch team and the System Data Analysis Team at the Space Flight Operation Facility in Pasadena, California, indicated that all assemblies of the TV Subsystem were functioning normally.

2. Launch

The Ranger VII Spacecraft was successfully launched from the Eastern Test Range (ETR) at 16:50:08 GMT on July 28, 1964. The launch was accomplished by an Atlas-Agena launch vehicle. The complete Ranger VII Mission Events List is presented in Table 10. At launch, the umbilical cable was disconnected from the launch vehicle, removing the full-power-inhibit circuit, which permitted only a reduced-power output of approximately 125 milliwatts from the TV Subsystem. TV Subsystem telemetry data was received by SDAT from the ETR during the first few minutes of launch. It was approximately 24 hours after lift-off before the ETR down-range data was available and evaluated. This data confirmed that the TV Subsystem parameters were normal during the entire launch phase.

The tracking station at Johannesburg, South Africa, acquired the spacecraft approximately 31 minutes after launch and started sending telemetry data to SDAT. The spacecraft entered the Earth's shadow at approximately the time of Johannesburg acquisition, where it remained for 39 minutes. The temperature sensors located on the external shrouds of the TV Subsystem indicated the resulting decrease in temperature during this time.

3. Cruise Mode

Agena-booster separation occurred at L + 32.5 minutes and generated a command to the TV Subsystem Clock to start its 67-3/4 hour count. Clock turn-on was verified four seconds later on cruise-mode telemetry. Agena-booster separation also provided a backup for the removal of the full-power-inhibit circuit, and started a mechanical timer which provided backup functions for the spacecraft. One of these functions was to provide a circuit which would enable the SCR gates in the TV Subsystem High-Current Voltage Regulators at separation plus 30 minutes. Approximately 43 seconds prior to start of the mechanical timer, the Spacecraft solar panels were deployed and activated a microswitch which provided the initial arming of the SCR gates. At L + 75 minutes, Spacecraft acquisition of the sun was accomplished, and 2 hours and 39 minutes later Earth acquisition occurred. Thus, the spacecraft was oriented in its normal cruise-mode position, with the z-axis pointing toward the sun and high-gain antenna pointing toward the earth. The 15-point telemetry continued to indicate normal performance with the 8- and 16-hour Clock telemetry steps occurring at their predicted times. Mid-course maneuver was initiated at approximately L + 17 hours. The channel-8 telemetry was placed into Mode II for 13 minutes and 58 seconds during the mid-course maneuver. While in this mode the 15-point telemetry data from the

TABLE 10
RANGER VII MISSION EVENTS LIST

Mission Event	Event Time (GMT)		Nominal Mission Time
	Actual	Predicted	
Day 210			
1. Cruise Mode On	13:44:00		L-116'
2. Reduced Power On	13:52:18		L-109'
3. TV Subsystem Off	13:54:26		L-106'
4. Cruise Mode On (special test during hold)	15:11:22		L-60'
5. Cruise Mode Off	15:15:23		L-60'
6. Cruise Mode On (final turn-on before launch)	16:25:25		L-15'
7. Launch (L)	16:50:08	16:50:00	L + 0
8. Shroud Ejection	16:55:13		
9. ETR-DSIF-71 Lost Lock (Spacecraft over horizon)	16:57:49		
10. Spacecraft Entered Earth's Shadow	*17:21	17:21:00	
11. DSIF-59 Acquired Spacecraft	17:21:01		
12. DSIF-51 Acquired Spacecraft	17:21:38		
13. Spacecraft/Agena Separation(S) (Mark-12)	17:22:36		S + 0
14. TV Electronic Clock-Start Indication	**17:22:40	17:22:36	S + 0
15. DSIF-51 and 59 Lost Lock (over horizon)	17:32:00		
16. DSIF-41 Acquired (one-way lock)	17:35:24		

*Approximate times, no definite indication of event.
**Tolerance is +0 seconds; −15 seconds.

TABLE 10
RANGER VII MISSION EVENTS LIST (Continued)

Mission Event	Event Time (GMT)		Nominal Mission Time
	Actual	Predicted	
Day 210 (Cont.)			
17. DSIF-41 Acquired (two-way lock)	17:38:48		
18. TV Subsystem SCR Gates Armed (Solar-Panel Microswitch)	*17:51:17		L + 61'
19. TV Subsystem SCR Gates Armed (Hydraulic Timer Backup)	*17:52:00		S + 30'
20. Spacecraft Exited Earth's Shadow	*18:00:00		
21. Spacecraft Acquired Sun	18:05:00		L + 100'
22. Spacecraft Acquired Earth	20:44:00		L + 241'
23. End of DSIF-41 Track Period and Start of DSIF-51 Track Period	21:57:00		
Day 211			
24. TV Electronic Clock 8-Hour Pulse	**01:22:40	01:22:40	S + 8 Hr.
25. End of DSIF-51 Track Period and Start of DSIF-12 Track Period	06:55:00		
26. TV Electronic Clock 16-Hour Pulse	**09:22:40	09:22:40	S + 16 Hr.
27. Start Midcourse Maneuver	10:00:39		M + 0
28. Mode II Telemetry on Channel 8	10:16:43	10:16:43	
29. Mode III Telemetry on Channel 8	10:30:40	10:30:39	M + 30'

*Approximate times, no definite indication of event.
**Tolerance is + 0 seconds; −15 seconds.

TABLE 10
RANGER VII MISSION EVENTS LIST (Continued)

Mission Event	Event Time (GMT)		Nominal Mission Time
	Actual	Predicted	
Day 211 (Cont.)			
30. Spacecraft Reacquired Sun	10:36:00		M + 60'
31. Spacecraft Reacquired Earth	10:58:39		M + 88'
32. TV Electronic Clock 24-Hour Pulse	**17:22:40	17:22:40	S + 24 Hr.
33. End of DSIF-12 Track Period and Start of DSIF-41 Track Period	18:37:00		
Day 212			
34. TV Electronic Clock 32-Hour Pulse	**01:22:37	01:22:40	S + 32 Hr.
35. End of DSIF-41 Track Period and Start of DSIF-51 Track Period	01:46:00		
36. End of DSIF-51 Track Period and Start of DSIF-12 Track Period	07:18:00		
37. TV Electronic Clock 48-Hour Pulse	**17:22:31	17:22:40	S + 48 Hr.
38. End of DSIF-12 Track Period and Start of DSIF-41 Track Period	17:55:00		
39. End of DSIF-41 Track Period and Start of DSIF-51 Track Period	22:39:00		
Day 213			
40. End of DSIF-51 Track Period and Start of DSIF-12 Track Period	07:36:00		

*Approximate times, no definite indication of event.
**Tolerance is + 0 seconds; −15 seconds.

TABLE 10
RANGER VII MISSION EVENTS LIST (Continued)

Mission Event	Event Time (GMT)		Nominal Mission Time
	Actual	Predicted	
Day 213 (Cont)			
41. TV Electronic Clock 64-Hour Pulse	**09:22:23	09:22:26	S + 64 Hr.
42. RTC-8 Initiated (Maneuver Inhibit Command)	11:55:00	11:55:00	
43. RTC-6 Initiated (Terminal Maneuver)	12:25:08	12:25:08	
44. CC&S Counter Started (C=0)	12:25:48	12:25:47	C + 0
45. Data Encoder Switched to Mode IV Telemetry	12:52:19		
46. Clock Turn-on of F-Channel (90-Pt Telemetry Received on Channel 8)	13:07:15	13:07:19	S + 37-3/4 Hr.
47. F-Channel in Full Power	13:08:35	13:08:35	
48. CC&S Warmup Command (P-Channel in Warmup)	13:10:49	13:10:48	C + 45'
49. P-Channel in Full Power	13:12:09	13:12:09	
50. CC&S Full-Power Command (Backup)	13:15:48	13:15:48	C + 50
51. Impact	13:25:49	13:25:49	

*Approximate times, no definite indication of event.
**Tolerance is + 0 seconds; −15 seconds.

TV Subsystem was interrupted so that propulsion and attitude control information would be available on the Channel-8 telemetry.

With motor burn complete, Channel-8 telemetry was stepped to Mode III returning this channel to the TV Subsystem's 15-point telemetry. When TV telemetry data was returned to Channel 8, the -y axis shroud temperature had decreased 10° F and the F_a Camera lens temperature had increased 12° F, indicating that the +y axis of the TV Subsystem was oriented toward the Sun during the midcourse maneuver. At the end of midcourse maneuver, the spacecraft was reoriented in its normal cruise-mode position, and 4 hours later the temperatures of the TV Subsystem had returned to their premidcourse values.

The 24- and 32-hour Clock telemetry steps occurred on time. At the time of the 32-hour step, the Clock also provided an output signal, which removed the Clock-output inhibit and the RTC-5 Clock-turn-off inhibit. Forty hours after launch, the TV Subsystem temperatures stabilized at the following values:

- F_a Camera Lens 66° F
- P-Channel Battery 75° F
- Top Hat (shroud) 82° F
- Lower Shroud 74° F
- F_b Camera Electronics 68° F

The 48- and 64-hour Clock telemetry steps occurred early, by 9 and 17 seconds, respectively. This indicated that the Clock was running fast but still well within its 5-minute overall tolerance. At this time, analysis of the Battery capacities and temperatures indicated that the F- and P-Channels could operate in the full-power mode for 56 and 37 minutes, respectively; the limiting factor being temperature.

4. Terminal Mode

Trajectory information revealed that the television cameras were properly oriented so that no terminal maneuver was required. Thus, an RTC-8 command was sent to inhibit the terminal maneuver, and then an RTC-6 command was sent to start the CC&S counter in the spacecraft, which supplies the warm-up (turn-on) and backup full-power commands to the TV Subsystem. The terminal sequence of events began with turn-on of the CC&S counter one hour before impact. The spacecraft Data Encoder switched to Mode IV telemetry 26.5 minutes later, indicating that the CC&S counter was operating. At 13:07:15 GMT, the TV Subsystem Clock turned on the F-Channel to warm-up mode and 90-point diagnostic telemetry was transmitted over Channel 8. Eighty seconds after the Clock turn-on pulse occurred, the TV Subsystem sequencer commanded F-Channel into full-power operation. At this time, strong F-Channel video signals were received by the Goldstone tracking station. Approximately 3 minutes after the turn-on of the F-Channel, the spacecraft CC&S commanded the P-Channel into warm-up mode, and 80 seconds later the TV Subsystem Sequencer placed the P-Channel in full-power operation. From this time until impact, both TV channels transmitted video pictures of the lunar surface. F-Channel operated for 17 minutes and 14 seconds, and P-Channel for 13 minutes and 40 seconds.

B. EVALUATION OF REAL-TIME DATA

1. General

TV Subsystem telemetry provided diagnostic information on the important Subsystem parameters so that any necessary, real-time adjustments could be made to correct or improve Subsystem performance, and in the event of a failure, an analysis could be made of the telemetry data to isolate the cause. A PAM/FM/FM* system was employed to monitor 104 parameters of the TV Subsystem. Telemetry data was transmitted by the TV Subsystem's two high-power Transmitters on a 225-kc subcarrier, and by the spacecraft's low-power Transmitter on an IRIG** Channel-8 3-kc subcarrier. Channel 8 was the prime data link. During cruise mode, a 15-point commutator sampled eleven Subsystem parameters and four telemetry references in the TV Subsystem. When either F- or P-Channel of the TV Subsystem is turned on into the warm-up mode, the cruise-mode telemetry data is switched off of Channel 8 and the diagnostic telemetry sampled by a 90-point commutator is transmitted over Channel 8. The format for the 90-point commutator is the same as for the 15-point commutator, except additional parameters are sampled. As a backup function, the 90-point commutator also modulates a 225-kc voltage controlled oscillator

*PAM/FM/FM: pulse amplitude modulated/frequency modulated/frequency modulated

**IRIG: Intra Range Instrumentation Group.

(VCO) whose output is transmitted over the P-Channel high-power Transmitter. Likewise, the telemetry data from the 15-point commutator is switched to and transmitted over the F-Channel high-power transmitter on a 225-kc subcarrier.

2. SDAT Data Accuracy (Computer Output)

In order to establish the accuracy of the various data stations, telemetry data point 15-9 (the Clock pulse) was selected as a reference and its incremental change was noted. The following variations were noted:

- Woomera variations averaged 0.3 volt;
- Goldstone variations averaged 0.12 volt; and
- Johannesburg variations averaged 0.3 volt.

Telemetry data from the Woomera, Goldstone, and Johannesburg tracking stations were plotted as minimum and maximum values sampled every hour during spacecraft view periods. Cruise-mode telemetry data from all tracking stations were further analyzed and compared. Telemetry data from Johannesburg were reading lower than the data from the other stations; the Clock pulse telemetry (15-9) was 200 millivolts lower, LCVR telemetry (15-2) was 100 millivolts lower, and lower-shroud temperature telemetry (15-8) was 100 millivolts lower.

3. Transition from Cruise-Mode to Terminal-Mode Telemetry

When terminal-mode operation occurred, 90-point telemetry was transmitted over Channel 8. The terminal-mode (90-point) telemetry included data on the same telemetry points sampled by the cruise-mode (15-point) telemetry and thus provided a basis of reference for determining the consistency of the telemetry readouts.

When the P-Battery voltage (data point 15-6) was readout as data point 90-59, the Primary Data Processor indicated an inconsistency of at least 0.1 telemetry volt in the readouts. In order to ascertain the source of this apparent inconsistency, the hard-line, semi-raw telemetry data from the Goldstone (DSIF-12) tracking station was reviewed. The zero-reference telemetry point was found to have increased from 115 data units as data point 15-13 to 131 data units as data point 90-88 in the terminal-mode telemetry. The full-scale-reference telemetry point (90-35) was also found to be erratic for the first six data points, so the alternate full-scale-reference telemetry point (90-87) was used to establish the gradient for interpreting the terminal-mode telemetry; the full-scale reference was found to have increased from 572 data units as data point 15-12 to 587 data units as data point 90-87. However, the data point in question (P-Battery voltage) increased from 526 data units as data point 15-6 to 556 data units as data point 90-59, a total of 30 data units or approximately 0.150 telemetry volts beyond the previously mentioned increase. The prelaunch tests of July 27, 1964, showed that full-scale reference averaged 573 data units as data point 15-12 and increased to an average value of 590 data units as data point 90-35/87, an increase of 17 data units.

Since the data-converter granularity is one order of magnitude smaller than the error, it would have to be a cumulative effect of programming combined with system noise to account for the entire increase of 30 units for the P-Battery voltage. In order to establish the semi-raw value for a particular data point, the raw pedestal values were sampled on either side of the data point to obtain an average "base band"; this was then subtracted from the raw-data-point value. This amount of programming would not have contributed a change of 30 units, and hence it must be concluded that the overall accuracy at this point is limited to 150 millivolts of telemetry (i.e., ±75 millivolts).

4. Telemetry Evaluation of TV Subsystem Performance

The cruise-mode telemetry was employed to monitor the TV Subsystem temperatures and power-supply operation. The temperatures during cruise and terminal mode were almost exactly as predicted in preflight calculations. Graphs typical of the actual and predicted cruise-mode temperatures are presented in Figures 17 and 18. Typical terminal-mode temperatures are plotted in Figures 19 and 20.

The TV Subsystem power supply consisted of a Battery and a High-Current Voltage Regulator (HCVR) for each of the F- and P-Channels, and a Low-Current Voltage Regulator (LCVR) on the P-Channel only. The power-supply units functioned normally throughout the mission. Figure 21 shows the budgeted and actual ampere-hour Battery capacity for each channel during the various phases of the Ranger VII Mission. The total capacity budgeted for the F-Battery was 27.0 ampere-hours, while the actual capacity expended was 12.8 ampere-hours. The F-Battery voltages during cruise mode are shown in Figure 22. The F-Battery voltages at launch, under a no-load condition was 39.1 volts. From Clock start (L + 32.5 minutes) until F-Channel turn-on, the F-Battery supplied 0.05* ampere to operate the TV Subsystem Clock. After the initial Battery-voltage drop to 37.4 volts at Clock start, the F-Battery voltage gradually decreased during cruise mode to 34.6 volts. At the start of F-Channel warm-up, the Battery voltage dropped to 33.5 volts at 7.7 amperes and finally to 32.5 volts at 13.5 amperes during full-power operation. (See Figure 25.)

For the P-Channel, the budgeted and actual Battery capacities were 30.0 and 21.0 ampere-hours, respectively. The P-Channel Battery, which powered the cruise-mode telemetry circuits (0.15 ampere*), had a prelaunch voltage of 35.6 volts, and at 16 hours after launch reached a plateau voltage of 34.4 volts and remained at this voltage until P-Channel warm-up (see Figure 23). The P-Battery voltages and currents were 32.5 volts at 10.5 amperes and 32.0 volts at 15.5 amperes in warm-up and full-power modes, respectively.

Both F- and P-Battery voltages remained constant throughout the terminal mode, full-power operation (see Figures 25 and 26).

The Low-Current Voltage Regulator (LCVR) supplied an output voltage of 27.70 volts during cruise-mode (Figure 24) and 27.78 volts during terminal-mode operation. The reason for the rise during terminal mode was that the Telemetry Power Supply assumed part of the load (see Figure 27). Both the F- and P-Channel High-Current Voltage Regulators performed as expected. Their output voltages were 27.52 and 27.50 volts for the F- and P-Channels, respectively, as shown in Figure 28.

At the start of F-Channel warm-up, the 90-point diagnostic telemetry data was switched onto Channel 8. A listing of the terminal telemetry parameters is given in Table 11. The signal profile from the full-power command telemetry points (55 and 60) indicated that both channels went into warm-up mode for 80 seconds and were then turned on into full-power operation by the TV Subsystem Control Programmer and Camera Sequencer. The Transmitter telemetry data indicated normal supply voltages and operating temperatures for both channels. The Power Amplifier cathode-current profiles for the Transmitters were almost identical to prelaunch full-power tests confirming a high-power output for both channels. All telemetry indications for the TV Camera assemblies, which included four partial-scan cameras, Video Combiner, and Control Programmer and Camera Sequencer for the P-Channel, and two full-scan cameras, Video Combiner, and Control Programmer and Camera Sequencer for the F-Channel, were normal.

*These values are based on prelaunch measurements as the cruise-mode telemetry was not sensitive enough to read less than 0.2-ampere changes.

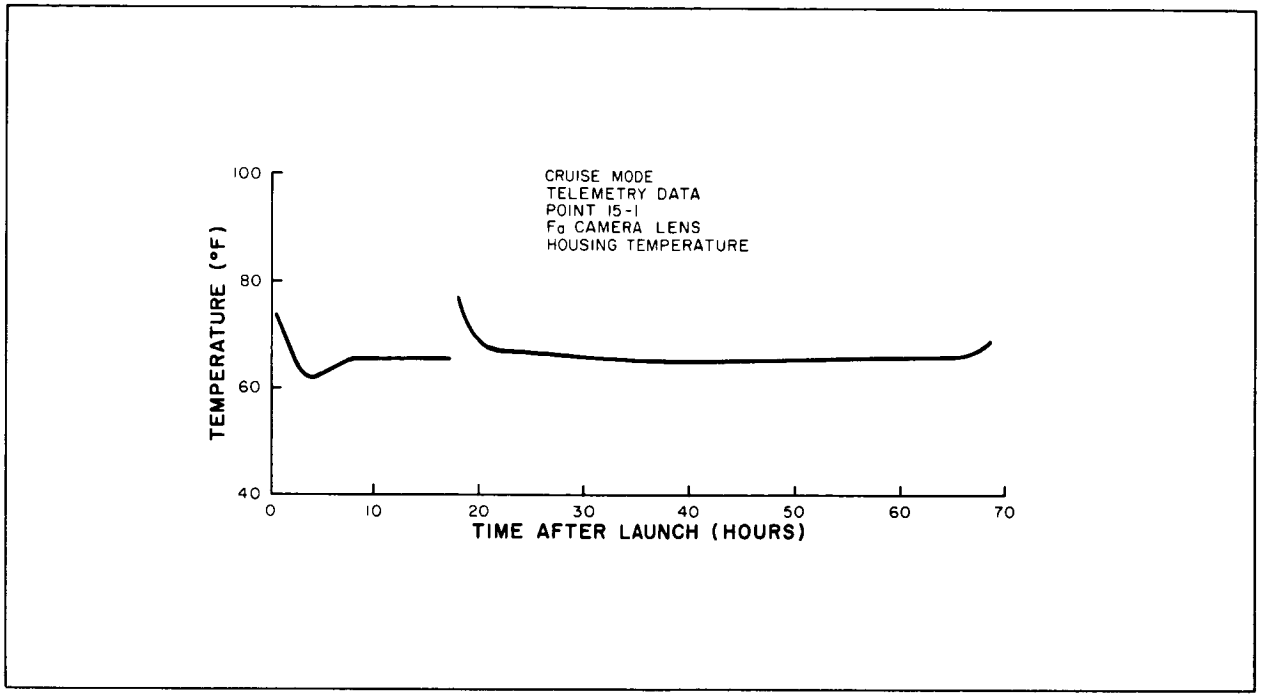

Figure 17. Ranger VII Actual F_a-Camera Lens Housing Temperature during Cruise Mode

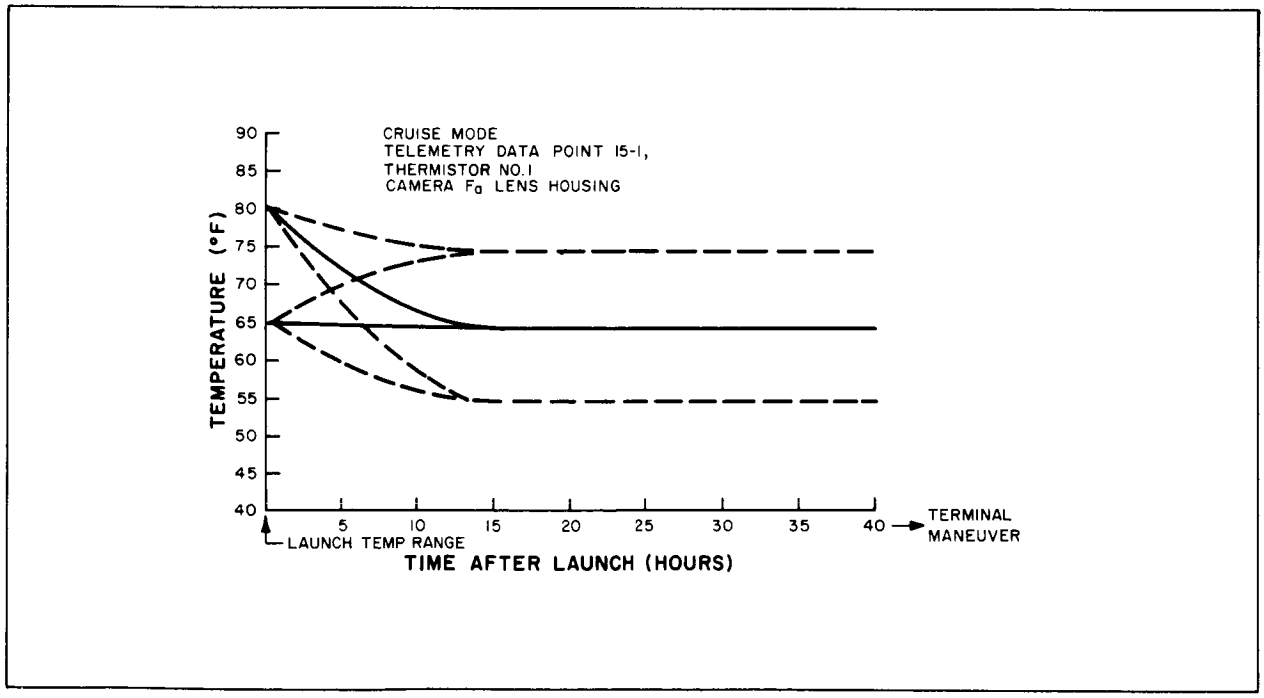

Figure 18. Ranger VII Predicted F_a-Camera Lens Housing Temperature during Cruise Mode

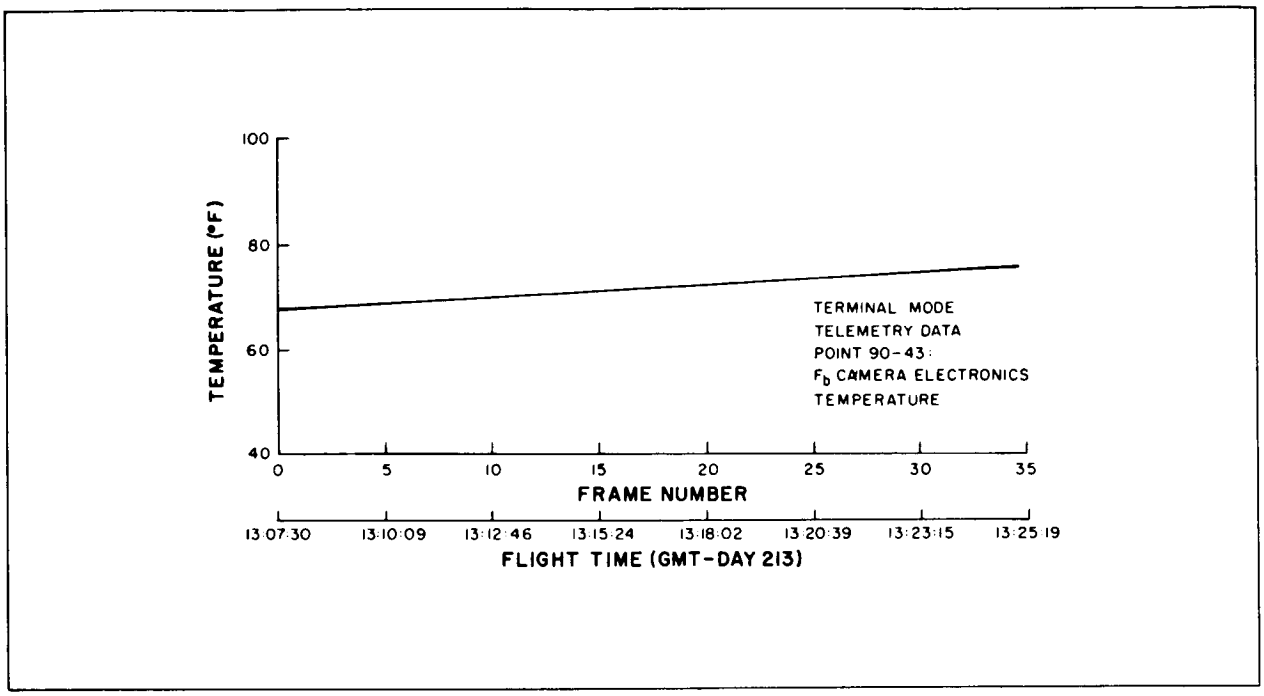

Figure 19. Ranger VII Actual F_b-Camera Electronics Temperature during Terminal Mode

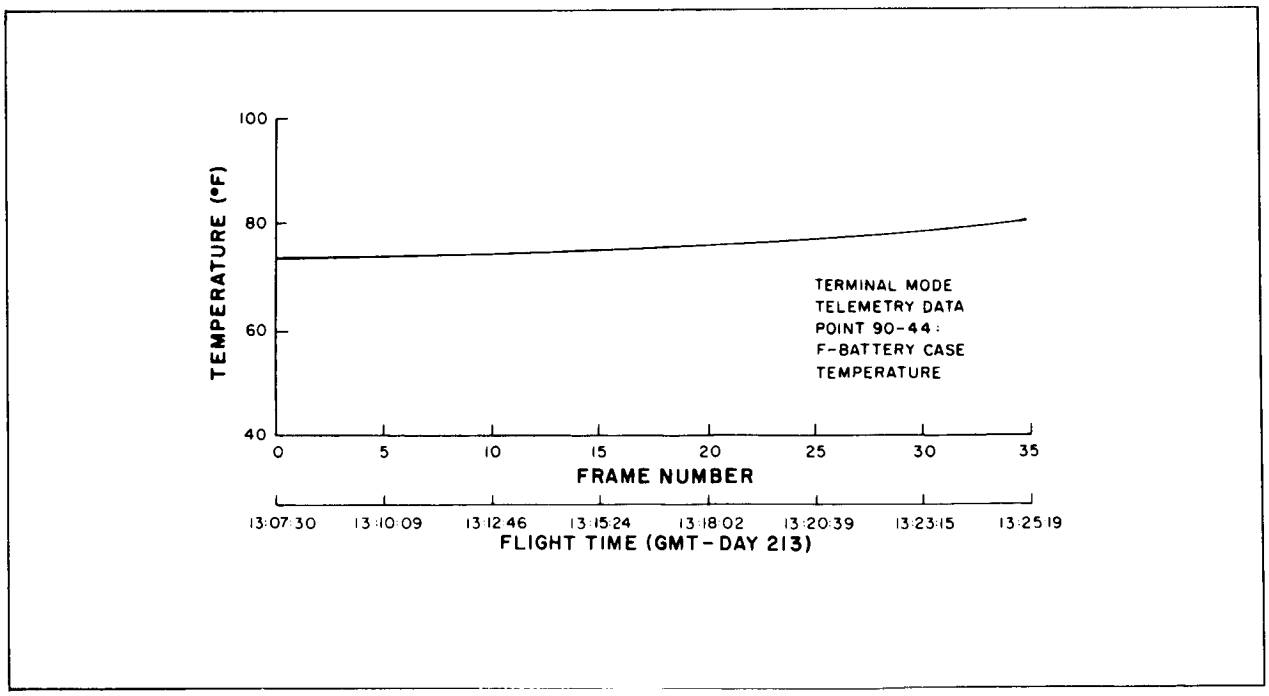

Figure 20. Ranger VII Actual F-Battery Case Temperature during Terminal Mode

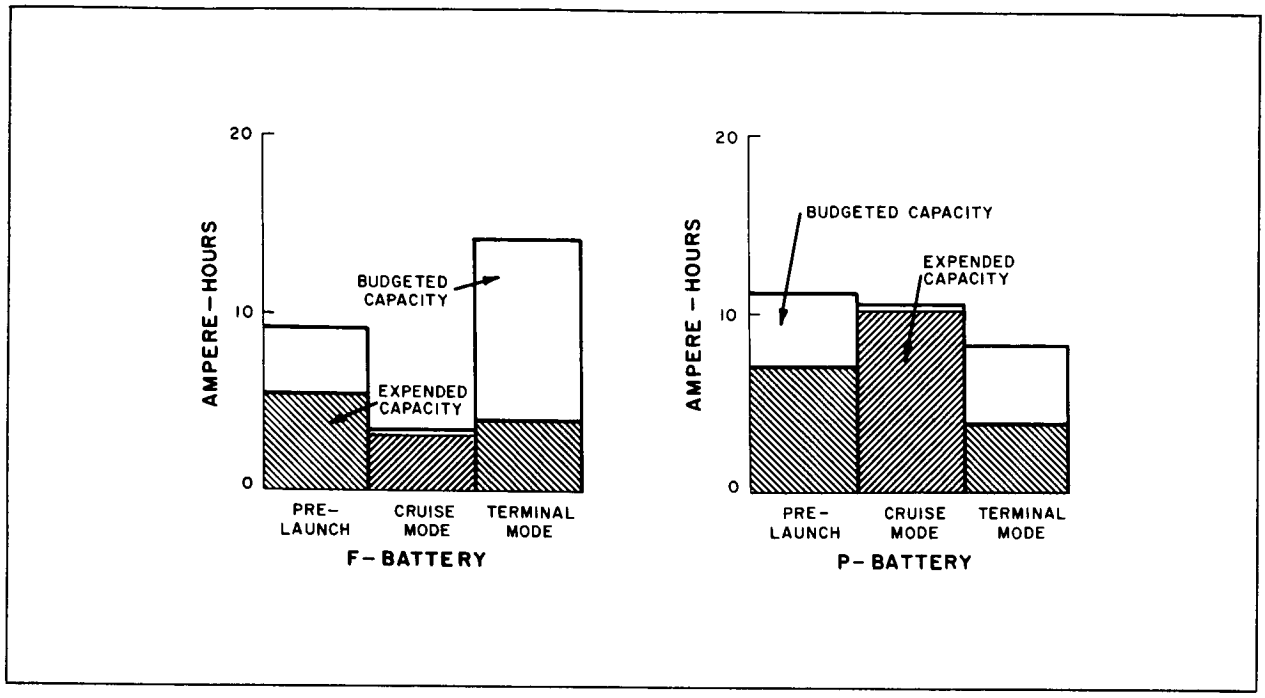

Figure 21. Ranger VII F- and P-Channel Budgeted and Actual Battery Capacities

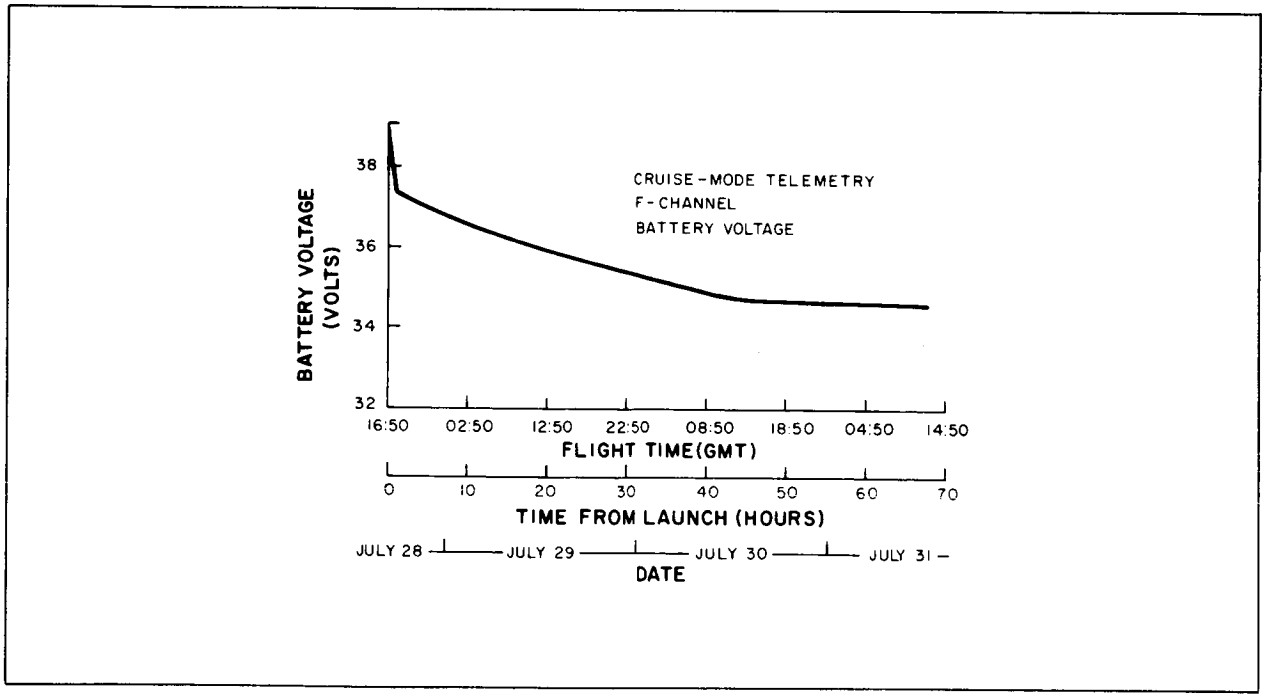

Figure 22. Ranger VII F-Channel Battery Voltage during Cruise Mode

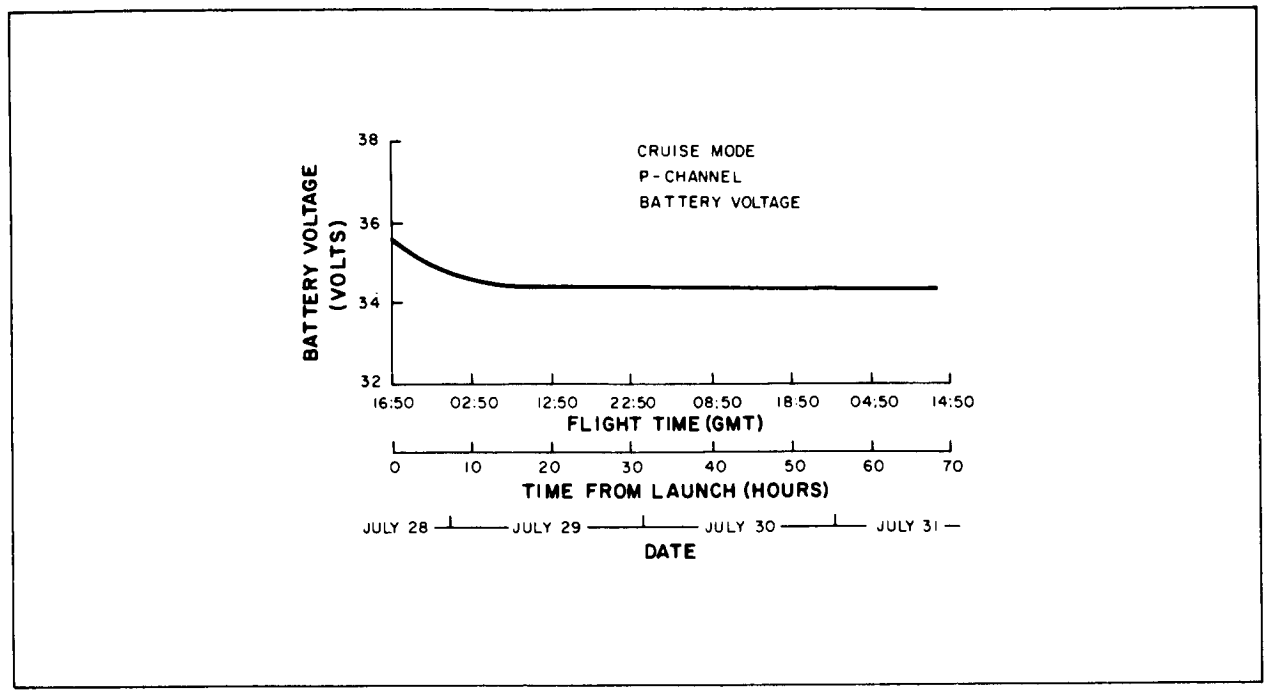

Figure 23. Ranger VII P-Channel Battery Voltage during Cruise Mode

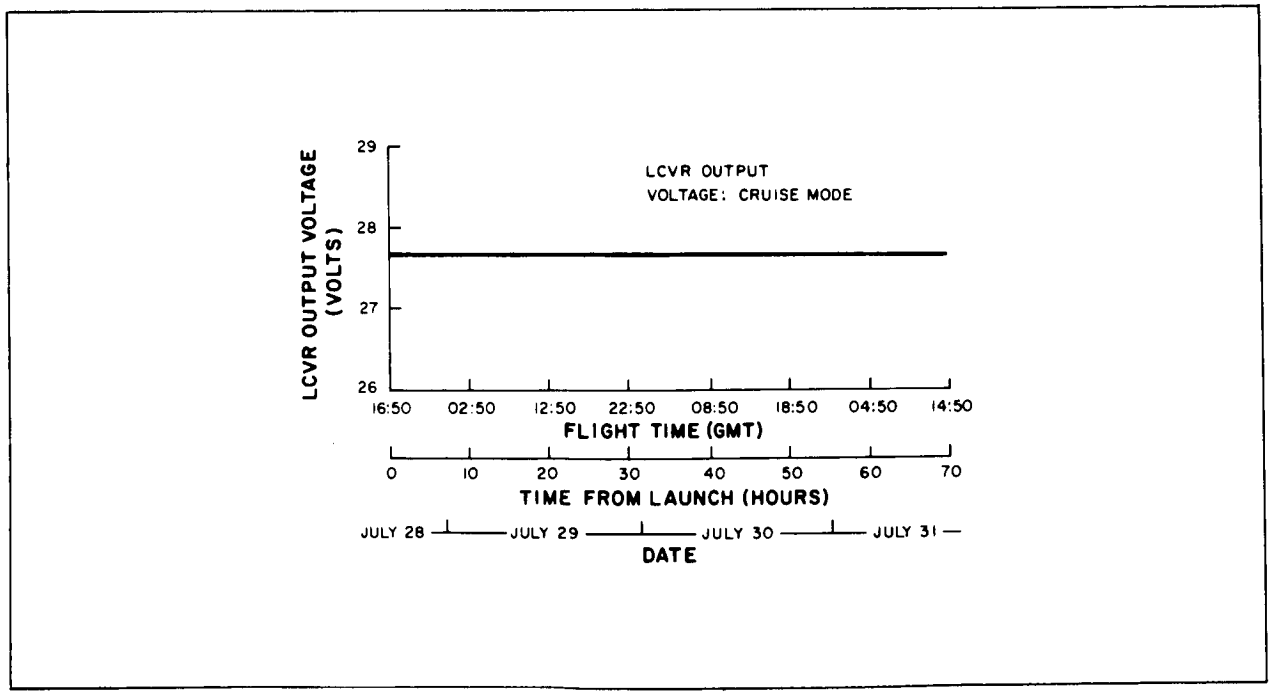

Figure 24. Ranger VII Low-Current Voltage-Regulator Output during Cruise Mode

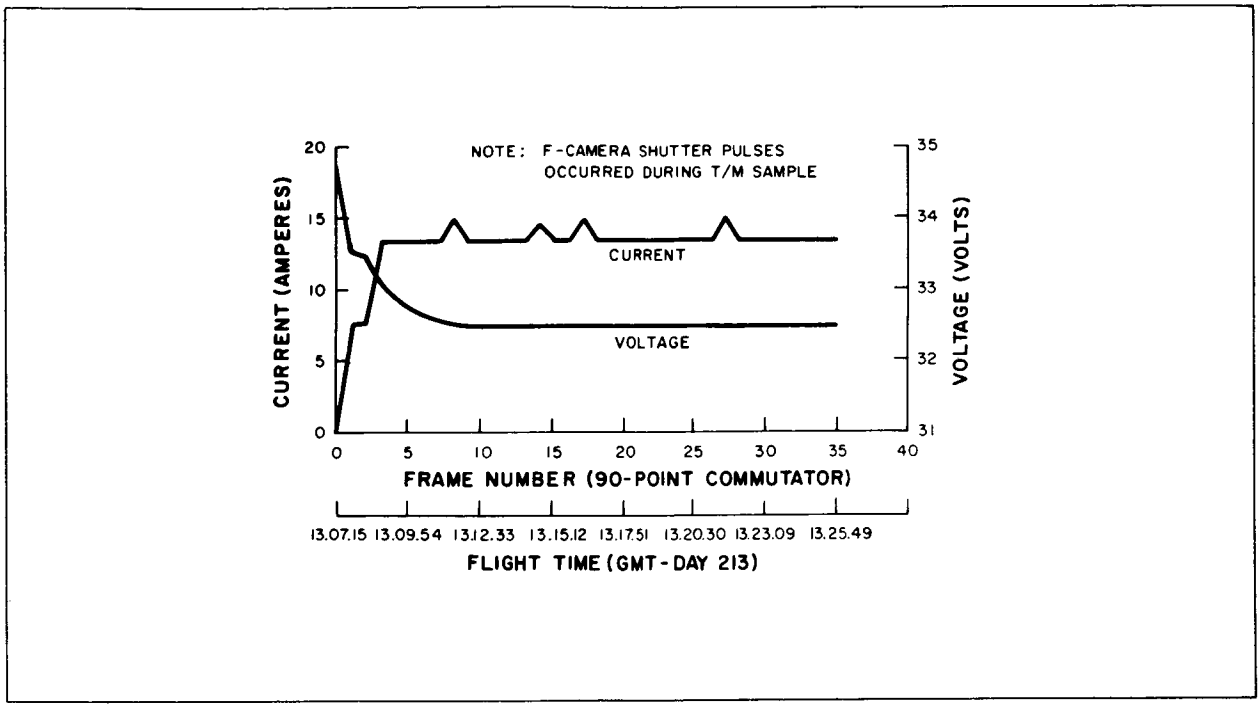

Figure 25. Ranger VII F-Channel Battery Voltage and Current during Terminal Mode

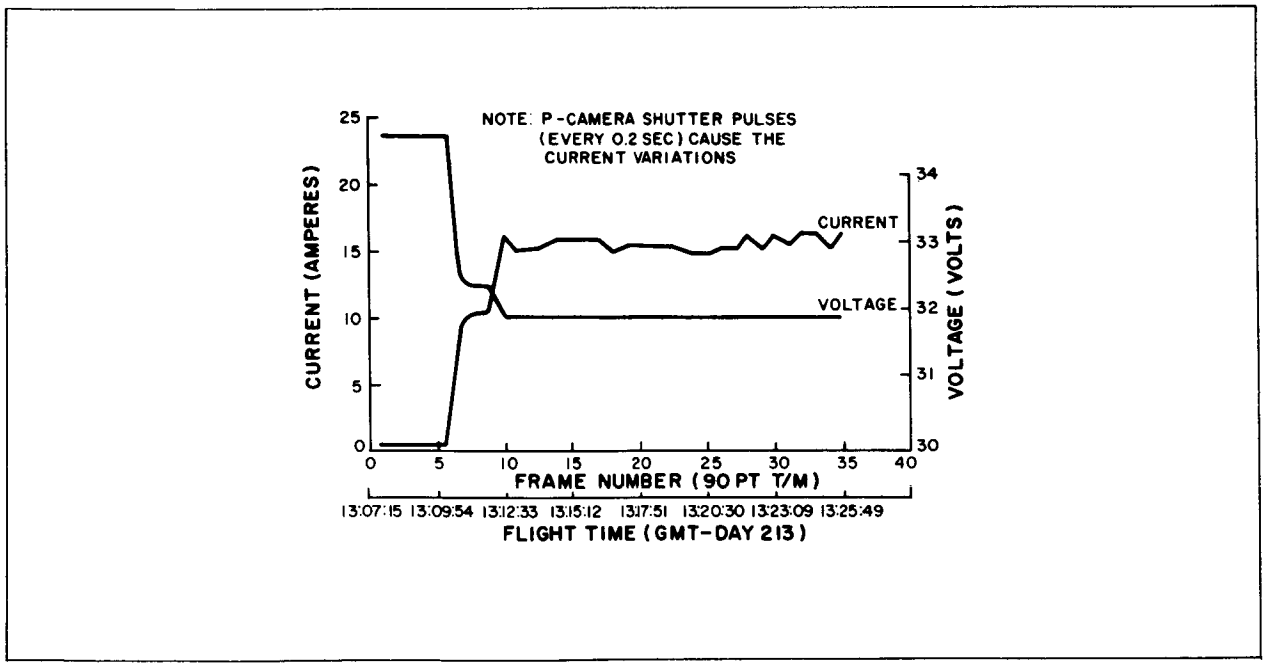

Figure 26. Ranger VII P-Channel Battery Voltage and Current during Terminal Mode

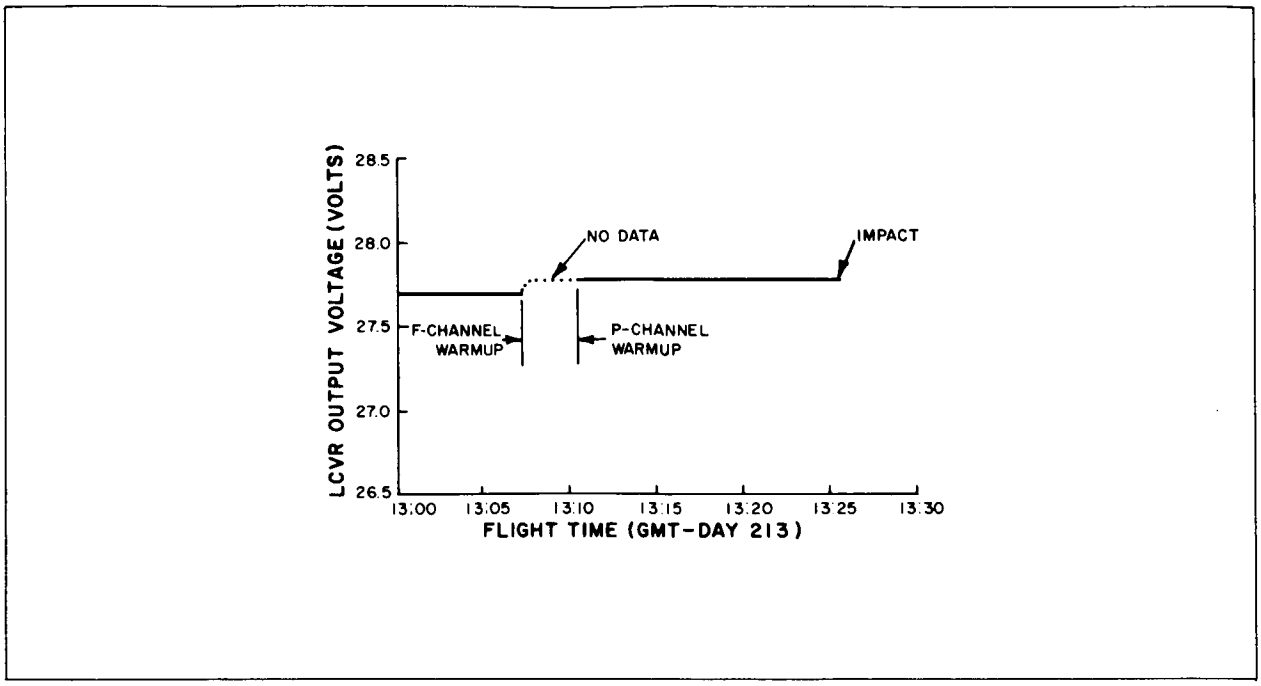

Figure 27. Ranger VII Low-Current Voltage-Regulator Output during Terminal Mode

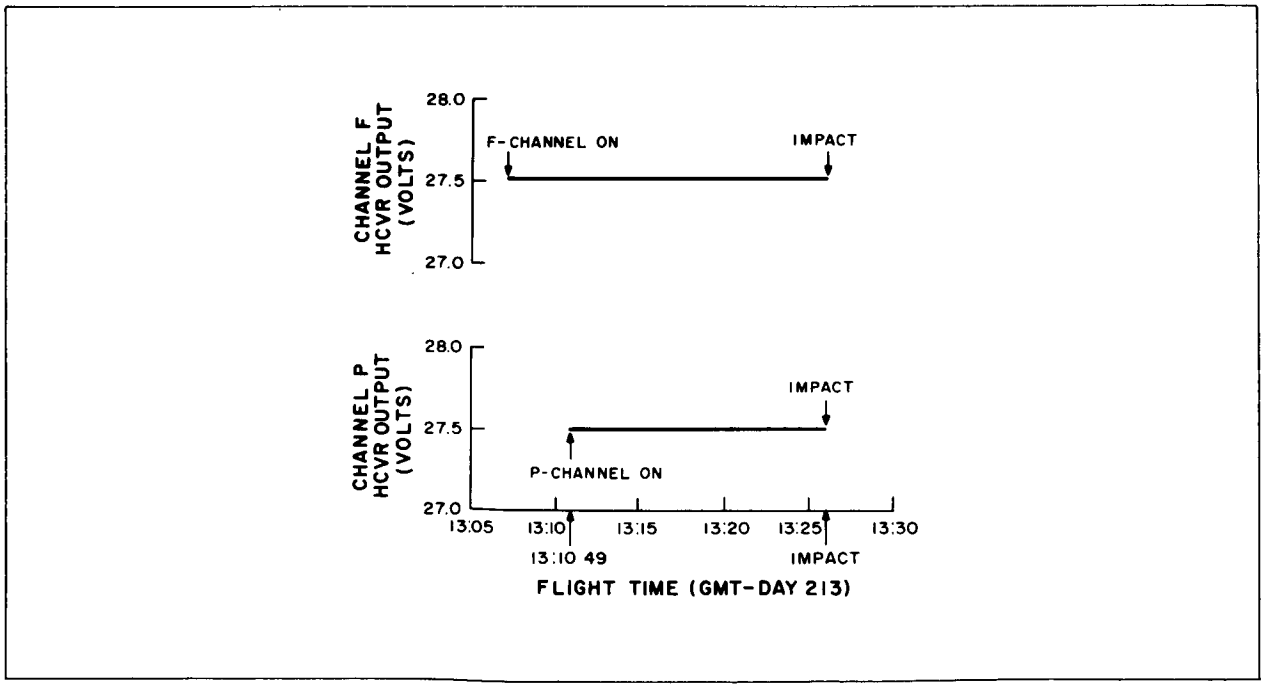

Figure 28. Ranger VII F- and P-Channel High-Current Voltage-Regulator Outputs during Terminal Mode

The telemetry data for the F-Channel Video Combiner output shown in Figure 29, indicated that the video output was greater than expected. This telemetry point (data point No. 72 of the 90-point telemetry) measures the amplitude of the composite video signal at the video combiner output, which has a range of 1.5 volts from sync tip to peak white for each camera, and is used only to indicate that a video signal is being applied to the modulator input. Its use as a light meter is quite limited because it monitors two cameras that have a four-to-one difference in their dynamic ranges and the data sample was not synchronized with the camera readouts.

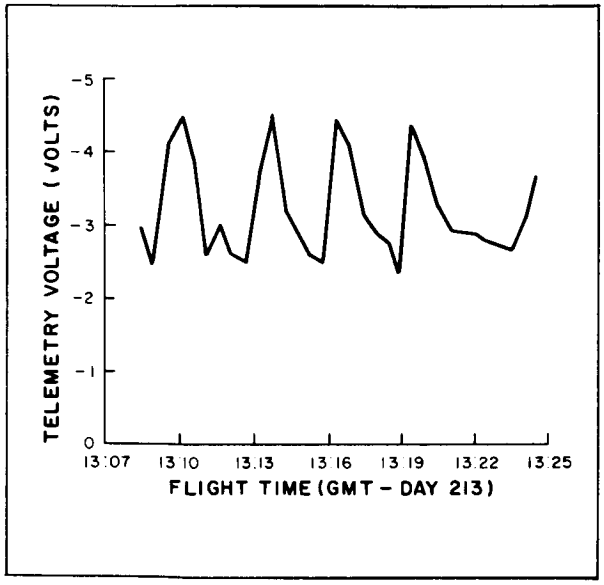

Figure 29. Ranger VII F-Channel Video-Combiner Output during Terminal Mode

The performance of the TV Subsystem telemetry was nominal throughout the mission. A slow shift in center frequency of the Channel-8 VCO was noted, which amounted to only one or two cycles and was within the ±2-cps VCO tolerance. The 90-point commutator stopped on data point 69 at the end of the prelaunch test and started on the same point at terminal mode, signifying no movement of the commutator during cruise mode. Thus, it may be concluded that the telemetry verified that the TV Subsystem performed a nominal mission.

5. Operational Support Equipment

a. FILM RECORDER CALIBRATION PROCEDURE

(1) General

The function of the Ground Recording Equipment of the Ranger Operational Ground Station at Goldstone was to record on 35-mm film an accurate reproduction of the lunar scene as seen by the TV cameras. All preflight calibrations were made to assure that picture detail and photometric characteristics were reproduced faithfully.

With the test specifications, the equipment was calibrated to obtain sufficient resolution and linearity to preserve the picture detail.

(2) Cathode Ray Tube and High Voltage Power Supply Calibrations

The first step in the Film Recorder Calibration is the designation of mission and backup Cathode Ray Tubes (CRT's) and High-Voltage Power Supplies (HVPS's). At all sites, grid drive as a function of 35-mm density runs were made on the following combinations:

- Mission CRT and Mission HVPS
- Mission CRT and Backup HVPS
- Backup CRT and Mission HVPS

Prior to the mission, a film development gamma was specified and held constant throughout the calibration. Upon initial installation, the lens f-stop was varied and a film record was made of discrete flat-field intensity settings on G1 of the CRT. Succeeding runs verified the results prior to removal of the calibration equipment from the film recorder. Table 12 summarizes the densities measured after a setup of all the camera recorders.

TABLE 11
TV SUBSYSTEM PARAMETERS MONITORED DURING TERMINAL MODE BY 90-POINT TELEMETRY COMMUTATOR

Data Point No.	Parameter Monitored
1	Camera P1 Vertical Sweep
2	Camera P1 Horizontal Sweep
3	Camera P1 G1 and Focus Current
4	Camera P1 +1000 volts and 300 volts
5	Camera P1 Shutter and Lamp Drive
6	Camera P1 Vidicon Filament
7	Zero Reference
8 thru 14	Same as 1 thru 7 except for P2 Camera
15 thru 21	Same as 1 thru 7 except for P3 Camera
22 thru 28	Same as 1 thru 7 except for P4 Camera
29 thru 34	Same as 1 thru 6 except for F_a Camera
35	Full Scale Reference
36 thru 42	Same as 1 thru 7 except for F_b Camera
43	F_b Camera Electronics Temperature (Sensor No. 2)
44	F Battery Case Temperature (Sensor No. 4)
45	P Battery Case Temperature (Sensor No. 5)
46	P Unregulated Bus
47	P Regulated Bus (-27.5 volts)
48	F Unregulated Bus
49	F Regulated Bus (-27.5 volts)
50	Lower Shroud Temperature (+y) (Sensor No. 12)
51	Bottom Deck Temperature (-x, -y quadrant) (Sensor No. 13)
52	Second Deck Temperature (-y) (Sensor No. 14)
53	Second Deck Temperature (+y) (Sensor No. 15)
54	LCVR Input Voltage
55	F-Channel Full-Power Command
56	P Battery Current
57	F Battery Current
58	F Battery Terminal Voltage
59	P Battery Terminal Voltage
60	P-Channel Full-Power Command
61	F Sequencer "T" Flip-Flop (No. 2)
62	Zero Reference
63	F Sequencer Oscillator (18 kc)
64	P Sequencer Voltage +12 volts
65	P Sequencer Voltage -12 volts
66	P Sequencer Oscillator (18 kc)
67	F Sequencer Voltage +12 volts
68	F Sequencer Voltage -12 volts
69	F Sequencer "T" Flip-Flop (No. 1)

TABLE 11
TV SUBSYSTEM PARAMETERS MONITORED DURING TERMINAL MODE BY 90-POINT TELEMETRY COMMUTATOR (Continued)

Data Point No.	Parameter Monitored
70	P Sequencer "R" Flip-Flop (No. 1)
71	P Sequencer "R" Flip-Flop (No. 2)
72	P Combiner Video Output
73	Zero Reference
74	F Combiner Video Output
75	P-Transmitter PA Heat Sink (Sensor No. 6)
76	F Battery Internal Temperature (Sensor No. 8)
77	F Transmitter PA +1000 volts
78	F Transmitter IPA -750 volts
79	F Transmitter PA Cathode Current
80	F Transmitter PA Heat Sink (Sensor No. 7)
81	Zero Reference
82	P Transmitter PA +1000 volts
83	P Transmitter IPA -750 volts
84	P Transmitter PA Cathode Current
85	F_a Camera Lens Housing Temperature (Sensor No. 1)
86	Camera Bracket Temperature (Sensor No. 3)
87	Full Scale Reference
88	Zero Reference
89	Frame Reference
90	Frame Reference

TABLE 12
BLACK AND WHITE DENSITIES FROM FILM RECORDERS NOS. 1 AND 2

Level \ Cameras	P1	P2	P3	P4	F_a	F_b
Black	0.34	0.32	0.37	0.35	0.35	0.32
Peak White	1.72	1.95	1.80	1.90	1.93	1.73

Calibration prior to terminal mode was completed with the following components:

- Film Recorder No. 1, CRT No. 1294 and HVPS No. 1007 (unchanged);
- Film Recorder No. 2, CRT No. 1214, and HVPS No. 1002; and
- Film Recorder No. 3, CRT No. 027, and HVPS No. 1008.

(3) Mission Data

As per the operational procedure, a film record of the Ranger VII camera calibration

data was made immediately following the mission, along with a grid drive, as a function of intensity run. Curves typical of these data are shown in Figure 30.

Camera transfer data from the mission film were not immediately available; however, using the available data, the curves such as those shown in Figure 31 were derived.

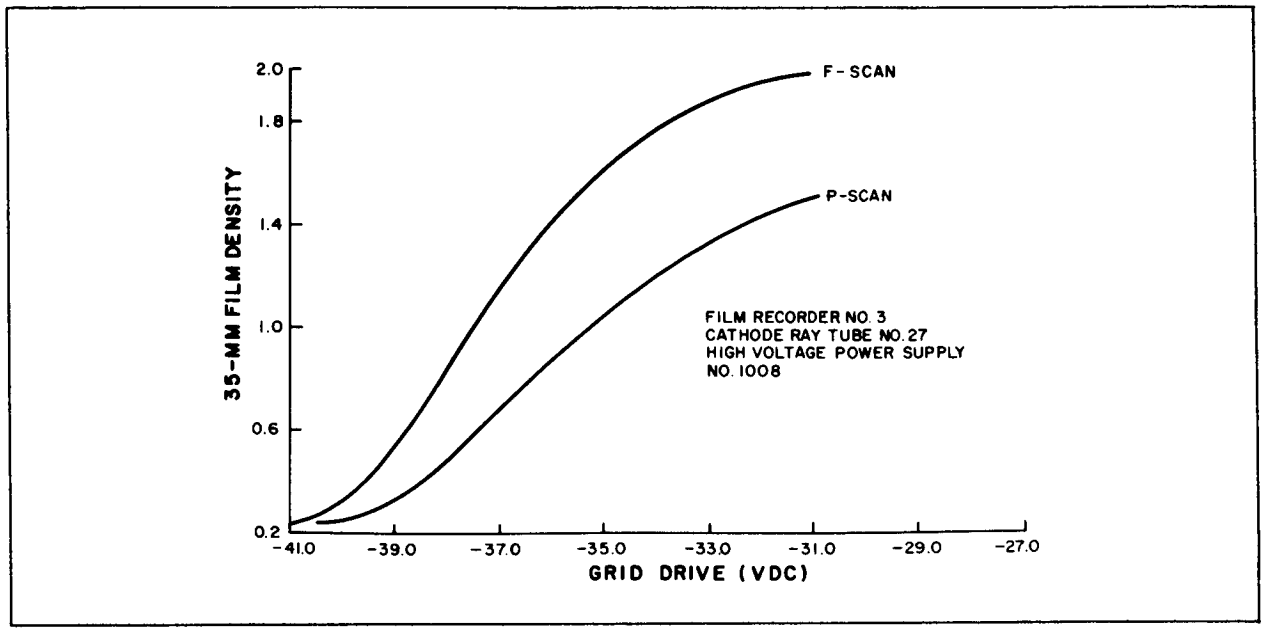

Figure 30. Grid Drive of a Typical Film Recorder as a Function of Film Density after Ranger VII Mission

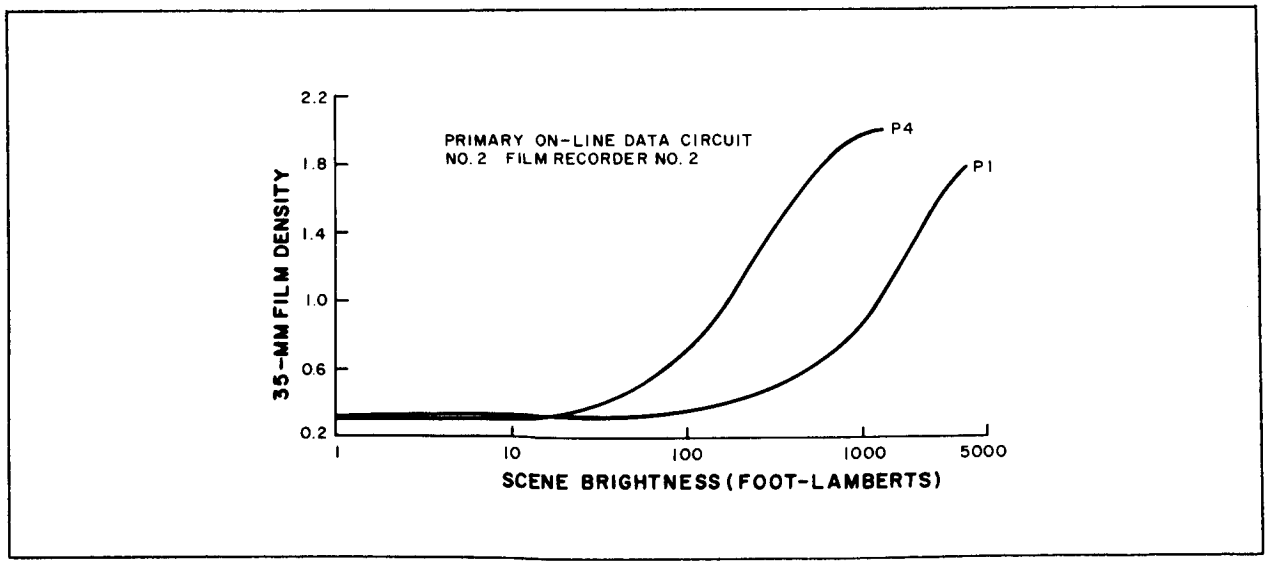

Figure 31. Scene Brightness as a Function of Film Density for a Typical Film Recorder

b. MISSION OPERATION OF TELECOMMUNICATIONS

(1) Power Output During Terminal Mode

The telemetry information for the Power-Amplifier cathode current indicated a normal power output and power profile.

The peak-to-peak noise on the sync tip was approximately 30 to 40 mv, which is equivalent to a 42 to 40 db peak-to-peak to rms noise ratio. A signal-to-noise ratio of 39 db was expected for a normal mission.

(2) Frequency Stability During Mission

The center frequency of each channel during the Ranger VII mission was determined. The F-Channel DC level, detected within 2 minutes of full-power operation, was approximately 100 mv higher than normal, which corresponds to center-frequency variation of plus 35 kc. During the mission, the center frequency remained within 5 kc of this value up to impact. During system test, the center frequency was approximately 20 kc high, and on the launch day, the frequency was 30 to 40 kc high.

The P-Channel center frequency was approximately 17 kc lower than normal at the start of the mission and approximately 25 kc low at impact. During final check on the launch pad, the center frequency was approximately 10 kc high.

(3) Deviation

The nominal voltage between the sync tip and the black level is 240 mv ±10 percent. This voltage was approximately 220 mv for the F_a Camera, 240 mv for the F_b Camera, and 250 mv for the P-Cameras.

(4) Telemetry

Only the telemetry broadcasted over the F-Channel transmitter was recorded on the strip-chart recorder. There was no noise on the telemetry.

The Channel-8 telemetry had a small amount of noise on the pedestal. However, the noise did not interfere with the data reduction.

C. FLIGHT MODEL III-2 (RANGER VII) EQUIPMENT PERFORMANCE

1. General

The receipt of 4,316 high-quality pictures of the lunar surface from the Ranger VII Spacecraft is indicative of the performance of each group of equipment of the Flight Model III-2 Ranger TV Subsystem. The level of performance of some portions of the TV Subsystem can be evaluated on the basis of specific information received during the mission. This is particularly true of the cameras and their associated electronic equipment, since the pictures themselves are evidence of the performance of this equipment. It is also true to a lesser degree of the telemetry equipment, thermal control equipment, power equipment, telecommunications equipment, and OSE equipment. The performance of the command and control circuitry, however, can only be evaluated in absolute terms; that is, all commands were processed and executed on-time and in good order, as expected.

Paragraph 2 of this subsection discusses the performance of the cameras and their associated electronic equipment. Paragraph 3 of this subsection is devoted to an evaluation of the thermal control equipment and a correlation of the predicted mission temperatures with those actually experienced. The performance of the power equipment, subsystem telemetry equipment, telecommunications equipment, and OSE equipment has been discussed previously in terms of the received telemetry data.

2. Camera Group

a. SATISFACTION OF MISSION REQUIREMENTS

The 35-millimeter photographs and the magnetic tapes of the video signals give ample

evidence that the Flight Model III-2 camera equipment met the mission requirements. The last partial-scan picture was a fragment from the P3 Camera which was outfitted with a one-inch, f/0.95 lens. A line selector was used to determine that the impact occurred on line 167 approximately 400 μs after the start of scan.

Exposure for the camera actually occurred about 80 milliseconds before the end of read-out for the P1 Camera. The total time before impact then is the sum

70	milliseconds during P1 readout
6.6	milliseconds blanking
111	milliseconds of P3 readout
187.6	milliseconds before impact.

A simple geometrical relationship for the 1-inch optical system and for a spacecraft traveling at 2.64 km/sec shows that the final picture was taken at an altitude of 500.0 meters from point of impact on the lunar surface and covered an area about 42 meters by 28 meters. Craters can be recognized that occupy one-fiftieth of picture height, a diameter of 0.8 meter. The bright rim and shadowed rim constitute image elements of 0.4 meter; hence, the mission resolution requirements were easily satisfied.

For the full scan cameras a fragment of a frame of the F_a Camera was the last to be scanned before impact. Video ceased after 350 microseconds on scan line No. 1074.

The mission requirements of wide area coverage and picture nesting were also satisfied. Examination of an image produced by the F_a Camera at an altitude of 480 miles from the Moon shows these two requirements satisfied. This image covers a wide area with several well known features such as the crater Lubiniezky and the Riphaeus Mountains. This image also nests all the remaining sequence of F_a Camera images and records the impact point.

The exposures for both the 76-mm, f/2 cameras and the 25-mm, f/0.95 cameras were such as to provide high signal-to-noise ratios. The peak illuminations appear not to exceed 1800 foot lamberts with average illuminations between 250 and 450 foot lamberts. The variations in exposure were noted and examined.

b. IMAGE DEGRADATION

Image degradation due to smear is difficult to assess from an examination of the images. The final P1 and P3 images are oblique views with the major axes of the elliptical images of the round craters being oriented from lower left to upper right.

Image degradation due to residual images from previous exposures is also difficult to assess. By viewing high-contrast crater images of both the F_a and F_b Cameras during the final 20- to 30-picture sequence, sufficient motion and size-changing of these images occur to attempt an observation of these residuals. The illuminated position of crators for succeeding frames shows a break in the highlight, which may be caused by the residual signal from the previous frame. A cautionary note is extended to the photo interpreters to consider this possibility when evaluating the craters for shadow detail.

There is evidence of coherent noise in the images, however, at a decidedly reduced level from prelaunch system tests. The F_a Camera shows the 15-kilocycle crosstalk from the F_b Camera erase raster. It is more evident in Camera F_b. There are two permanent spots of a detail near the size of the smallest recognizable crater in each full-scan camera. They can be detected as black and white spots with the black opposite to the normal crater shadowing. There is also evidence of four kinescope spots which appear as four tiny white spots on each image. In the F_a Camera pictures, there is evidence of shadowing at top left and bottom left of each image which is

typical of shading in the vidicon electron optics, or possibly of lens vignetting.

In the F_a Camera pictures, there are a few images that show evidence of the 12 to 13 nearly evenly spaced disturbances that are characteristic of microphonics excited by partial-scan camera shutter actuations. The Camera F_b pictures show evidence of a loss of a line or lines of video in occasional frames. This is due to the clamp acting upon a noise spike and drawing that line either up to peak white or down to peak black. Some evidence of this exists in F_a Camera video output for a noise pulse caused by the actuation of the P1 and P3 shutters.

The black region at the bottom of the F_a pictures as mounted is due to mask used as a black reference at the start of each horizontal scan of the vidicon target. The transition into the picture region from the mask is gradual, or appears fuzzy, because the mask is mounted externally on the vidicon, removed from the image plane.

The P1 Camera pictures also showed evidence of occasional electrical noise spikes on alternate frames, in a time-coherence with the end of stroke on the P3 shutter.

The P1 and P2 Camera pictures show low level microphonics in time-coherence with the end of stroke of the P3 and P4 shutters respectively.

c. EVALUATION OF PERFORMANCE

The evaluation of the performance of the Camera group on Flight Model III-2 (Ranger VII) can be made on two levels. The first level would entail a comparison of the information content and overall performance of the Ranger VII cameras to those of the mission requirements and the general specifications. A second level of evaluation would involve a review of the performance of each camera against the specification for that camera type.

(1) General Specifications

The general specification for the Ranger television cameras was written to provide the following:

- High-quality images of the lunar surface at a surface resolution of better than 0.5 meter;
- Wide-area coverage; and
- Picture nesting.

A review of the 4,316 pictures taken by the Ranger VII cameras indicates that the general specifications were met. The satisfying of the first specification can be attributed, in part, to the superior performance of the overall system in that: (1) The camera platform was placed in an impacting trajectory such that sufficient light and shadow detail was available for the imaging system, and (2) Sufficient transmitter power was available to overcome system losses by an ample margin. These facts contributed to a high signal-to-noise video output for each Ranger VII camera, this being an essential factor for high-quality images. Resolutions of lunar detail at the level of one-half meter have been conservatively estimated from the image produced by the final two partial-scan-exposures made immediately prior to impact. The final fragment of the last partial-scan picture was exposed approximately 500 meters before impact and produced an image of an area 42 meters in width and 28 meters in height. In examining this last image, craters one-fiftieth of the picture height, a diameter of 0.8 meter, can be easily recognized. A crater is recognized by its deeply shadowed and brightly luminant image. On the basis of this achieved detail, the resolution requirement of one-half meter was surpassed.

The second and third specifications, wide-angle coverage and picture nesting, were imposed as a basis for correlation of the expected data

output of the Ranger cameras to the well-defined telescopic photographs presently on hand. The success with which Ranger VII cameras met the objectives of these specifications is illustrated by Figure 32. This image, produced by the twenty-five-degree camera, was taken 480 miles before impact. It covers a wide area within which several well known features such as the crater Lubiniezky and the Riphaeus Mountains, can be distinguished by their characteristic images and their geographical relationships. Also indicated on this Figure are the areas covered by pictures taken in the picture-taking sequence, at a higher level of resolution, including the point of impact as shown in Figures 33, 34 and 35. The realization of the design to satisfy this specification is contained in the interplay of camera fields of view, the camera mounting bracket that physically ties the six-camera array into appropriate overlapping fields of view, the camera exposure sequence, and the design of the impacting trajectory.

(2) Detailed Specifications

To achieve television pictures capable of high information content, detailed specifications were imposed on the Ranger cameras. The specifications were formulated to insure that:

- The ratio of the voltage excursion created by the camera when exposed to illumination ranging from black-to-peak-white to the root-mean square of the random noise of the camera would exceed 30 db;
- The ratio of the peak-to-peak signal to the peak-to-peak coherent noise would exceed 20 db;
- The scanned area of the tube would maintain an aspect ratio of unity to within four percent;
- The cameras would have adequate exposure; and
- Image distortion due to smear would be minimized.

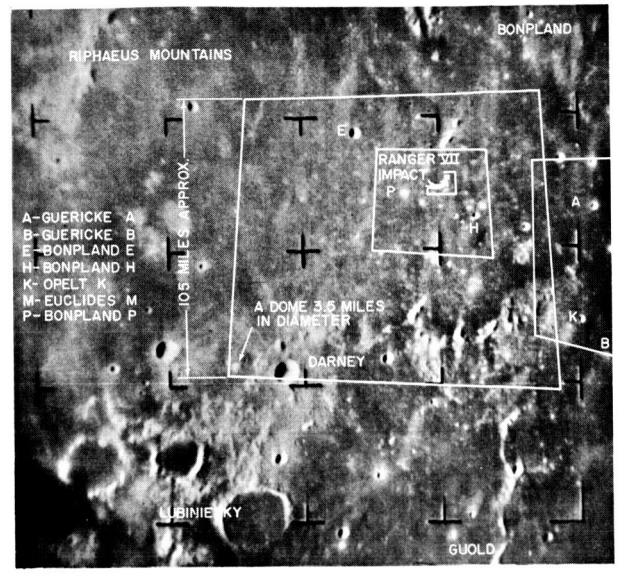

Figure 32. Ranger VII F_a-Camera Picture of Northwest Lobe of Mare Nubium, Showing Picture Nesting

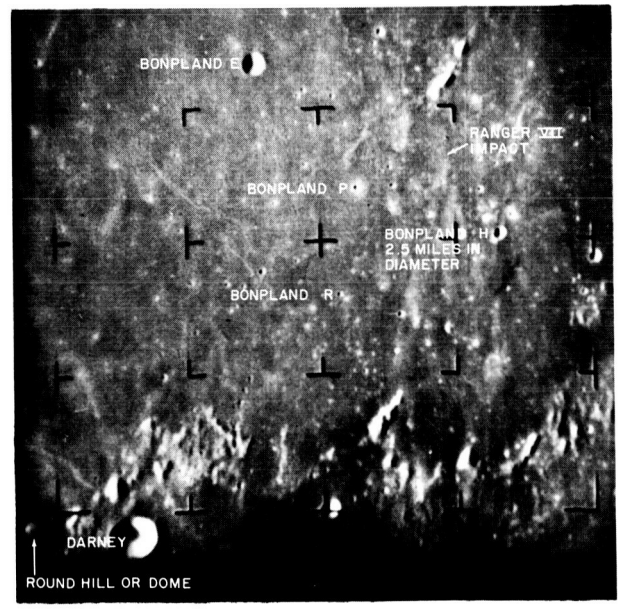

Figure 33. Ranger VII F_a-Camera Picture Taken 2 Minutes 46 Seconds Before Impact (235 miles altitude)

This last specification is a commentary on the ability to calculate and predict the luminance of the lunar surface and the ability of the spacecraft system to direct the cameras

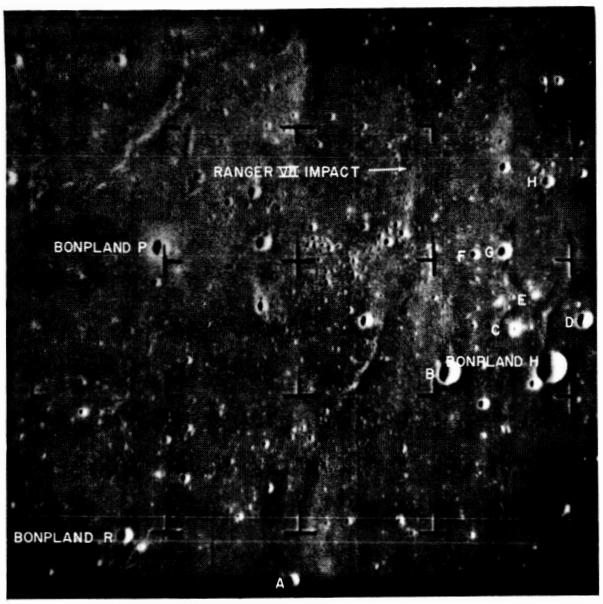

Figure 34. Ranger VII F_a-Camera Picture Showing Last of Previously Known Craters (85 miles altitude)

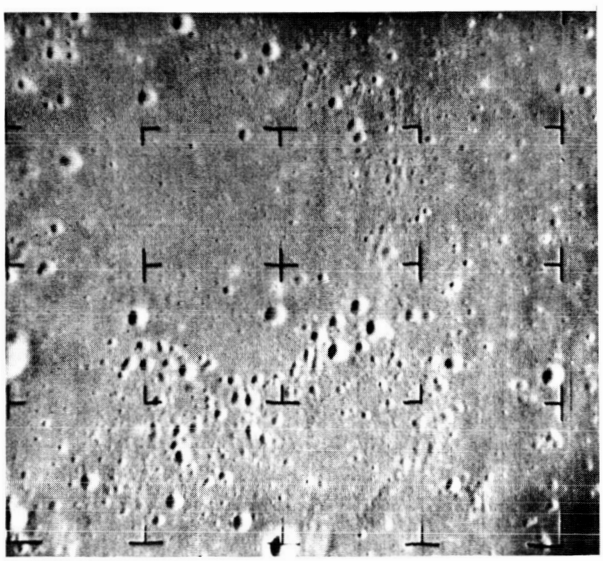

Figure 35. Ranger VII F_a-Camera Picture Showing Rays of Crater Copernicus (34 miles altitude)

to a specific location on the lunar surface. The shutter speed and the velocity projection were calculated to maintain image smear to less than a TV element. These shutter-actuated exposures were 2 milliseconds for the partial-scan cameras and 5 milliseconds for the full-scan cameras.

A duplicate negative of the 35-millimeter primary on-line film data (POD) was examined by projection. In addition, the dubs of the secondary on-line magnetic tape data (SOD) were replayed through a Range Kinescope recorder and polaroid records were made of the video signals at the input of the kinescope film recorder. These observations and data were evaluated in regard to previous test data and to the detailed camera specifications.

The camera subsystem was aligned and calibrated for video output as a function of scene luminance at the Eastern Test Range, preceding the launch. Thie procedure utilizes a brightness source simulating the spectral emission and luminance of the Moon. For the Ranger VII cameras, the F_b, P1, and P2 Cameras were adjusted for a peak luminance of 2700 footlamberts, and the F_a, P3, and P4 Cameras for a peak luminance of 650 footlamberts. Transfer curves, shown in Figures 36 and 37, were plotted for each camera by varying the luminance of the calibration source and recording the corresponding video excursions at the input to the kinescope recorder. Observations of the video excursions at the kinescope recorder were reported during the Ranger VII mission five minutes after video was received. These values are noted on the transfer curves and are also listed in Table 13. These voltage measurements are related to the measured footlamberts of the simulated brightness source and provide an indication of camera exposure.

The choice of the lunar area to be imaged was fortuitous and resulted in maximum use of the conversion capabilities of all six cameras in that adequate camera exposure resulted in a high signal-to-noise ratio.

Some of the variations in the apparent relative luminances are due to variations within the tolerances of camera components. One of these is tolerance on the nominal shutter speed and

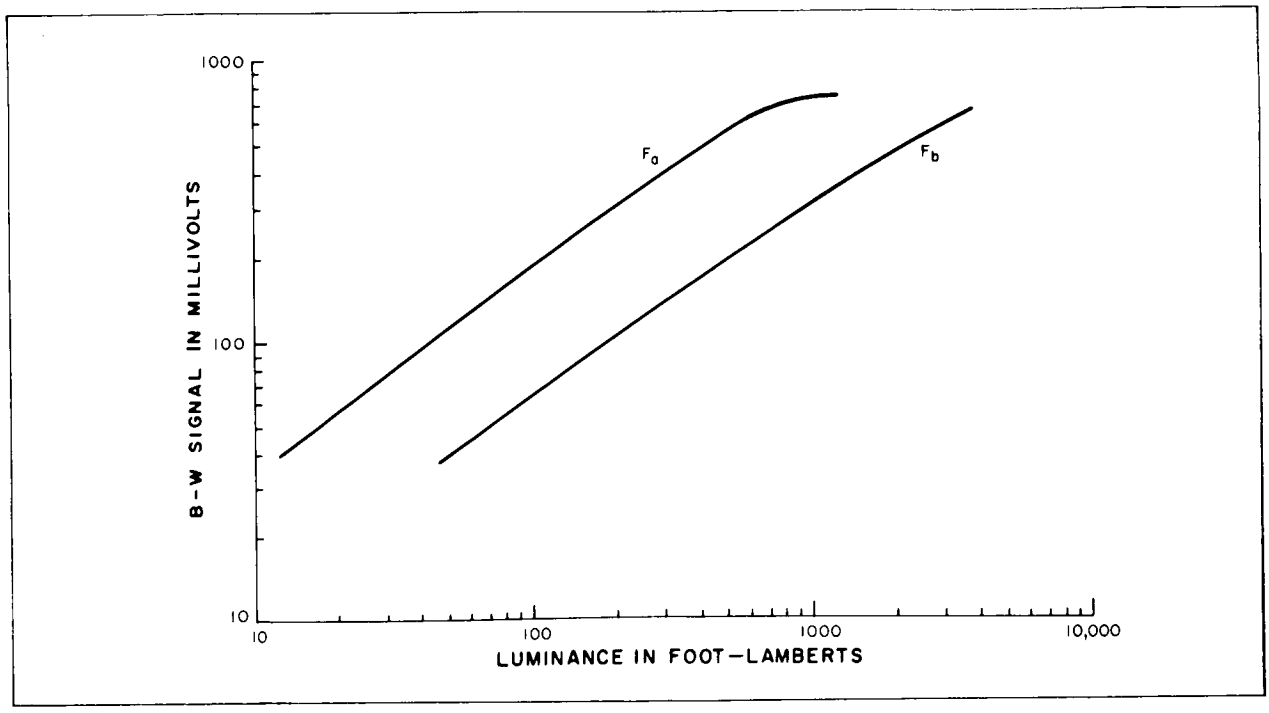

Figure 36. Light-Transfer Characteristics Curves for Ranger VII Full Scan Cameras

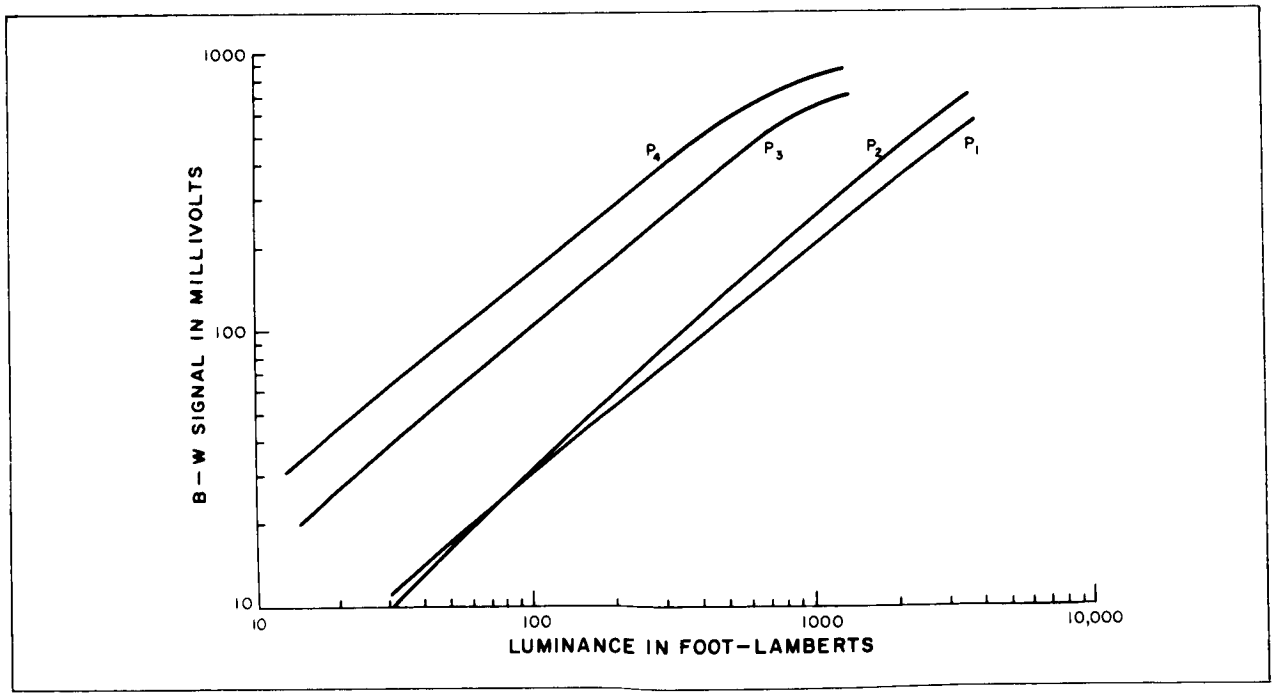

Figure 37. Light-Transfer Characteristics Curves for Ranger VII Partial-Scan Cameras

TABLE 13
LIGHT LEVELS 8 MINUTES BEFORE IMPACT

Camera	Average Light Level (footlamberts)	Peak Light Level (footlamberts)
F_a	520	1300
F_b	600	2100
P1	600	1800
P2	900	2000
P3	410	1350
P4	240	840

on the variation in shutter speeds for the in-stroke and out-stroke. Camera video output is a measure of this variance, all other parameters remaining constant. From the magnetic-tape playback, oscilloscope traces of alternate exposures were made for each camera. The scene luminance is assumed to be invariant during an alternate exposure sequence. The primary cause of variance in camera signal amplitude, then, is the difference in speed for the alternate shutter strokes.

The oscilloscope records of the video for each camera, derived from the secondary original data (from the tape recorders), are shown in Figures 38 and 39.

The variation in exposure for alternate frames is listed in Table 14.

An examination of the video shows that on the three 25-millimeter, f/0.95 cameras, the peak illuminations are occasionally detected near the saturation level of the camera, but the camera did not actually saturate or clip. Maximum exposure without saturation was then achieved on Cameras F_a, P3 and P4. The remaining three Cameras, F_b, P1, and P2 had average

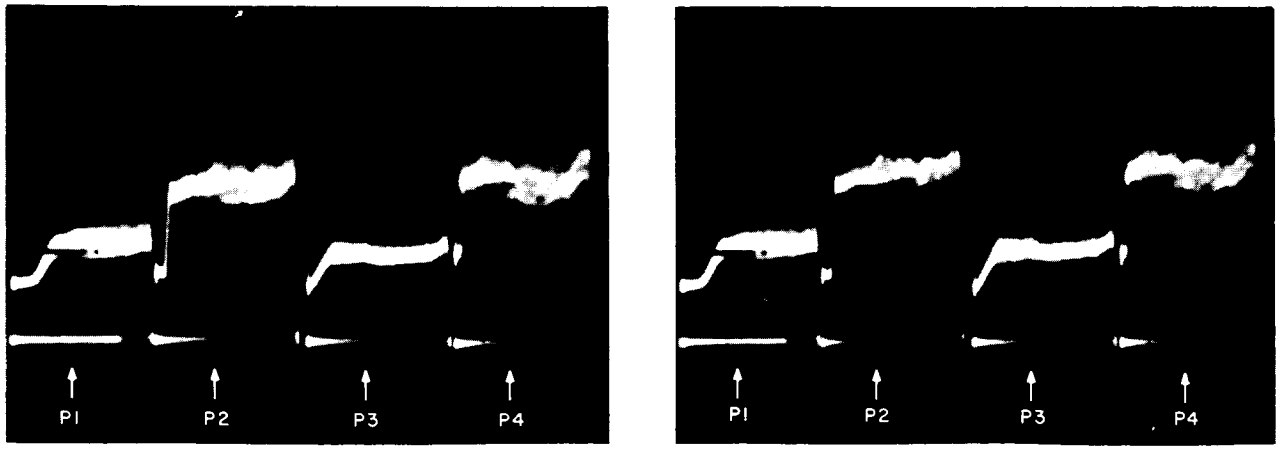

Figure 38. Video Signals for Alternate Exposures of Ranger VII Partial-Scan Cameras

TABLE 14
VARIATION IN ALTERNATE FRAME EXPOSURE ATTRIBUTABLE TO VARIATION IN SHUTTER SPEED

Camera	Variation in Exposure (percent)
F_a	0+
F_b	8
P1	3
P2	10
P3	25
P4	10

exposures with signal-to-noise ratios three to four db lower than for Cameras F_a, P3 and P4. If image smear is evident, it would have occurred in the final two partial-scan pictures. In these pictures, image motion during the shuttered exposure is near the order of the image element being recorded. The final P1 and P3 images are oblique views, causing the major axes of the eliptical views of all round craters to be oriented from lower left to upper right. The elongation of the many smaller craters, whose major axes would be oriented roughly toward the impact point would be most evident in Figure 40. If the final picture had been taken by either the P1 or P2 Cameras, considerable smear would have been evident for this photogeometry.

The evaluation of the Ranger VII pictures against specifications for exposure and image smear indicates that all cameras received adequate exposure for high signal-to-noise pictures and that degradation of image smear was minimized during the final sequence of the Ranger VII mission.

Video line selections from the final F_a and P3 camera frames, shown in Figure 41, indicate that the first specification of a high signal-to-noise ratio was also satisfied. A video signal at the input to the kinescope recorder with a signal-to-noise ratio in excess of 30 db will produce a picture considered to be of high quality. Exmination of the video from the final F_a and P3 frames shows it to be on the order of 34 db. Transmission of video with a signal-to-noise ratio of 35 db through the communication channel, which has a signal-to-noise ratio

F_b CAMERA F_a CAMERA

Figure 39. Video Signals for Alternate Exposures of Ranger VII Full-Scan Cameras

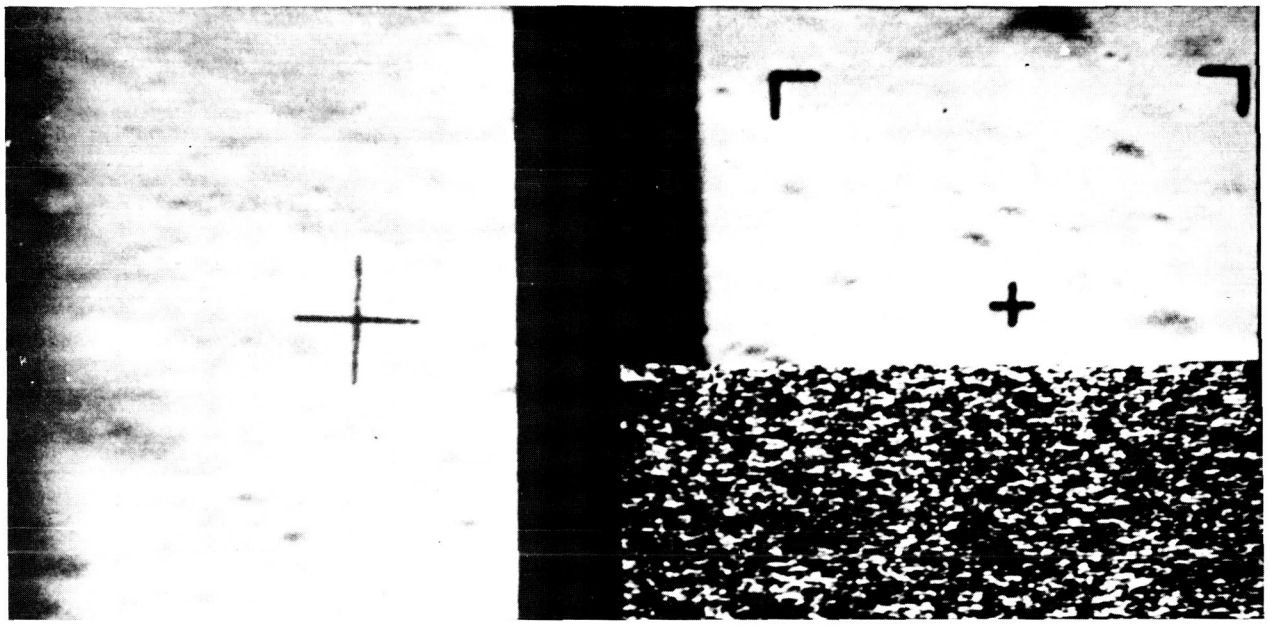

Figure 40. Ranger VII Final Pl- and P3-Camera Pictures

of 39 db would result in a received signal-to-noise ratio of 34 db. Thirty-five db then is taken as the average signal-to-noise ratio for the F_a, P3 and P4 Cameras. The average signal-to-noise ratio for the F_b, P1 and P2 Cameras is taken, in like manner, as 31 db.

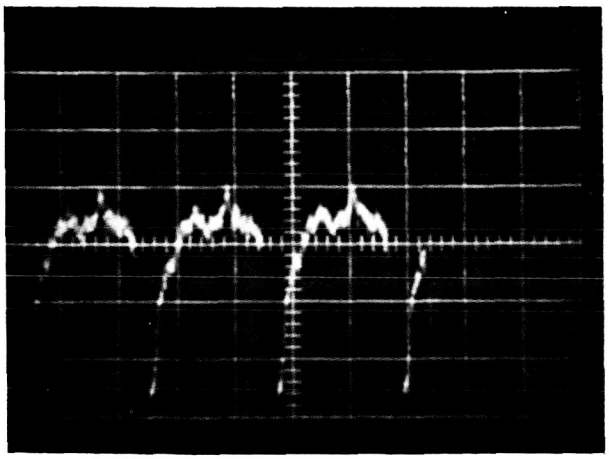

Figure 41. Video Lines 1070, 1072, 1073, and 1074 of Ranger VII Final F_a-Camera Picture

Each of the six cameras then provided video signal with more-than-adequate signal-to-noise ratios to satisfy the first specification and the video criterion for high-quality images.

(3) Image Degradation

In the total record of Ranger VII pictures, some image-degrading factors were noticed that can be described and their effect on the final images evaluated. Some of these factors have remained in the cameras in spite of the best efforts to eliminate them. In general, they were present in the Ranger VII pictures to a degree considerably reduced from prelaunch test experiences. They are, at worst, nuisance factors and result in a loss of less than 1 percent of actual data. Some of these factors are:

- 15-kilocycle crosstalk;
- Vidicon or nuvistor microphonics; and
- Residual images.

Some of these effects will be described in the order of their objectionableness.

(a) 15-KILOCYCLE CROSSTALK

In the full-scan Camera channel, Cameras F_a and F_b are exposed and read out in sequence. While Camera F_a is being read out, Camera F_b is being erased and prepared for exposure, as shown in Figure 42. Part of this prepare cycle involves switching for exposure, as shown in Figure 42. Part of this prepare cycle involves switching the vertical sweep from an 0.39-cps read rate to a 15-kc-per-second erase rate. This high rate is necessary to cause the scan-erase image to be beyond the bandwidth of the scanning aperture and video amplifier. To insure that sufficient photoconductor area will be scanned at this high rate, the sweep voltages must be increased to a high level. It is this signal which is picked up by the readout camera. The pickup mechanism is not entirely defined; however, it is known that part of it is picked up in the power supply grounds and part by electromagnetic or electrostatic pickup in the vicinity of the camera heads.

The signal produced by this crosstalk is on the order of 20 to 25 millivolts, about 28 db below the peak-white video. It varies in amplitude from 15 millivolts in scene areas that approach black to about 40 millivolts in the peak-white areas. It is evident in each full-scan camera, though its amplitude appears to be slightly higher in Camera F_a. This signal is identified by vertical marks with the subtitle of a in Figures 43 and 44.

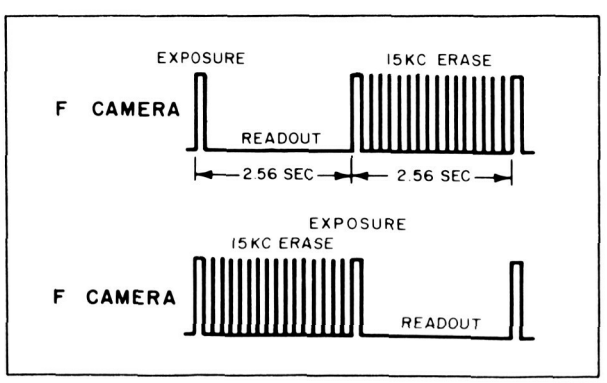

Figure 42. Readout Sequence of the Ranger VII Full-Scan Cameras

This high-frequency vertical-erase scan signal is also the dominant source of noise in the P2 Camera. It occurs in the P2 Camera during the erase period of one of the F-Cameras. The signal causes 8.5 vertical bars in the picture which persist for three consecutive frames, then are absent for three frames.

(b) VIDICON OR NUVISTOR MICROPHONICS

Disturbances in the video signals that can be correlated to exposure sequence are due either to electrical pickup at the high impedance of the vidicon target or actually due to mechanical displacements of either the vidicon or the nuvistor preamplifier. This type of interference is illustrated in Figure 44 where twelve disturbances caused by P-Camera shutters are each indicated by a subscript b. Microphonic performance was generally satisfactory with occurrences in four-to-five F_a Camera frames showing objectionable levels. Similar disturbances are evident in the lower third of the P1 and P2 frames in time coherence with the end-of-travel of the P3 and P4 shutter strokes.

Another noise which is observed occasionally in the F_a Camera and P1 Camera frames is a very short noise pulse which goes into the saturated white region. While the duration of the noise is only about 15 microseconds, the kinescope beam is overdriven causing an elliptical-shaped spot which appears to be several scan lines wide, as shown in Figure 45. In Camera P1 these saturated noise pulses occur during the bottom third of the frame in time coherence with the end-of-shutter stroke of alternate exposures of Camera P3. It also occurs about six times in the F_a Camera. In frame 105 of the F-Channel POD there is a loss of 2 lines of video caused when this shutter-induced noise occurs in time with the clamping actions. This noise also appears to be caused by the partial-scan Camera P3, is

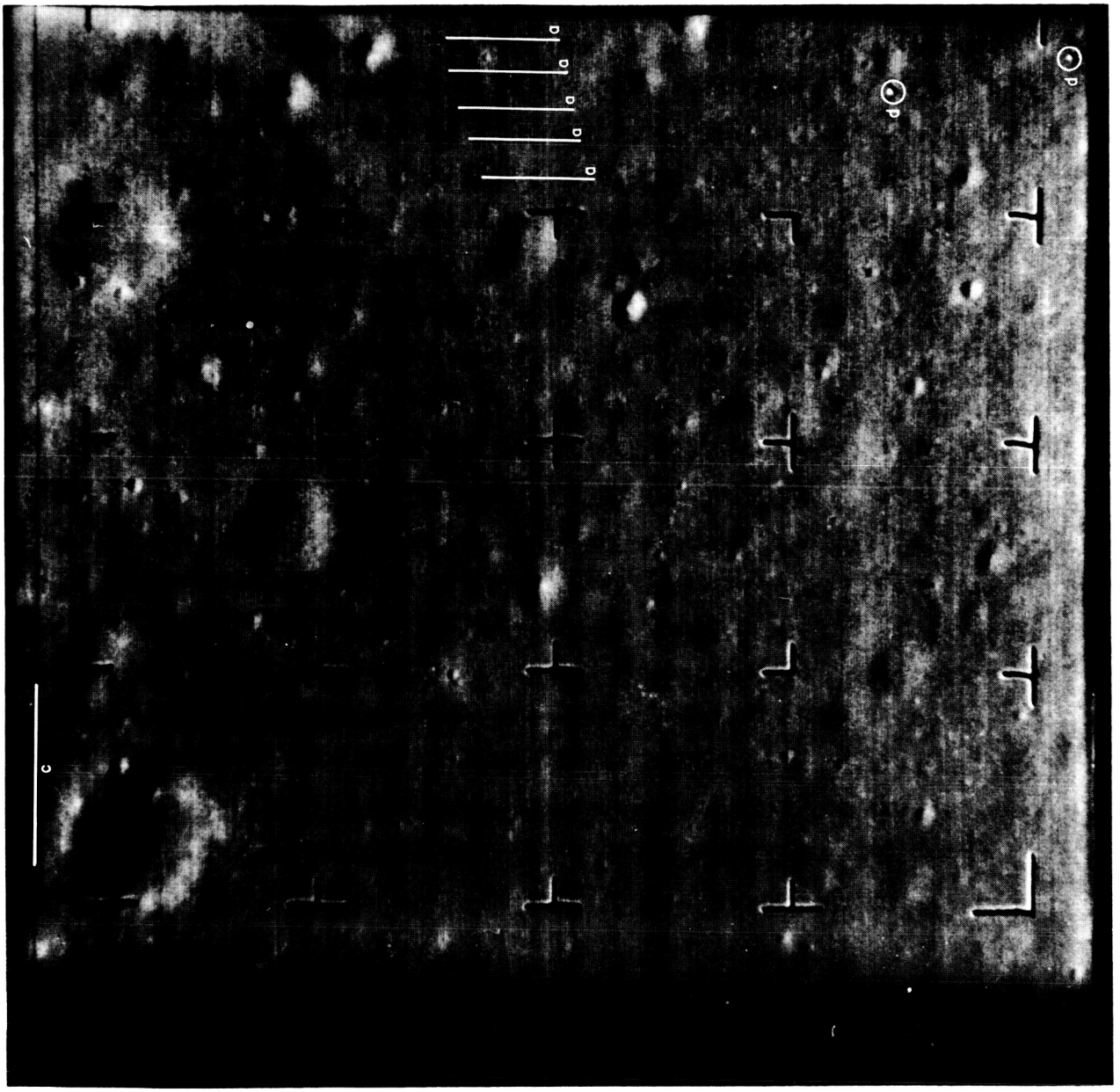

Figure 43. F_a-Camera Video Output Indicating Image Degradations

synchronous with shock-wave microphonics, and is similar to the more prominent noise of Camera P1. Video loss due to clamp displacement is shown as subscript c of Figure 43. A third type of video disturbance due to the shock wave produced by the shutter's end-of-stroke is nuvistor microphonics which is the dominant noise present in the P1 Camera, as shown in Figure 40. The nuvistor appears to be excited primarily by its own shutter and by

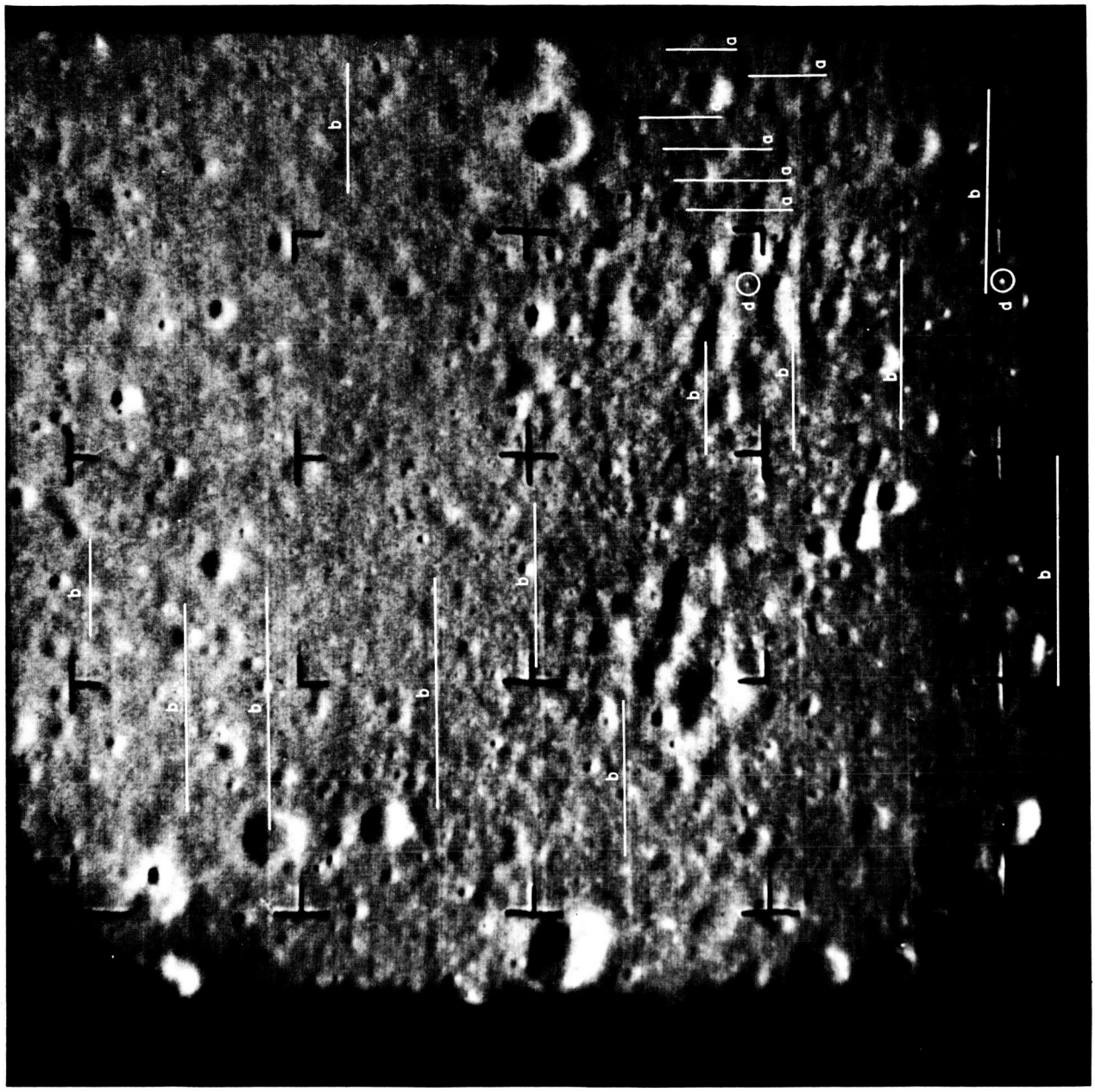

Figure 44. F_b-Camera Video Output Indicating Image Degradations

the F-Camera shutters. The microphonic signal is a 13-kc signal which appears as a series of vertical bands in the picture. There are approximately six-and-a-half bands present in every P1-Camera picture.

(c) RESIDUAL SIGNALS

Perhaps the most difficult image degradation to identify in the Ranger VII image is that due to residual images. After the normal erase

Figure 45. Noise Pulses Induced by End of Shutter Stroke in Ranger VII PI-Camera

procedure has been applied to a camera, there will generally remain a residual signal amounting to about 5 percent of the previous exposure for the full-scan cameras and as much as 10 percent for the partial-scan cameras. Its effect on the image produced by the subsequent exposure depends on the image contrast and the effectiveness of the camera's erasure. The F_b Camera frames numbers 230 through 240 of the POD, were observed. The crater in the lower right area appears to be a typical example of image degradation due to residual image. There is a definite brightness discontinuity correlated to the region of high illumination in the previous frame, shown as an increase of white level due to frame-to-frame memory. This is a very subtle degradation and does not affect the overall image quality; it is categorized here only as a cautionary measure to the image interpreters who may confuse it with image detail.

(d) VIDICON BLEMISHES

There are at least two spots in Cameras F_a and F_b that may be due to vidicon blemishes. They are identified by the subscript d in Figures 43 and 44 and were found to be present also in prelaunch system tests. They have the appearance of the tiniest of craters but betray themselves by having the characteristic white and black rims opposite in-sense to actual craters, and by their presence in the same raster position of all pictures from a given vidicon.

(e) SHADING

Shading is the combined vidicon and lens effect which causes some modification in dynamic range over the scanned area. In the F_a-Camera it is produced primarily by lens vignetting and manifests itself as a dark shadow in three of the four corners of the picture.

(4) Summary

In total, image degradations that have been detailed here detract only in a small way from the overall image quality and information content of the Ranger VII pictures.

The analysis and evaluation of the Ranger VII pictures indicated that modest improvements in camera performance could eliminate several of the more pronounced image disturbances. A program to reduce the shock wave produced by the camera shutters was instituted which eliminated the characteristic vidicon and nuvistor microphonics. The program culminated in an improved shock-isolator design for the shutter-to-camera mounting. The analysis also indicated that camera effects such as residual images and lens vignetting, previously considered serious, did not, in fact, degrade the usability of the image.

In the discussion on camera exposure, it was pointed out that the signal-to-noise ratios for the F_b, P1 and P2 Cameras were three- to four-db lower than those for the F_a, P3, and P4 Cameras. It was also noted that only few peak-white signals exceeded 1800 footlamberts on any of the cameras. The recommendation was to increase the video amplifier gain in the F_b, P1, and P2 Cameras to produce the

maximum output voltage for an 1800-footlambert signal. This ensured higher signal-to-noise ratios on all cameras for the closer-to-the-terminator Ranger VIII picture-taking.

The final recommendation was to implement a spectral-response measurement program to accomodate all cameras for Ranger IX and Spares, to increase the radiometric interpretation capability.

3. Thermal Control Group

The thermal configuration of the Ranger VI and VII TV Subsystems is shown in Figure 46. Primary temperature-control surfaces are:

- Thermal shroud (polished aluminum vehicle skin);
- Thermal fins; and
- Thermal shields (insulators).

The construction of the shroud and fin assembly is such that solar energy striking the spacecraft parallel to its axis illuminates only the top surfaces of the fins, i.e., no direct sunlight is incident upon the thermal shroud. The flow of thermal energy with this condition is as follows:

- Sunlight strikes the fin surface as a normal angle of incidence and a portion is absorbed. The remainder is reflected to space and other parts of the spacecraft.
- Part of the energy absorbed by the fin is radiated from the front and rear surfaces of the fin; the remainder flows into the thermal shroud.
- The energy flowing into the thermal shrouds from the fins is radiated from the shroud surface (polished aluminum), establishing a temperature field on the shroud surface.
- The temperature field established on the shroud is essentially isothermal. Since the shroud envelops all electronic equipment, the equipment will come to this same temperature at steady-state conditions. During full-power operation of the equipment, the temperatures of individual components are maintained below maximum temperature limits due to the "heat-sinking" properties of the spacecraft.

a. METHODS USED TO PREDICT FLIGHT TEMPERATURES

Three equilibrium-temperature calculations were performed for the Ranger VII flight. The calculation methods used are as follows.

- The energy input to the TV Subsystem was considered to be only direct solar energy which was incident upon the top surfaces of the temperature-control fins. No additional energy input was considered. This is the "direct-input" method.
- The energy input to the TV Subsystem was calculated in essentially the same manner as the "direct-input" method. However, it included calculations for the energy input due to multiple reflections of solar energy from surfaces of the Subsystem to other viewed Subsystem surfaces, and solar energy input from the solar panels and the Bus. This is called the "input including reflections" method.
- The energy input to the TV Subsystem was calculated using ratio factors applied to the results of the "direct-input" method. (These ratio factors were determined from an analysis of the Ranger VI flight data and empirically account for the greater-than-expected energy input for Ranger VI.) This is called the "input-with-ratio-applied" method.

The use of any of the three methods results in an effective energy input into each of the thermal control fins.

Using the three methods of calculation outlined above and inputs determined from the solar

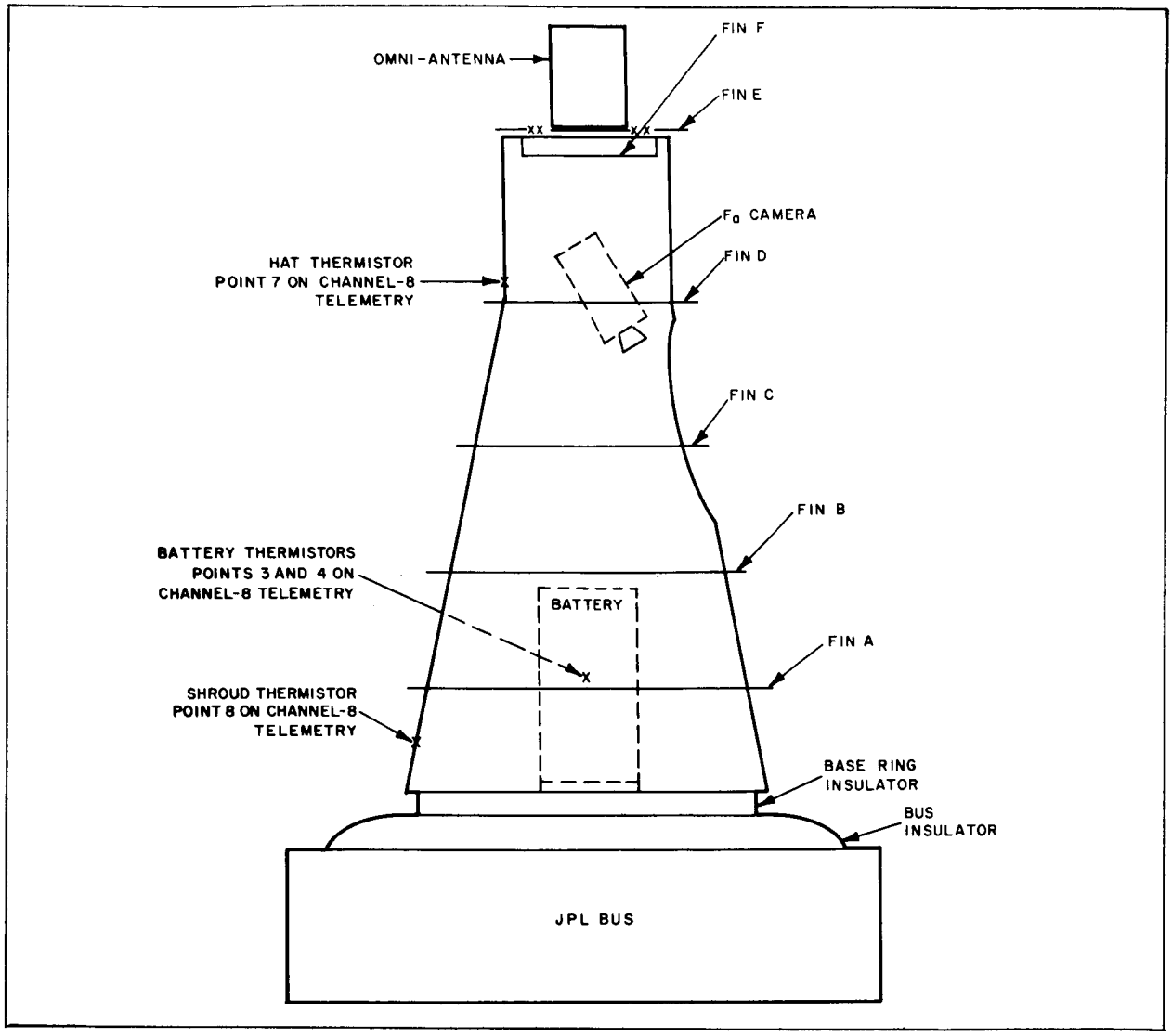

Figure 46. Thermal Configuration of the Ranger TV Subsystem

absorptivity values, a set of equilibrium temperatures for the Ranger VII flight was predicted for each method. The values of absorptivity were determined by both RCA and JPL/STL; consequently there were six sets of predicted equilibrium temperatures. The resulting dual sets of values are reported in the following paragraphs. All calculations were performed using the minimum solar constant value of 0.87 watt per square inch, which was applicable for the Ranger VII flight. The results of the calculations for cruise telemetry data points are tabulated in Table 15.

The thermal design for Ranger VII was primarily based upon the data received from the flight of Ranger VI. The temperature data in Table 15, calculated using the "input with ratio factors applied" method, was considered to be nominal.

It was considered, however, that if the Ranger VI temperature data were not accurate,

TABLE 15
CRUISE-MODE EQUILIBRIUM TEMPERATURE PREDICTIONS FOR SUBSYSTEM LOCATIONS MONITORED BY CRUISE-MODE TELEMETRY

Method of Calculation	Hat (-Y)		Vidicon Housing		Shroud		Internal Battery (Ch. P)		Camera Electronics		Remarks
	°F	°C	°F	°C	°F	°C	°F	°C	°F	°C	
RCA values of α (0.71, 0.50), no reflections included	52	11	34	1	34	1	34	1	32	0	Establishes absolute minimum values, highly unlikely to occur
JPL/STL values of α (0.76, 0.56), no reflections included	66	19	45	7	46	8	45	7	45	7	Unlikely to occur
RCA values of α, reflections included	59	15	39	4	52	11	46	8	46	8	Probable minimal temperature
JPL/STL values of α, reflections included	70	21	48	9	61	16	57	14	55	13	Most probable minimal temperature
RCA values of α using ratio factors from Ranger VI (1.37, 0.85)	70	22	55	13	66	19	64	18	68	20	Nominal temperature range (assuming accuracy of Ranger VI information)
JPL/STL values of α using ratio factors from Ranger VI	84	29	66	19	79	26	77	25	79	26	
Telemetry received from Ranger VI with α values of 0.41, 0.65, 0.82, and solar constant = 0.93 w/in^2	102	39	84*	29*	97	36	99	37	99*	37*	Establishes absolute maximum values, highly unlikely to occur

* Estimated

then the remaining entries in the tabulation might become significant. Since emphasis was placed on obtaining battery temperatures of not less than 10° C, conservative methods were employed for selecting the finishes. The calculations indicating battery temperatures of 1 and 8° C for Ranger VII were considered highly unlikely in light of the results obtained from the Ranger VI flight and the limited adjustment of inputs to this area.

b. THERMAL-CONTROL PAINTS APPLIED TO RANGER VII

Two thermal-control fin paints were to be applied to the TV Subsystem of Ranger VII. This was at variance with the procedure followed for Ranger VI where a third paint was applied to both Fin B and the antenna. During final assembly at Cape Kennedy, it was discovered that the Ranger VII omni-antenna did not reflect the change from a light gray paint to white paint; it was neither convenient nor practical to repaint at that time since the effect of light gray as compared to the effect of white in that area is almost negligible. All calculations for temperature shown in Table 15 (which were made before the launch of Ranger VII) were made considering Fin E, the antenna ring, as being painted white PV-100. A comparable tabulation that takes the light gray paint on the antenna ring, Fin E, into account in the calculation is shown in Table 16.

The thermal-control paints used on the fins of Ranger VII were a mixture of PV-100 white paint and MIL-E-5557 type III black paint and are identified as follows:

Description	Drawing Number
Light Gray (antenna)	1758619-19
Light Gray	1758619-27
Dark Gray	1758619-28

Mixtures of gray paints were prepared in March 1964 for Ranger VII. The desired values of solar absorptivity (α) for the paints were 0.58 and 0.77 (as compared to 0.62 and 0.82 for Ranger VI. Samples of the paints were sent to JPL for spectral evaluation by JPL/STL. The values of α measured by JPL/STL on the Ranger VII samples were 0.04 to 0.05 higher than those measured at RCA and resulted in values that were almost the same as measured on Ranger VI. It was decided, therefore, to use JPL/STL solar absorptivity measurements as the design reference values or "true" values and the RCA values were used as a lower bound.

New mixtures of gray paint were prepared for spectral analysis to obtain the new values of 0.55 and 0.75. The discrepancy between RCA and JPL/STL measurements indicated that the RCA values of 0.51 and 0.71 were reversed. The spectral-measurement history of these paints is given in Table 17.

Measurements of absorptivity at ETR on the Ranger VII thermal shroud fins were obtained using the Lion Model 25A portable reflectometer and RCA prepared calibration standards. The accuracy of this reflectometer is estimated to be ±5 percent. The light gray paint on the antenna was prepared and measured in a series of spectral measurements similar to those employed for Ranger VI and checked at ETR on Ranger VII. Therefore, the measurements program data indicates the values of solar absorptivity on the Ranger VII fins to be as given in Table 18.

c. RANGER VII CRUISE-TEMPERATURES VS. FLIGHT PREDICTIONS

(1) Thermal Shroud Hat

The temperature of the hat was monitored during cruise mode by channel 8, data point 7. Immediately after launch, the Spacecraft traveled into the shadow of Earth. The hat, being of low thermal mass, dropped steadily from a launch temperature of 78° to 61° F before the spacecraft was out of the shadow and exposed to solar radiation. Within 10 hours

TABLE 16
CRUISE-MODE EQUILIBRIUM TEMPERATURE PREDICTIONS FOR FLIGHT MODEL III-2

Location on TV Subsystem	RCA Calculations			JPL/STL Calculations		
	σT^4	Temperature		σT^4	Temperature	
		0° C	0° F		0° C	0° F
Thermal Shroud, Hat, -Y Side	0.294	26	78	0.317	32	90
Camera Lens Housing	0.257	16	61	0.276	22	72
Thermal Shroud, -Y Side, Below Fin A	0.271	20	68	0.297	27	81
Battery (Internal), Channel P	0.269	20	68	0.293	26	79
Camera Electronics, -Y Side, Unit (upper)	0.273	21	70	0.296	27	81
Power Amplifier, -X Side, Unit (cavity end) Channel F	0.273	21	70	0.297	27	81
Power Amplifier, +X Side, Unit (cavity end) Channel P	0.273	21	70	0.297	27	81
Camera Mounting Bracket	0.286	24	75	0.307	30	86
High Current Voltage Regulator, +Y Side, Channel P	0.260	18	64	0.281	23	73
Transmitter Power Supply, +X Side, Channel P	0.264	19	66	0.288	25	77
Temperature Control Plate, Center (Fin F)	0.341	38	10	0.364	43	109
Thermal Shroud, +Y Side, Below Fin A	0.268	20	68	0.293	26	79
Thermal Shroud, -Y Side, Between Fins B and C	0.290	25	77	0.315	32	90
Deck No. 3, -Y Side	0.284	24	75	0.296	30	86
Deck No. 4, -Y Side	0.272	21	70	0.298	27	81
Deck No. 5, -Y Side	0.257	17	63	0.281	23	73

*Considering Gray Paint with α of 0.41 on the antenna ring, using Ratio Factors from the RA-6 Spacecraft.

TABLE 17
SPECTRAL-MEASUREMENT HISTORY

Description	Desired Design Values Absorptivity	Samples Painted at RCA 5/8/64	Samples Painted at JPL 5/26/64	Samples Prepared During Painting of Ranger VII Fins at JPL 6/12/64	Values Measured on Ranger VII Fins at ETR with Portable Reflectometer 6/24/64
Light Gray	RCA 0.51	RCA 0.522	RCA 0.513	RCA 0.517	RCA 0.50
RCA 1758619-27	JPL/STL 0.55	-	JPL/STL 0.56	JPL/STL 0.56	-
Dark Gray	RCA 0.71	RCA 0.716	RCA 0.720	RCA 0.716	RCA 0.71
RCA 1758619-28	JPL/STL 0.75	-	JPL/STL 0.76	JPL/STL 0.76	-

after launch, the temperature of the shroud hat had reached equilibrium at 82° F, but took a drop again during midcourse when it went to about 75° F. One hour after midcourse maneuver was initiated, the temperature of the hat was back to equilibrium at 84° F.

Using the "input-with-ratio-applied" method, the predicted temperature was calculated to range from 76° F (RCAα) to 90° F (JPL/STLα). The hat, being large in area and low in thermal mass reacts significantly to small changes in energy input and it is for this reason that the temperature drops occurred within Earth's shadow and during midcourse maneuver. (See Paragraph B of this section for graphs of the cruise mode telemetry.)

(2) Camera Lens Housing

The temperature of the camera lens housing was monitored during cruise mode by channel 8, data point 1. This point indicated a decrease in temperature of about 10° F while the vehicle was in the Earth's shadow. Temperature drifted still lower to 62° F until about an hour after spacecraft exposure to solar radiation at which time the temperature began to rise and reached equilibrium at 66° F, 14 hours after launch.

During midcourse maneuver, the spacecraft was rotated in such a way as to subject the lens housing to an increased solar input, as indicated by a sharp rise in temperature to 76° F. A large mass, such as the six cameras and the bracket, took this rise as indicated by the time required to reestablish equilibrium at 66° F (8 hours from the time midcourse maneuver was initiated).

TABLE 18
VALUES OF SOLAR ABSORPTIVITY ON THE RA-7 FINS

Location	Solar Absorptivity
Fins A, B, F	0.50 to 0.56
Fins C, D	0.71 to 0.76
Fin E (White Paint)	0.19 to 0.22

Using "the input-with-ratio-applied" method the predicted temperature was calculated to range from 61° F (RCAα) to 72° F (JPL/STLα). The camera lens housing remained steady at 66° F after midcourse maneuver until the final few hours of flight at which point a slight rise occurred due to lunar inputs, as described in paragraph d that follows.

(3) Thermal Shroud (-Y side, below Fin A)

The temperature of the thermal shroud in this area was monitored during cruise mode by channel 8, data point 8. Passage through Earth's shadow allowed the temperature of the lower portion of the shroud to drop to 65° F before exposure to solar radiation which allowed this area to stabilize at 74° F. Temperature equilibrium was reached within 8 hours from launch.

Analysis of the data indicates the -Y side of the vehicle was shadowed during midcourse maneuver and a decrease to 70° F occurred at this time. This apparent shadowing is somewhat substantiated by the increased input to the cameras since the field-of-view hole is on the +Y side. Within 90 minutes, however, the shroud in this area was once again at a stable 74° F.

Using the "input-with-ratio-applied" method the predicted temperature at this data point was calculated to range from 68° F (RCAα) to 80° F (JPL/STLα). Flight temperature fell at the midpoint of this range.

(4) Battery, P-Channel

The temperature of the Battery is monitored during cruise mode by an internally located thermistor on channel 8, data point 4.

The batteries were not affected by transient changes in solar input as occurs when the Spacecraft is in the Earth's shadow and during midcourse maneuver, due to their high thermal mass and location.

Battery temperature decreased steadily and reached equilibrium at 75° F within the 40-hour time constant determined from thermal-vacuum testing. From using "the input-with-ratio-applied" method, the predicted temperature of the batteries ranged from 66° F (RCAα) to 79° F (JPL/STLα).

(5) Camera Electronics

The Camera Electronics temperature was monitored during cruise mode by Channel 8, data point 11. Reaction to brief changes in solar input, as during passage through Earth's shadow and midcourse maneuver, was limited by the thermal mass location within the Subsystem.

Temperature of this component decreased steadily and obtained equilibrium within 24 hours from launch. Stability was reached at 68° F, 12° below the launch temperature of 80° F. The predicted temperature range, calculated by the "input-with-ratio-applied" was 70° F (RCAα) to 81° F (JPL/STLα). Flight temperature fell slightly below the lower limit of the prediction. This can be explained only as being an inaccuracy of the prediction equation due possibly to insufficient knowledge of the temperature of this area from the flight of Ranger VI. This data point was not telemetered on Channel 8 and during the Ranger VI mission no information was obtained from that flight.

(6) Summary

Of the five points which were monitored for temperature during cruise mode, four points were close to the midpoint temperature of the predicted range.

Three were right at midpoint, the Hat being 2° below mid-temperature. The Camera Electronics was 7° F below the midpoint of the predicted range, but well within the range of desirable operation temperature. A comparison of predictions to actual flight temperatures obtained from Channel-8 telemetry is listed in Table 19.

TABLE 19
COMPARISON OF PREDICTED TO ACTUAL FLIGHT TEMPERATURES

Location	Data Point	Predicted by RCA (°F)	Predicted by JPL/STL (°F)	Flight (°F)
Hat	7	78	90	82
Lens Housing	1	61	72	66
Shroud	8	68	81	74
Battery	4	68	79	75
Camera Electronics	11	70	81	68

d. TEMPERATURE RISE OF RANGER VII CAMERA LENS HOUSING DURING FINAL HOURS PRIOR TO LUNAR IMPACT

As the Spacecraft approaches the moon, the effects of lunar solar reflections and moonshine began to be noticed. These factors will not affect the overall spacecraft temperature to any noticeable extent due to the high reflectance of the surfaces which face the moon. The solar cell paddles and the cameras, however, have a highly absorptive surface facing the moon, and both these areas experienced heating during the final hours of flight.

The thermal energy flux is a summation of the reflected solar radiation and the IR radiation of the moon, referred to as moonshine. Calculations of the flux density at various distances from the moon were plotted to provide the curve in Figure 47. The curve is not absolute due to the approximations that were used in the calculations, but it is accurate enough to explain the conclusions that were reached by its usage.

From the curve, the average flux during the last three hours of flight can be reasonably approximated at 0.01 watts per square inch to within 1000 miles from the moon's surface. Within 1000 miles to impact, the average flux is 0.12 watts per square inch for a period of 15 minutes. Using these values as an input, the increase in temperature of the camera lens can be calculated. Although the entire projected area of the cameras is exposed to this energy flux, the front end of the camera can be treated separately due to its limited conductivity to the balance of the mass. This is evident by the fact that the camera bracket does not rise in temperature at the same rate as the lens housing. The temperature increase, ΔT, during the last 15 minutes can be calculated from:

$$\Delta T = \frac{Q}{mc}$$

$$= \frac{(flux)\,(area)\,(minutes)}{(weight)\,(specific\ heat)}$$

$$\frac{\left(0.12 \frac{w}{in^2}\right)\left(0.0569 \frac{BTU}{min/w}\right)(12.5\ in^2)\ (15\ min)}{(1.5\ lbs)\left(0.22 \frac{BTU}{lb\,°F}\right)}$$

$$\Delta T = 3.8\,°F$$

and the ΔT for the previous three hours using the same relationship:

$$\Delta T = \frac{\left(0.01 \frac{w}{in^2}\right)\left(0.0569 \frac{BTU}{min/w}\right)(12.5\ in^2)\,(180\ min)}{(1.5\ lbs)\ \left(0.22 \frac{BTU}{lb\,°F}\right)}$$

$$\Delta T = 3.9\,°F$$

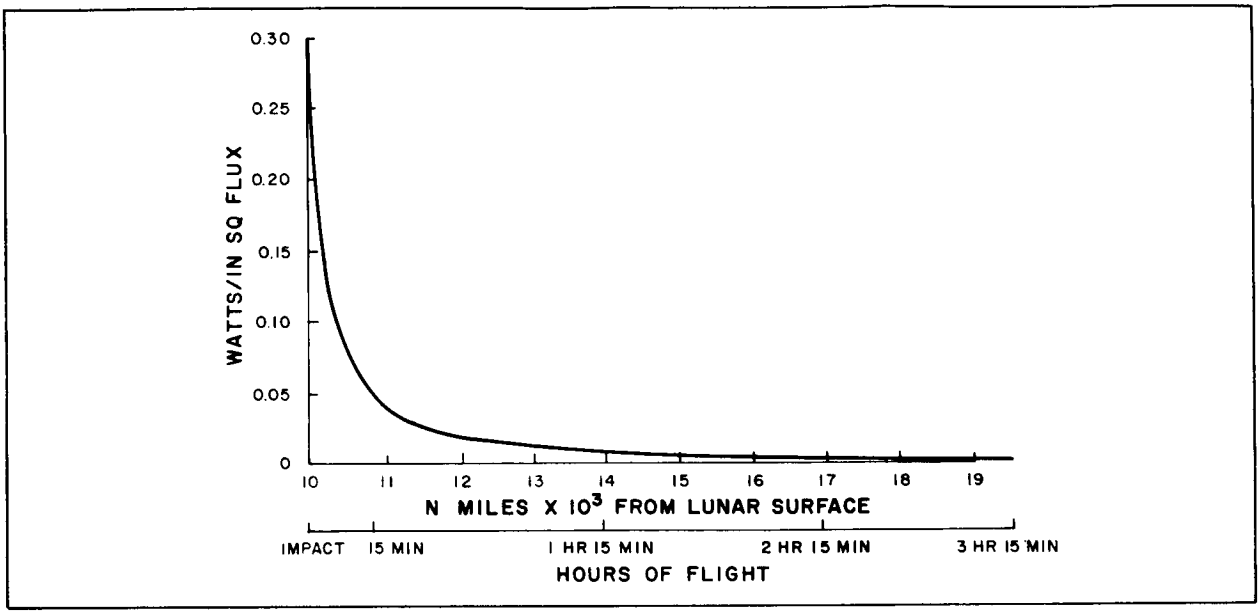

Figure 47. Reflected Solar Radiation and Moonshine ($\theta_s = 40°$, 11° S Lat., 21° W Long.)

These calculations indicate a rise in temperature of the front end of the cameras on the order of 7 to 8° F. Using this approach, the increase of 6 to 10° F from telemetry, in the area of the camera lens during Ranger-VII flight can be explained. Lunar inputs can provide heating on the same order as that experienced by the Ranger-VII spacecraft.

Other data points indicate little or no temperature increase due to the lunar inputs since conditions of mass and high reflectance limit the effects.

Section IV

Ranger VIII Mission Evaluation

A. SUMMARY OF RANGER VIII MISSION

1. Prelaunch

Three hours before launch (Day 48 - 14:00:00 GMT), the TV Subsystem was turned on in the reduced-power mode for a final check. Telemetry and video indications were normal at this time. The countdown continued, and at launch minus 15 minutes, cruise-mode (15-point) telemetry was initiated and received from the spacecraft. Again the telemetry data, evaluated by both the ETR launch team and SDAT, indicated that all assemblies of the TV Subsystem were functioning normally in accordance with the predicted values.

2. Launch

The Ranger VIII Spacecraft was successfully launched from the Eastern Test Range at 17:05:01 GMT on February 17, 1965 (Day 48). The launch was accomplished by an Atlas-Agena launch vehicle. A complete Ranger VIII mission events list is presented in Table 20. At launch, the umbilical cable was disconnected from the launch vehicle, removing the full-power inhibit circuit which had limited the RF power output from the TV Subsystem to a reduced level of approximately 125 milliwatts. TV Subsystem telemetry data were received by SDAT from the ETR during the first seven minutes of launch. These data confirmed that all TV Subsystem parameters were normal during the entire launch phase.

The tracking station at Johannesburg, South Africa (DSIF 51), acquired two-way lock of the spacecraft approximately 28 minutes after launch (Day 48 - 17:33:20 GMT) and commenced to relay telemetry data to SDAT with message No. 1 taken at 17:43:00 GMT.

The Woomera, Australia, Tracking Station (DSIF 41) first viewed the spacecraft at 17:54:00 GMT, with message No. 1 to SDAT reporting all TV Subsystem parameters normal. Temperature sensors on the camera lens housing and the top hat indicated initial temperature increases whick leveled off at less than 90° F and then began to decrease toward the predicted cruise-mode values.

3. Cruise Mode

Agena booster separation (S) occurred at L + 25 minutes and initiated the 64-1/4 count of the TV Subsystem Clock. Overseas Tracking Station DSIF 51 at Johannesburg, South Africa, verified that the Clock was operating, by means of a cruise-mode telemetry indication received at 17:43:00 GMT. Agena booster separation also provided a backup for the removal of the full-power inhibit circuit, and started a mechanical timer which provided backup functions for the spacecraft. At separation plus 30 minutes (S + 30), a contact closure of the wafer-type timer switch provided initial arming of the silicon controlled rectifier (SCR) gates in the High-Current Voltage Regulators (HCVR) of the TV Subsystem. At separation plus 35 minutes, the spacecraft solar panels were deployed. This activated a microswitch which provided a backup function for the enabling of the SCR gates. At L + 69 minutes, spacecraft acquisition of the Sun was accomplished, and 2 hours and 35 minutes later, the Earth acquisition occurred. Thus, the spacecraft was oriented in its normal cruise-mode position, with the z-axis pointing toward the Sun and high-gain antenna pointing toward the Earth. The 15-point telemetry continued to indicate normal TV Subsystem performance with temperatures slowly stabilizing toward nominal cruise-mode values. The 8- and 16-hour

TABLE 20
RANGER VIII MISSION EVENTS LIST

Mission Event	Event Time (GMT)		Nominal Mission Time
	Predicted	Actual	
DAY 48			
1. Prelaunch Test	—	13:59:59	T-116'
2. Cruise-Mode Telemetry On	—	16:40:00	T-15'
3. Spacecraft on Internal Power	—	17:00:00	T-5'
4. CC&S Uninhibit	17:03:00	17:03:01	T-2'
5. CC&S Clear	17:04:01	17:04:01	T-1'
6. Launch (L)	17:05:01	17:05:01	T = L
7. Spacecraft/Agena Separation (S)	17:30:00	17:30:14	L + 23' (=S)
8. Transmitter Power Up	17:28:01	—	—
9. TV Clock Start	17:30:00	17:30:14	S + 0
10. DSIF-51 View Period Start	—	17:34:00*	—
11. DSIF-41 View Period Start	—	17:52:00*	—
12. Solar Panels Extend Command	18:05:01	18:05:01	L + 60'
13. Solar Panels Extended	18:06:01	18:05:40	—
14. Sun Acquisition Command	18:08:01	18:08:01	L + 63'
15. Sun Acquisition Complete	—	18:14:20	—
16. Earth Acquisition Command	20:36:01	20:36:01	L + 211'
17. Earth Acquisition Complete	—	20:40:10	—
18. DSIF-41 View Period End	—	23:15:00*	—
DAY 49			
19. TV Clock 8-hour Pulse	01:30:14	01:30:12	S + 8 hours
20. DSIF-12 View Period Start	—	06:08:00*	—
21. DSIF-51 View Period End	—	08:40:00*	—
22. TV Clock 16-Hour Pulse	09:30:12	09:30:36	S + 16 hours
23. Midcourse Maneuver Start (M)	—	10:00:39	M + 0
24. Roll Correction Start	10:00:44	10:00:45	—
25. Roll Correction End	10:01:37	10:01:38	—
26. Pitch Correction Start	10:10.09	—	—
27. Pitch Correction End	10:21:30	—	—
28. Midcourse Motor Ignition	10:27:09	10:27:09	M + 26.5'
29. Midcourse Motor Turn-off	10:28:08	10:28:11	—
30. Sun Reacquisition Command	10:30:39	10:30:40	M + 30'
31. Sun Reacquisition Complete	—	10:40:12	—

*Approximate time

TABLE 20
RANGER VIII MISSION EVENTS LIST (Continued)

Mission Event	Event Time (GMT)		Nominal Mission Time
	Predicted	Actual	
DAY 49 (Cont'd)			
32. Earth Reacquisition Command	10:58:39	10:58:40	M + 58'
33. Earth Reacquisition Complete	—	11:00:42	—
34. DSIF-41 View Period Start	—	12:00:00*	—
35. DSIF-12 View Period End	—	16:01:00*	—
36. TV Clock 24-Hour Pulse	17:31:00	17:30:48	S + 24 hour
37. SDIF-51 View Period Start	—	20:00:00*	—
DAY 50			
38. DSIF-41 View Period End	—	00:36:00*	—
39. TV Clock 32-Hour Pulse	01:31:00	01:30:52	S + 32 hours
40. DSIF-12 View Period Start	—	06:11:00*	—
41. DSIF-51 View Period End	—	07:30:00*	—
42. DSIF-41 View Period Start	—	12:00:00*	—
43. DSIF-12 View Period End	—	16:37:00*	—
44. TV Clock 48-Hour Pulse	17:31:00	17:31:08	S + 48 hours
45. DSIF-51 View Period Start	—	20:00:00*	—
DAY 51			
46. DSIF-41 View Period End	—	00:47:00*	—
47. DSIF-12 View Period Start	—	06:10:00	—
48. DSIF-51 View Period End	—	08:00:00*	—
49. Terminal Maneuver Start (T)	08:48:10	08:48:10	T + 0
50. Pitch Correction No. 1 Start	08:48:15	08:48:16	—
51. Pitch Correction No. 1 Complete	08:48:16	—	—
52. Yaw Correction Start	08:57:40	08:57:40	T + 9.5'
53. Yaw Correction Complete	08:57:41	—	—
54. Pitch Correction No. 2 Start	09:14:40	09:14:40	T + 26.5'
55. Pitch Correction No. 2 Complete	09:14:41	—	—
56. TV Clock 64-Hour Pulse	09:31:24	09:31:29	S + 64 hours
57. CC&S TV Turn On (Warm-up)	09:33:10	09:33:09	T + 45'
58. TV Full-Power On	09:34:30	09:34:28	T + 46' 20"
59. TV Full-Power Backup	09:38:10	—	T + 50'
60. TV Clock Warm-up	09:46:29	—	I - 11'
61. TV Clock Full Power	09:47:49	—	—
62. Impact	—	09:57:38.1	I

*Approximate time

Clock telemetry steps occurred on time within the Clock tolerance. A midcourse maneuver was initiated at approximately L + 17 hours during a Goldstone tracking station (DSIF-12) contact which began with two-way RF lock at 05:57:00 GMT on Day 49. Data from Goldstone indicated perturbations of the top-hat and lower-shroud temperatures as a result of the midcourse maneuver. The temperature of the top hat (data point No. 7 of the 15-point telemetry) increased to a peak of 110° F at 10:37:00 GMT; dropped to 79° F at 10:47:00 GMT; and then slowly increased to a stabilizing temperature of 84° F. The lower-shroud temperature (data point No. 8 of the 15-point telemetry) increased to a peak of 100° F at 10:37:00 GMT and then dropped rapidly to 80° F. When the midcourse maneuver was completed, the spacecraft was reoriented in its normal cruise-mode position, and within 16 hours, all temperatures of the TV Subsystem had returned to their pre-midcourse values.

The 24- and 32-hour Clock telemetry steps indicated that the Clock was operating slowly by approximately one second per hour, but well within specification. At the time of the 32-hour telemetry step, the Clock also provided an output signal which removed the Clock-output inhibit function and the RTC-5 Clock turn-off inhibit.* Thirty hours after launch, the temperatures of the TV Subsystem had stabilized at the following values:

- F_a Camera Lens Housing 65° F
- P-Channel Battery 80° F
- Top Hat (shroud) 84° F
- Lower Shroud 80° F
- F_b Camera Electronics 71° F

The display of analog telemetry data from DSIF-41 on the SDAT strip-chart recorder revealed about twelve noise spikes in the cruise-mode telemetry. Checks with the tracking station revealed that the origin of the noise was the communication link between SDAT and the DSIF-41 tracking station.

The 48-hour Clock telemetry step further confirmed a slow Clock operation of one second per hour. At this time, analysis of the battery capacities and temperatures indicated that the F- and P-Channel could operate in the full-power mode for 45 and 41 minutes, respectively, with the constraint being temperature.

4. Terminal Mode

An RTC-8 command was transmitted to the spacecraft which inhibited the terminal maneuver. An RTC-6 command was transmitted at 08:47:30 GMT of Day 51 to initiate the CC&S terminal sequence, which would result in turn-on of both television channels by CC&S command. Because of the sequence of events, the TV Clock would be used only as a backup command for F-Channel turn-on at Impact minus 11 minutes, if required. The 64-hour TV Clock step occurred about two minutes before the CC&S warm-up command. TV Subsystem was placed in warm-up mode by the CC&S TV-2 command at 09:33:09 GMT. The F- and P-Channels of the TV Subsystem were commanded into full-power operation by the outputs of the 80-second timers in the Camera Sequencer Assembly. The full-power backup command (TV-3), initiated by the CC&S five minutes after the TV-2 command, was not required. Video data were received at the Goldstone Station at 09:34:28 GMT. The TV Subsystem operated normally until impact, with video pictures of the lunar surface transmitted on both F- and P-Channels for 23 minutes and 10 seconds.

B. EVALUATION OF REAL-TIME DATA

1. General

As in the Ranger VII flight, 15-point telemetry was used in the cruise mode and 90-point telemetry was used for the terminal mode.

Figure 48 shows sample 15-point telemetry frames and defines the parameter monitored

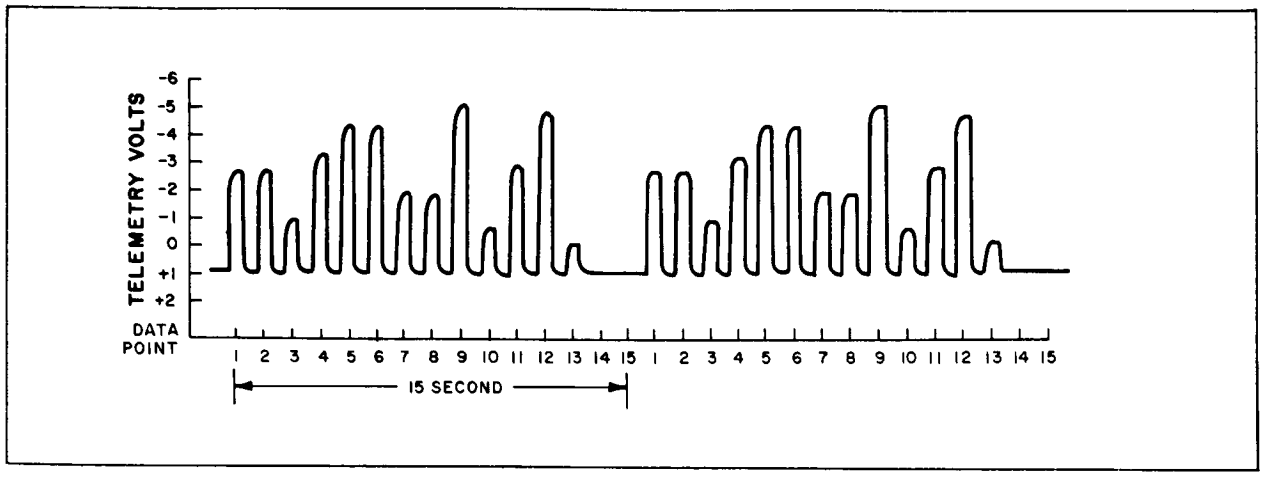

Figure 48. Sample Frames of Ranger VIII Cruise-Mode Telemetry Data from 15-Point Commutator

by each data point. When either F- or P-Channel of the TV Subsystem is turned on into the warm-up mode, the 15-point cruise-mode telemetry data are switched off Channel 8 and the diagnostic telemetry data sampled by a 90-point commutator are transmitted over Channel 8. The format for the 90-point commutator is similar to that of the 15-point commutator shown in Figure 48, with more and different parameters being sampled. The TV Subsystem parameters sampled by the 90-point commutator are identical to those of Ranger VII except that two of the Zero Reference points have been used to monitor F- and P-Transmitter IPA cathode currents, and the monitored F- and P-Transmitter IPA voltages have been reduced from -750 to -500 volts. As a backup function, the 90-point commutator also modulates a 225-kc voltage-controlled oscillator (VCO) whose output is transmitted over the P-Channel high-power Transmitter. Likewise, the telemetry data from the 15-point commutator are switched to and transmitted over the F-Channel high-power Transmitter on a 225-kc subcarrier.

Just before TV Subsystem turn-on in warm-up mode, the computer was programmed (switch to Mode 4) for the reception 90-point diagnostic telemetry data. The data outputs available to the TV Subsystem SDAT during terminal mode were:

- Strip-chart recording of the analog telemetry signal in real time;
- Real-time computer printouts of 13 selected telemetry points;
- Matrix printouts of all 90-point telemetry data about 1-1/2 to 2 minutes behind real time; and
- Telephone and administrative teletype messages of selected telemetry points are read out on the strip-chart recorders from the Goldstone tracking station.

After impact, complete computer tabulations and plots of the 90-point telemetry data were available.

2. SDAT Data Accuracy (Computer Output)

As with the Ranger VII flight, data point No. 9 of the 15-point telemetry (the Clock pulse) was selected as a reference and its incremental change was noted as a means of establishing the accuracy of the data from the various tracking stations. The telemetry from all tracking stations varied no more than 0.1 telemetry volt from the nominal value.

The telemetry points analyzed were data points No. 9 (Clock pulse), No. 2 (LCVR output), and No. 8 (lower-shroud temperature) of the 15-point telemetry. Computer-processed CCC data from analog information supplied by Woomera and Goldstone tracking stations exhibited a spread of less than 0.2 telemetry volt; data forwarded from the Johannesburg tracking station was comparable in accuracy.

3. Transition from Cruise-Mode to Terminal-Mode Telemetry

When warm-up mode of the TV Subsystem was initiated, 90-point diagnostic telemetry data were transmitted over Channel 8, as with the Ranger VII flight. A strip-chart recording of analog telemetry data transmitted over the F-Channel and Channel 8 and recorded at the Goldstone tracking station on Day 51 at 09:47:40 (approximately 10 minutes before impact) was examined for incremental changes in telemetry voltages. The results of this comparison are presented in Table 21.

4. Telemetry Evaluation of TV Subsystem Performance

The cruise-mode telemetry was employed to monitor TV Subsystem temperatures and power-supply operation. The actual temperatures of the TV Subsystem assemblies during cruise and terminal modes were almost exactly as predicted in preflight calculations, repeating the performance established by the Ranger VII flight.

The TV Subsystem power supply was of the design used on the Ranger VII flight and all units functioned normally throughout the mission.

At the start of F-Channel warmup, 90-point diagnostic telemetry data were transmitted over Channel 8. The signal profile from telemetry data point Nos. 55 and 60 (full-power commands) indicated that both channels went into warm-up mode for 80 seconds and were then turned on into full-power operation

TABLE 21
COMPARISON OF 15-POINT AND 90-POINT TELEMETRY READOUTS DURING TERMINAL MODE

Parameter Monitored	Telemetry Readout (Telemetry Volts)	
	15-Point (F-Channel)	90-Point (Channel 8)
F_a Camera Lens Housing Temperature	2.7	2.7
P-Battery Current	4.55	4.6
F-Battery Terminal Voltage	3.4	3.4
P-Battery Terminal Voltage	3.4	3.4
F-Battery Current	4.2	4.2
F_b Camera Electronics Temperature	2.9	2.9

by the Control Programmer and Camera Sequencer. The Transmitter telemetry data indicated normal supply voltages and operating temperatures for both channels. The Power-Amplifier cathode-current profiles for the Transmitters were almost identical to prelaunch full-power tests, thus confirming a high-power output for both channels. All telemetry indications for the TV Camera equipment were normal.

The telemetry data for the F-Channel Video Combiner output indicated that the video output was greater than expected.

The performance of the TV Subsystem telemetry was normal throughout the mission. The 90-point commutator had stopped on data point No. 70 at the end of the prelaunch test and started on the same point at the initiation of full power. It can be assumed that there was no movement of the commutator during cruise mode. Thus, on the basis of the analysis of the telemetry data, it may be concluded that the TV Subsystem performed a normal mission.

5. Operational Support Equipment

Approximately 72 hours before launch of the Ranger VIII Spacecraft, a complete alignment of the Ranger Operational Support Equipment (OSE) at the Echo site (DSIF-12) and Pioneer site (DSIF-11) of the Goldstone tracking station was ititiated. This alignment was performed in accordance with the procedures of the Ranger specifications as specified in the Ranger operational procedure. The data from the alignment procedures were submitted to JPL more than 24 hours before launch. No discrepancies were noted in any of the test data obtained.

After launch, an abbreviated check of overall OSE operation was performed before each pass of the Ranger VIII Spacecraft over the Goldstone tracking station. The pretrack checkouts were performed in accordance with Ranger operational procedure. No discrepancies were noted in the test data obtained.

The evaluation of cathode ray tubes (CRT) to select the most suitable units for use in the OSE film recorders during the Ranger VIII mission followed the same general procedures employed during previous Ranger missions. Curves for 35-mm film density as a function of CRT grid-drive voltage were obtained for eight selected cathode ray tubes, and a record of CRT performance was obtained with different lens f-stops on the 35-mm film cameras. All 35-mm film for the evaluation was developed to a gamma of 1.40, as determined from previous Ranger missions. The criteria utilized during the film-density calibration were:

- Black was defined as the lowest video signal (peak-to-peak voltage from sync tip) obtained with the TV camera lens capped. The G1 bias of the CRT was then adjusted to obtain a 35-mm film density of 0.4 ±0.05 for that video signal; and
- Peak white was defined as the highest peak white signal (peak-to-peak voltage from sync tip) given on the TV camera-calibration data sheets. The G1 gain of the CRT was then adjusted to obtain a 35-mm film density of 1.9 ±0.1 for that video signal.

C. FLIGHT MODEL III-3 (RANGER VIII) EQUIPMENT PERFORMANCE

1. General

The receipt of 7,140 high-quality television pictures of the lunar surface attests to the overall performance of the Flight Model III-3 TV Subsystem during the Ranger VIII mission, and in particular to the performance of the TV

Camera Assemblies. The telemetry data received throughout the Ranger VIII mission indicated that the thermal-control, power, and telecommunications equipment functioned as predicted from the results of prelaunch system tests. Proper operation of the control circuitry is evidenced by the fact that all commands were processed and executed on time and in good order.

The level of performance of the TV cameras and associated video processing equipment can be evaluated by a review of the 35-mm film and magnetic-tape recording of the video information obtained. The large bandwidth in the RF channel permits an accurate determination of all important parameters for the Camera Group. The quality of the pictures, the video-signal levels, and signal strength measured during the mission are used to evaluate the performance of the Communications Group. The Thermal Control and Power Groups are best evaluated from the telemetry received.

2. Camera Group

a. PICTURE ANALYSIS

(1) General

The four partial-scan and two full-scan TV cameras aboard the Ranger VIII Spacecraft obtained 7,140 pictures during the 23-minute 10-second full-power mode of the mission. All pictures were of good quality with the exception of the pictures obtained by the P2 Camera during the final 5 minutes of terminal-mode operation. The mesh of the vidicon in the P2 Camera became microphonic during this period, and although the microphonic signal was objectionable, there was very little loss of information. The microphonic signal produced a number of horizontal bars across the picture. The amplitude of these bars is less than 20 percent of the dynamic range, so that lunar-surface details are still visible in all frames.

The exposure settings of the cameras with 3-inch focal-length, f/2 lenses (F_b, P1, P2) provided balanced pictures during the entire mission, while the exposure settings of the cameras with 1-inch focal-length, f/0.95 lenses (F_a, P3, P4) provided optimum pictures only during the last 10 minutes of the mission. There was considerable compression of video in the "on-line" kinescope display of the F_a, P3, and P4 pictures during the first thirteen minutes of operation. There is, however, very little saturation in the video signals from the TV Cameras. This problem can be corrected by adjusting the drive signal to the OSE kinescope and recording video on 35-mm film from the playback of the magnetic tape.

The Camera Assemblies performed satisfactorily throughout the mission and would have met mission requirements for ground resolution if a terminal maneuver had been performed to align the common optical axis of the six cameras with the spacecraft velocity vector. Examination of film reproduced from magnetic tape playback revealed that impact occurred after 13 percent of a P4-Camera picture had been read out. The preceding picture from the P2 Camera represented an area of approximately 23 by 29 meters. Craters as small as 0.3 meter in diameter would have been visible; however, the lack of a terminal maneuver caused approximately 1.3 meters of smear in each of these partial-scan pictures. The last picture from the P1 Camera represented an area of approximately 56 by 70 meters, and would have shown craters as small as 0.75 meter in diameter. Table 22 lists the resolution, area coverage, and translational smear in each of the final 24 partial-scan pictures and the final four full-scan pictures. The geometry of the spacecraft approaching impact is presented in Figure 49.

(2) Final Partial-Scan Picture

The final partial-scan picture was a fragment from the P4 Camera and is shown in Figure 50. By use of a line selector, it was determined that impact occurred approximately 340

TABLE 22
CHARACTERISTICS OF FINAL PARTIAL-SCAN AND FULL-SCAN PICTURES

Camera	Time from Impact (msec)	Range (kilo-meters)	Emission Angle (degrees)	Resolu-tion (m/olp)*	Approximate Coverage (meters x meters)	Translational smear (meters)
P4	86.8	0.19	38.0	0.21	21 x 27	6.2
P2	286.8	0.627	37.0	0.233	23 x 29	5.6
P3	486.8	1.080	37.8	1.21	121 x 154	1.07
P1	686.8	1.5061	36.8	0.56	56 x 71	2.33
P4	926.8	2.07	38.0	2.31	231 x 294	0.56
P2	1126.8	2.48	37.8	0.93	93 x 118	1.40
P3	1326.8	2.95	37.8	3.30	330 x 420	0.39
P1	1526.8	3.355	36.8	1.25	121 x 159	1.04
P4	1766.8	3.95	38.0	4.42	442 x 560	0.30
P2	1966.8	4.33	37.0	1.61	161 x 205	0.81
P3	2166.8	4.83	37.8	5.40	540 x 686	0.24
P1	2366.8	5.203	36.8	1.94	195 x 248	0.67
P4	2606.8	5.83	38.0	6.53	653 x 830	0.20
P2	2806.8	6.18	37.0	2.31	231 x 293	0.56
P3	3006.8	6.70	37.8	7.50	750 x 950	0.17
P1	3206.8	7.05	36.77	2.63	263 x 333	0.50
P4	3446.8	7.70	38.0	8.63	863 x 1100	0.15
P2	3646.8	8.04	37.0	3.00	300 x 381	0.43
P3	3846.8	8.57	37.77	9.60	960 x 1220	0.14
P1	4046.8	8.895	36.75	3.32	332 x 422	0.39
P4	4286.8	9.58	38.0	10.70	1070 x 1360	0.12
P2	4486.8	9.89	36.94	3.69	369 x 470	0.35
P3	4686.8	10.44	37.75	11.7	1170 x 1500	0.11
P1	4886.8	10.74	36.74	4.00	400 x 510	0.32
F_a	2070.0	4.21	29.0	4.70	1880 x 2150	0.86
F_b	4650.0	10.99	41.9	4.10	1640 x 2200	0.43
F_a	7210.0	14.51	28.8	16.2	6500 x 7400	0.25
F_b	9770.0	23.06	41.8	8.6	3440 x 4600	0.21

m/olp: Resolution is given in meters per optical line pair

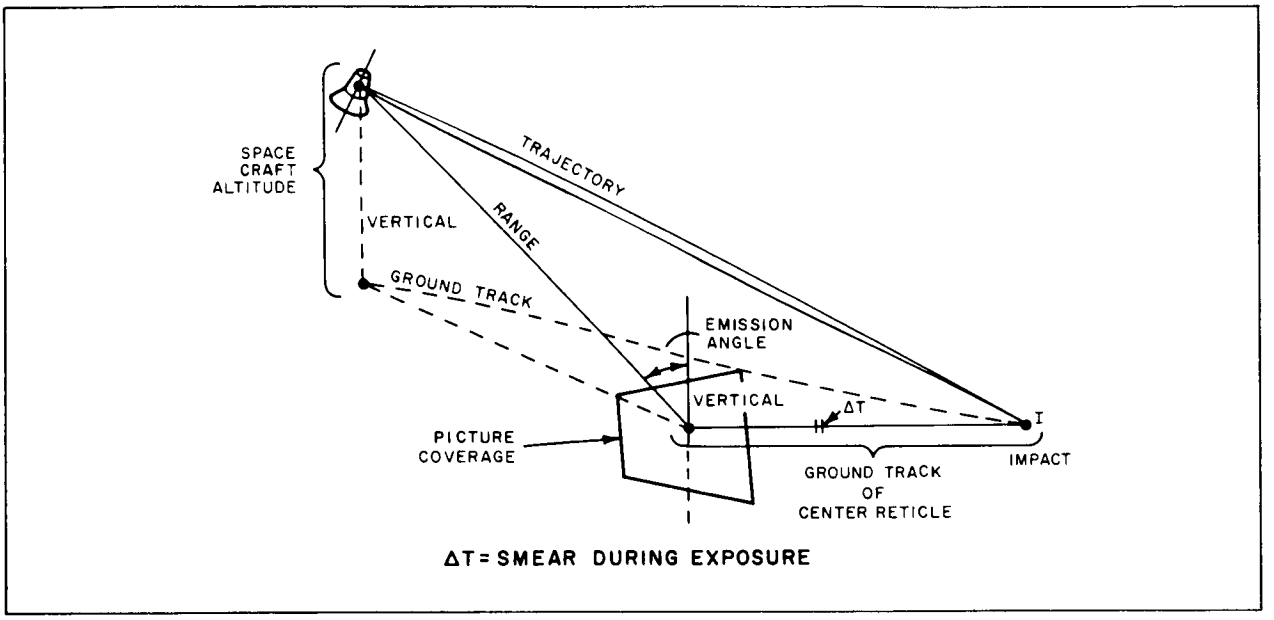

Figure 49. Ranger VIII Spacecraft Geometry Prior to Impact

microseconds after the start of scan line 036. By measuring the projected image, it was determined that 13 percent of the P4 picture had been read out at impact, or that approximately 25.1 milliseconds of the total 193-millisecond readout time of the P4 camera had been completed. Knowing the vertical-blanking time (6.6 milliseconds) and the time from the end of P4 shutter travel to the beginning of P4 Camera readout (55 milliseconds) that occurs during P2 Camera readout, the approximate time of P4 Camera exposure before impact can be determined:

25.1 milliseconds of P4 Camera video readout

6.6 milliseconds of vertical blanking

55.0 milliseconds during P2 Camera video readout

86.7 milliseconds; APPROXIMATE TIME OF P4 CAMERA EXPOSURE BEFORE IMPACT.

The 55-millisecond period during P2 Camera readout is an optimistic figure. The average time of this interval was measured as 60 to 65 milliseconds in tests performed at RCA, so that exposure may have taken place as much as 97 milliseconds before impact.

Computation of the distance from the camera to the lunar surface during shutter operation requires knowledge of the time of exposure before impact, the velocity vector of the spacecraft, and the orientation of the spacecraft with respect to the velocity vector. Spacecraft velocity is determined by tracking of radio signals from the spacecraft. Spacecraft orientation is determined from attitude data transmitted from the spacecraft, which is processed by a computer in the ground station to determine the lunar-surface features that will be photographed. Some inaccuracies exist in the computer printouts because of measurement precision and errors in the attitude-control system of the spacecraft.

Based on the information available, it was determined that the final picture from the P4 Camera was taken at a distance of 160 meters from the lunar surface.

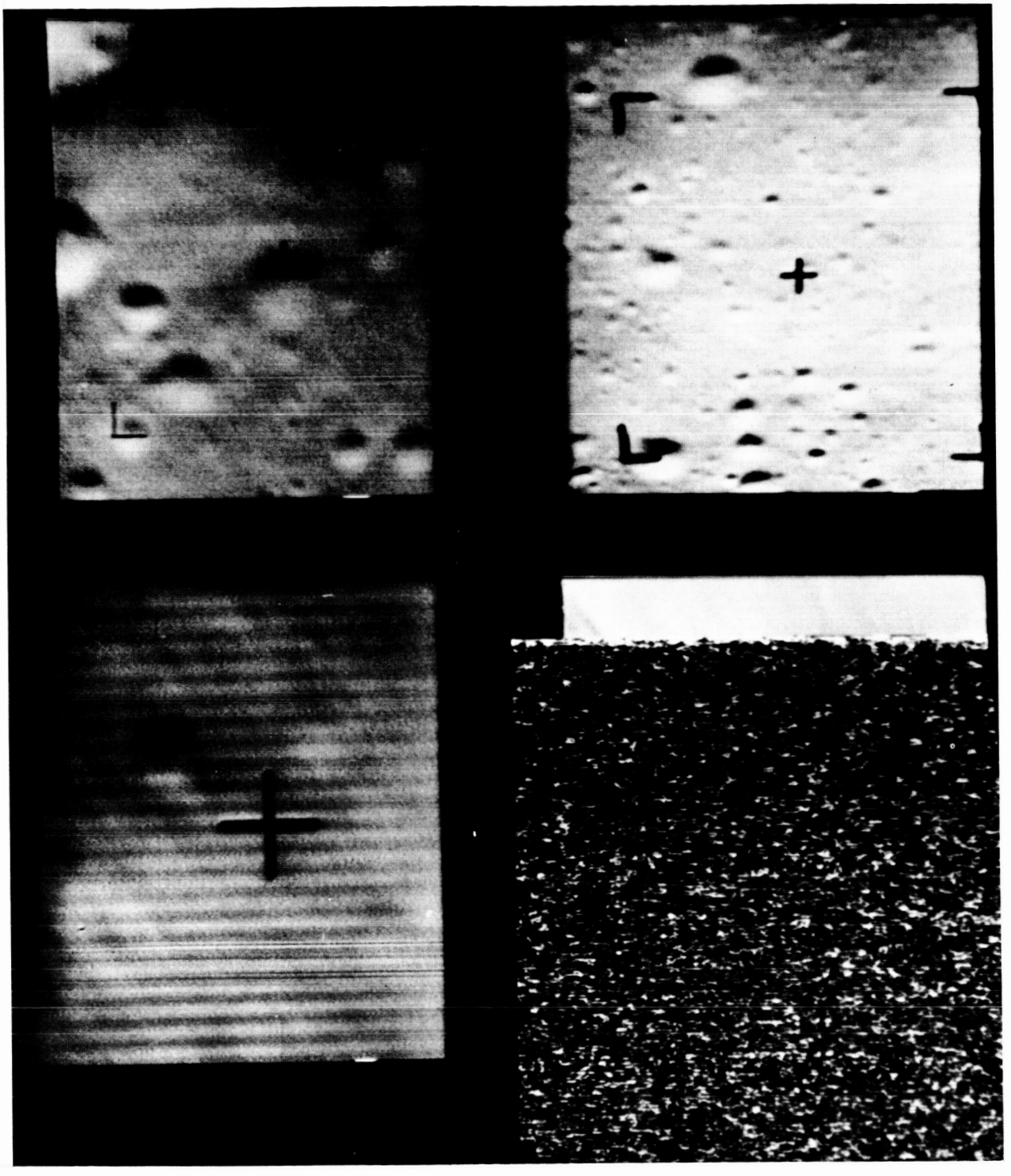

Figure 50. Ranger VIII Final Partial-Scan Pictures

(3) Final Full-Scan Picture

The final full-scan picture, shown in Figure 51, was taken by the F_a Camera. The line selector indicated that impact occurred on scan line 889, after 1.97 seconds of video had been read out. From the vertical blanking time (46 milliseconds) and the time from the end of F_a shutter travel to the start of F_a Camera readout (65 milliseconds) the approximate time of exposure of the final F_a Camera picture can be determined:

1.97	seconds of F_a Camera video readout
0.046	second of vertical blanking
0.065	second during F_b Camera video readout
2.08	seconds; APPROXIMATE TIME OF F_a CAMERA EXPOSURE BEFORE IMPACT.

The F_a Camera was approximately 3.7 kilometers from the moon at the time of the last exposure. The coverage provided by the last F_a-Camera picture was approximately 1.8 by 2.1 kilometers, and craters down to 6 meters in diameter could be seen. The translational smear in the final F_a picture was about 4 meters.

The final F_b picture, shown in Figure 52, was taken 2.56 seconds earlier, or 4.65 seconds before impact. This picture represents lunar-surface coverage of approximately 1.6 by 2.7 kilometers. The final F_b picture had only 1.7 meters of translational smear so that much more detail can be discerned than in the final F_a picture.

(4) Picture Nesting

Because a terminal maneuver of the Ranger VIII Spacecraft was not performed, the mission requirement of picture nesting was not accomplished. The fulfillment of picture nesting was based on the prerequisite that the common optical axis of the television cameras is aligned along the spacecraft velocity vector.

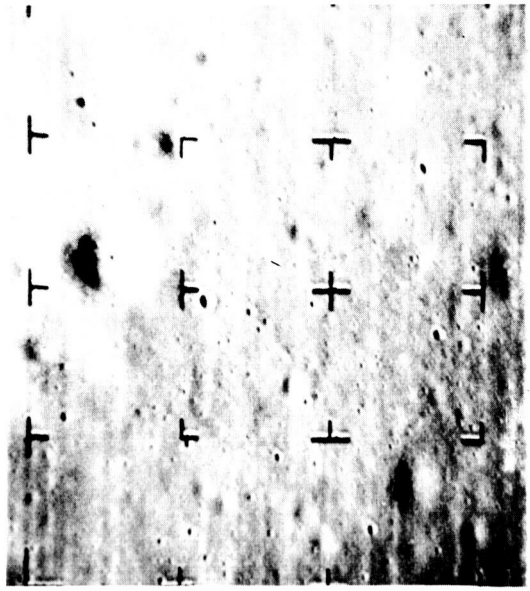

Figure 51. Ranger VIII Final F_a-Camera Picture

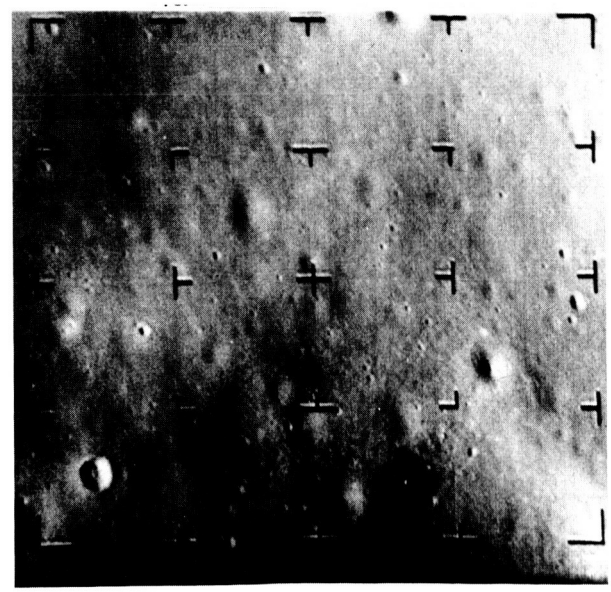

Figure 52. Ranger VIII Final F_b-Camera Picture

Although there was no nesting in the pictures, considerable coverage overlap existed in all but the final few pictures from the partial-scan cameras.

The pictures provided continuous coverage of the lunar surface over a distance of more than 750 miles, and more than 50 percent overlap existed in all pictures but those taken during the final 30 seconds. As the spacecraft approached the lunar surface, the degree of overlap in successive F_b pictures and successive F_a pictures was reduced. The overlap in the successive pictures decreases until the final picture is approximately tangent to the previous F_a picture. There is less reduction in picture overlap in the final F_b pictures. The field of view of the F_b Camera, however, does overlap the field of view of the F_a Camera, and the combined coverage of the F_a and F_b pictures provides more than 50 percent overlap on all pictures transmitted by the full-scan cameras. The overlap is high even in the last F_a and F_b pictures. Figures 53 through 58 show the lunar surface at successively closer ranges extending from seven minutes before impact to 0.4 second before impact of Ranger VIII.

b. EVALUATION OF CAMERA PERFORMANCE

An evaluation of camera performance during the Ranger VIII mission was made by reviewing 35-mm film copies of the Prime on-line Data (POD) and Secondary on-line Data (SOD). These data were analyzed to determine whether the camera performance during the mission deviated from the performance observed in prelaunch test at RCA, JPL, and ETR. In particular, the performance of the cameras during System Test No. 7, performed at ETR on February 6, 1965, was used as the basis of comparison.

(1) Image Degradation

Shutter-Induced Noise. - Review of the partial-scan data revealed the presence of some shutter-blade discharge noise. The noise was equally distributed between the video outputs of the P2 and P3 Cameras, and was limited to only a few of the 1600 frames of

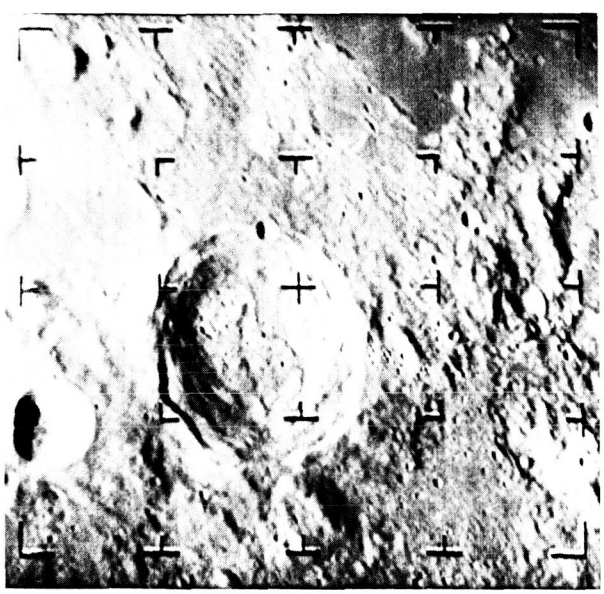

Figure 53. Ranger VIII F_b-Camera Picture Taken 7 Minutes Before Impact (470 miles altitude)

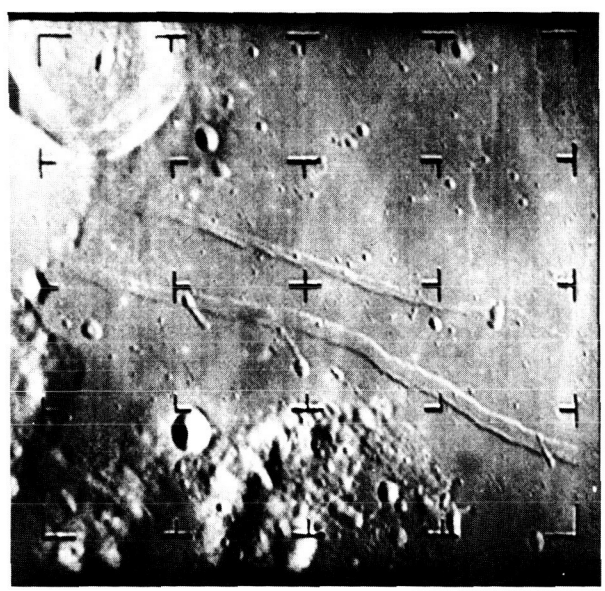

Figure 54. Ranger VIII F_b-Camera Picture Taken 4 Minutes Before Impact (270 miles altitude)

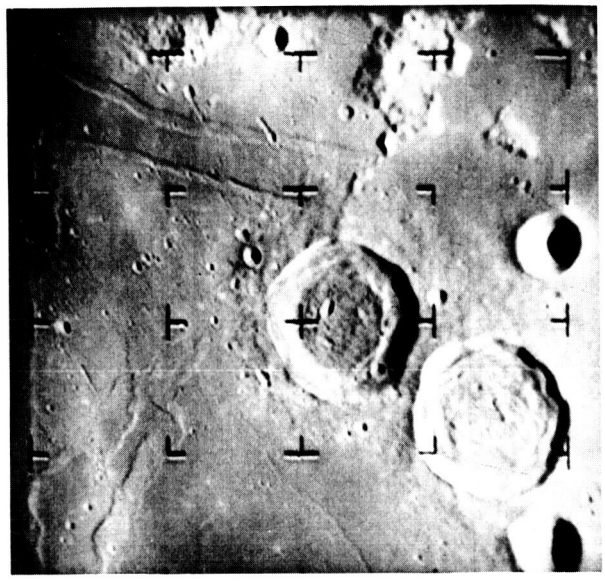

Figure 55. Ranger VIII F_a-Camera Picture Taken 2 Minutes 15 Seconds Before Impact (151 miles altitude)

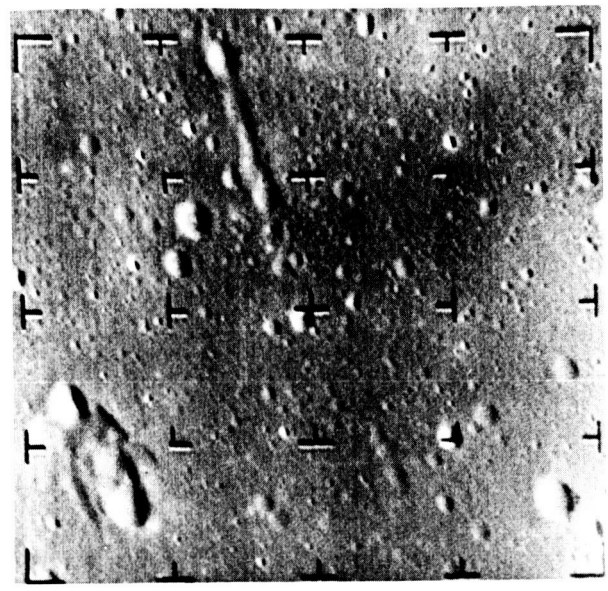

Figure 56. Ranger VIII F_b-Camera Picture Taken 45.6 Seconds Before Impact (50 miles altitude)

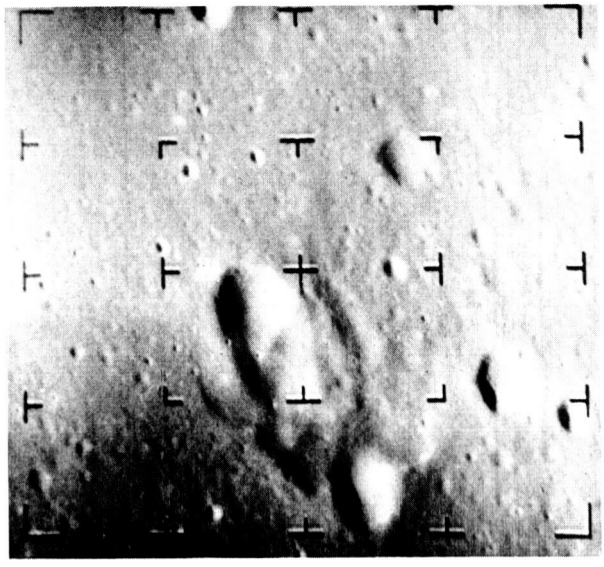

Figure 57. Ranger VIII F_b-Camera Picture Taken 25.13 Seconds Before Impact (27.5 miles altitude)

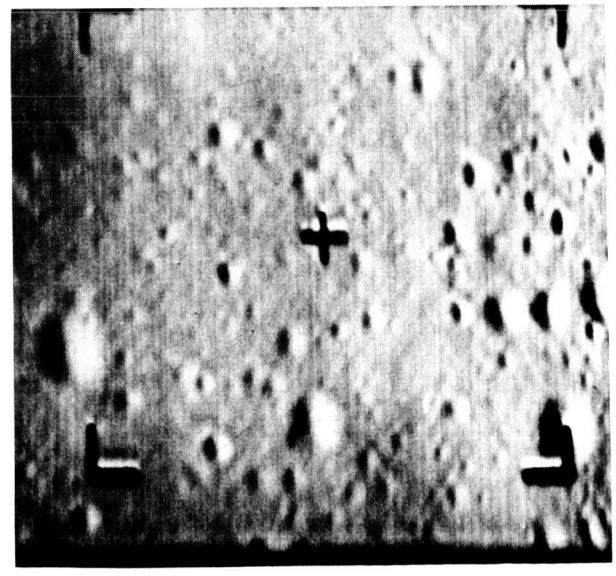

Figure 58. Ranger VIII P3-Camera Picture Taken 0.4 Second Before Impact (2400 feet altitude)

video data received. These fast noise pulses had been observed in test to be predominantly in time-coherence with the end-of-shutter stroke. They are induced into the video output by an electrostatic discharge from the shutter blade to the detent spring. When the shutter blade travels along the nyloc blade guide in the shutter assembly, it acquires an electrostatic charge. The blade then discharges when gravity causes it to contact the grounded detent spring.

The amount of shutter blade discharge noise observed in the P2 Camera video output was considerably less during the mission than in the system testing. Less than 1 percent of the P2 pictures contained shutter-blade discharge noise pulses compared with 40 percent during System Test No. 7. This reduction in noise was anticipated, based on the results of the Ranger VII mission compared with test results. The reduction is attributed to the fact that during a mission, the shutter is operating in a zero-gravity field so that no force existed to cause blade contact with the detent spring.

Vidicon and Nuvistor Microphonics. - The vidicon microphonic level of the P2 Camera was higher during the final 5 minutes of the Ranger VIII mission than the level observed during prelaunch system testing. The vidicon mesh of the P2 Camera became microphonic after 18 minutes of full-power operation. This problem was not experienced during the major portion of prelaunch testing since most simulated missions and tests entailed less than 15 minutes of camera operating time. During the tests at RCA, however, a 30-minute operational test of the P-Channel was performed. During this test, the P2 Camera exhibited a similar microphonic signal near the end of the test run. This camera also revealed some microphonic characteristics during thermal-vacuum testing at 95°F, which were similar to the performance experienced after 18 minutes of full-power operation during the Ranger VIII mission.

The 35-mm films of the P2 Camera video output were studied to determine the effect of the mesh microphonics on picture quality. The magnitude of the microphonics was judged subjectively by assigning a 0-to-10 rating to each video frame. With this technique of rating the severity of observed microphonics, a video frame assigned a rating of 10 exhibits severe microphonics; a level of 5 indicates moderate microphonics; and a level of 1 indicates that the microphonics are scarcely discernible. A picture assigned a rating of 10 would have horizontal bars going from black to white.

From the 1600 frames of P2 Camera video reviewed, 120 frames were assigned a microphonic level of 4 or 5, and 40 frames were rated at a level of 6, 7, or 8. Therefore, 160 video frames were found to have a moderate or objectionable level of mesh microphonics. Even with this number of microphonic frames, there was very little loss of video information, because the lunar scene changed very little in adjacent pictures. The microphonic level was not constant in a series of exposures, so there are nonmicrophonic pictures in each series of exposures of a given point on the lunar surface. Examples of P2 Camera video exhibiting moderate and severe levels of microphonics are presented in Figure 59.

15-Kilocycle Crosstalk. - Some 15-kc crosstalk noise was observed in the video output from the F_b Camera. This noise originates in the erase deflection circuitry of the F_a Camera. The F_b Camera is being read out while the F_a Camera is being erased and prepared for exposure. Part of the prepare cycle of the full-scan cameras involves increasing the vertical sweep read rate from 0.39 cps to 15 kc so that the scan-erase image is beyond the bandwidth of the scanning aperture and video amplifier. The sweep voltages must also be increased to ensure that a sufficient area of the photoconductor will be scanned at the 15-kc rate. The 15-kc signal present in the vertical deflection coil of the F_a Camera appears in the F_b Camera video output as a

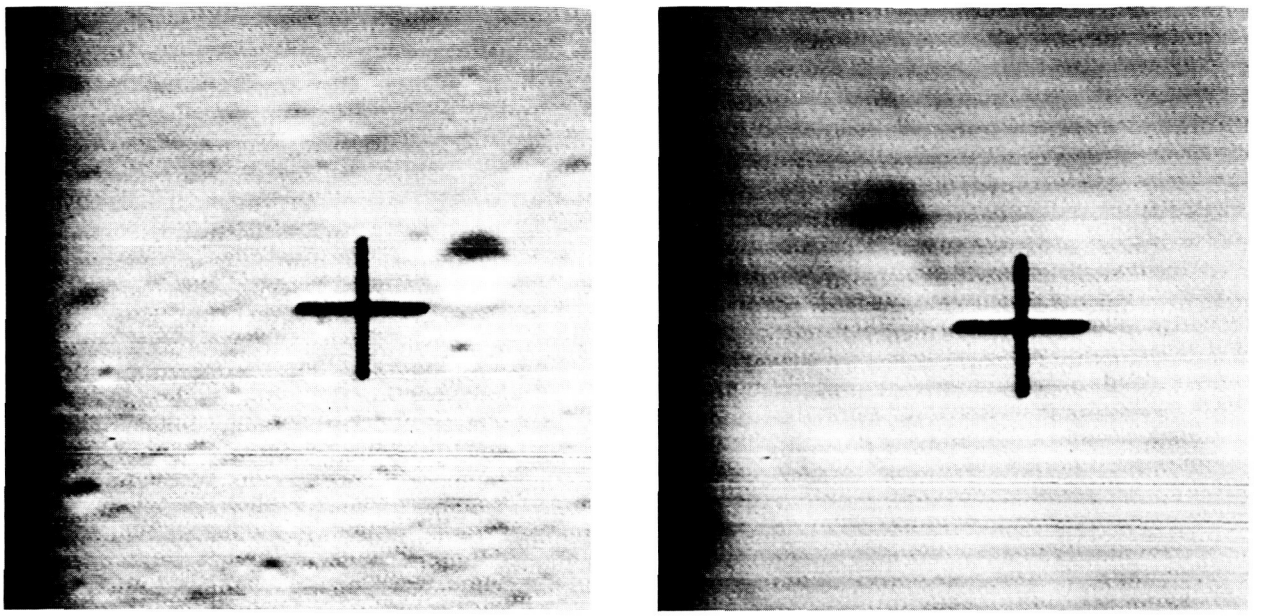

Figure 59. Examples of Ranger VIII P2-Camera Video Data Exhibiting Moderate and Severe Vidicon Microphonics

low-amplitude sine wave of 30 cycles on each horizontal scan line. The phase between the 15-kc signal and the horizontal sweep signal is nearly constant so the effect is the 30 vertical bands appearing on the picture. The amplitude of the crosstalk signal is generally less than 50 microvolts, peak-to-peak. The output of the F_a Camera was not affected by 15-kc crosstalk during the Ranger VIII mission.

(2) Shutter-Exposure Variations

The variations in exposure between the "in" and "out" strokes of the shutters were relatively minor during the Ranger VIII mission. The speed of the shutter blade is approximately the same for all cameras. The Ranger VIII shutters were selected to give uniform exposure, and much smaller variations were noted as compared to the Ranger VII mission.

(3) Residual Image

Very little or no evidence of any residual signal from previous exposures existed in the Ranger VIII video data. The partial-scan cameras displayed less than one percent of residual image. The pictures from the full-scan cameras also had very little residual image, and no residual information could be observed in the final full-scan pictures.

(4) Light Transfer Characteristics

Prior to launch, the light transfer characteristics of each Ranger VIII camera were determined. This was accomplished by measuring the response of the camera to a narrow white bar of known luminance. The response was measured at the center of the scanned format. The gains of the F_b, P1, and P2 Cameras were adjusted for a peak scene luminance of 1500 footlamberts, and the gains of the F_a, P3, and P4 Cameras were adjusted for a peak scene luminance of 650 footlamberts. The luminance of the calibration source was varied and the video excursions at the output of the distribution amplifier were recorded. Light transfer curves were plotted from the data recorded for each camera. A

tape playback of the video recorded during these tests was recorded on the 35-mm film copy of the video received during the mission. By using a densitometer, the luminance of points on the lunar surface can be determined approximately.

c. RANGER VIII CAMERA MODIFICATIONS

The several modifications incorporated into the cameras of the Ranger VIII TV Subsystem provided improved performance over the Ranger VII mission. Most of the modifications to the cameras were intended to reduce the level of microphonics experienced with particular cameras.

Some of the nuvistors used in the preamplifier circuit of the Ranger VIII cameras were preselected for minimum microphonic susceptibility. During the Ranger VIII mission, only the video output of the P3 Camera, for which the nuvistor was not specially selected, revealed any indications of nuvistor microphonics. In addition, the revised method of mounting the nuvistor in the camera head contributed to the reduction of microphonics. The use of polyurethane for encapsulating the nuvistor greatly reduced the sensitivity of the nuvistor to microphonics.

Another camera modification credited with suppressing the level of microphonics was the new-design shutter isolator installed on the Ranger VIII cameras. The modification involved a change of the shutter shock isolators from individual grommet configurations to a complete castellated-gasket configuration designed to provide an interference fit in the camera head. The new isolator was fabricated from blue polyurethane (Thiokol formulation 5).

The new technique for aligning the vidicon and focusing the cameras resulted in higher-resolution video data during the mission. The new technique, was developed after a shift of the best focal plane of the cameras, between ambient and vacuum conditions, was discovered during Ranger VIII prelaunch tests. An additional change in the location of the focal plane resulted from the thermal expansion and contraction of camera components. The new focusing technique minimized this problem by compensating for the anticipated change in focal length in vacuum. The cameras were focused at ambient condition with a 0.0025-inch shim installed between the lens and vidicon faceplate. When the shim was removed, the camera was properly focused for operation in a vacuum environment.

3. Thermal Control Group

The thermal configuration of the Ranger VIII TV Subsystem is identical to that of the Ranger VI and Ranger VII Subsystems.

a. FLIGHT TEMPERATURE PREDICTIONS

To predict the flight temperatures for Ranger VIII, the ratio factors determined from the analysis of the Ranger VI flight data were used. The determination of these factors is discussed earlier in this report. The equations used in the temperature calculations were derived from a least squares fit of spacecraft temperatures.

The energy input to the TV Subsystem was calculated by applying the ratio factors to the results of the calculations for the direct solar energy input, which was incident upon the top surfaces of the temperature-control fins. The ratio factors empirically account for reflections and deviations from predicted inputs as experienced in the Ranger VI flight. Table 23 summarizes these predictions and the telemetered cruise-mode temperatures.

b. THERMAL-CONTROL PAINTS APPLIED TO RANGER-VIII

The paints used on the fins of the Ranger VIII TV Subsystem were a mixture of PV-100 white paint and MIL-E-5557 type III black paint and are identified as light gray (RCA Drawing 1758619-29) and dark gray (RCA Drawing

1758619-30), respectively. Mixtures of the gray paints were prepared in November 1964 for use on the Ranger VIII TV Subsystem. In an effort to obtain the same flight temperatures on Ranger VIII as occurred on Ranger VII, the solar absorptivities of the paints were decreased. This decrease allowed for the increased solar constant at the time of the anticipated February launch. The desired values of solar absorptivity for the Ranger VIII paints were 0.48 and 0.67 as compared with 0.51 and 0.71 for Ranger VII. Samples of the paint were sent to JPL for measurement at STL.

c. SUMMARY

Temperatures of the five points monitored during cruise mode were all within 5°F of

TABLE 23
CRUISE-MODE EQUILIBRIUM TEMPERATURE PREDICTIONS FOR FLIGHT MODEL III-2

Location on TV Subsystem	Temperature Calculated by RCA Absorptivity		Temperature Calculated by JPL/STL Absorptivity[1]		Actual Flight Temperature (Telemetry, RA-8)	
	°C	°F	°C	°F	°C	°F
Thermal Shroud, Hat, (-Y side)	23	73	26	79	29	84
Camera Lens Housing	13	55	16	61	18	65
Thermal Shroud, (-Y side, below fin A)	21	70	24	75	26	79
P-Battery, Internal	20	68	23	73	27	80
Camera Electronics, (-Y side)	21	70	24	75	22	71
F-Channel Power Amplifier, (-X side, cavity end)	21	70	24	75	-	-
P-Channel Power Amplifier, (+X side, cavity end)	21	70	24	75	-	-
Camera Mounting Bracket	21	70	23	73	-	-
P-Channel HCVR, (+Y side)	17	63	20	68	-	-
P-Transmitter Power Supply, (+X side)	18	64	21	70	-	-
Temperature Control Plate (fin F)	30	86	33	91	-	-
Thermal Shroud, (+Y side, below fin A)	20	68	23	73	-	-
Thermal Shroud, (-Y side, between fins B & C)	26	79	29	84	-	-
Deck No. 3, (-Y side)	25	77	28	82	-	-
Deck No. 4, (-Y side)	21	70	24	75	-	-
Deck No. 5, (-Y side)	17	63	20	68	-	-

the midpoint of the predicted range of stabilized cruise-mode temperatures. Thus, the temperatures of the spacecraft were within the range of desirable operation for the initiation of terminal operation as verified during a number of tests at this same level. A comparison of test temperatures and flight temperatures for the same period of operation is listed in Table 24.

4. Telecommunications Group

a. RF POWER OUTPUT DURING TERMINAL MODE

Evaluation of telecommunications performance during the Ranger VIII mission is based on the RF power transmitted by the F- and P-Channel Transmitters. The data obtained during the Ranger VIII mission supports the contention that the communications performance compared closely with the results of prelaunch final system tests, which were nominal.

The results of the different power-measuring techniques used vary by ±1 db; however, this is of no consequence, since the received RF signal level was 10 db above receiver threshold. At such a strong signal level, the peak-to-peak signal-to-rms noise ratio was approximately 40 db, and no degradation of picture quality would have occurred as the result of a 1-db decrease in the received signal level.

Figure 60 is a plot of the power profiles for the F- and P-Channels that result from the diode-detector power-monitor technique, using full values of power losses provided by JPL. The power output for each minute of full-power operation is presented in Table 25. The power profile was excellent, as anticipated.

b. TRANSMITTER

Performance of the F- and P-Channel Transmitters can be evaluated by a review of operational characteristics during the mission.

(1) Center Frequency

The center frequency of the F-Channel carrier signal was 7 kc below nominal, as expected. The center frequency of the P-Channel carrier signal was 20 kc above nominal, as expected.

(2) Frequency Stability

The frequency of the F-Channel carrier drifted 7 kc during the 23 minutes of full-power operation. This was expected. The frequency of the P-Channel carrier drifted 8 kc during the first 2 minutes of full-power operation, and then only 3 kc for the remainder of the mission, as expected.

(3) Deviation

Deviation of the F- and P-Channel carriers was normal.

(4) Transient Response

The rise time of the F-Channel signal was normal. The rise time of the P-Channel signal was slow during the first half of terminal mode, but improved during the later half of the mission. This variation of rise time was not a serious problem, since trailing-edge sync timing is employed. The slow rise time of the P-Channel signal was the result of a negative rate response at higher frequencies, which goes positive after the modulator warms up.

c. TELEMETRY COMPONENTS

Performance of the telemetry components of the Communications Group can be evaluated by a review of the operating characteristics during the mission.

(1) Cruise Mode

All telemetry components operated satisfactorily during cruise mode. The center frequency of the Channel-8 3-kc voltage-controlled

TABLE 24
RA-8 TEST TEMPERATURES vs FLIGHT TEMPERATURES

Telemetry Point Location	III-3 Test, Cruise		III-3 Test, 23 Min Full Power		III-3 Test, 23 Min Full Power		RA-8 Flight, Stabilized Cruise Mode Prediction		RA-8 Actual Flight, Stabilized Cruise		RA-8 Impact, 23 Min Full Power	
	°C	°F	°C	°F	°C	°F	°C	°F	°C	°F	°C	°F
P-Channel Battery, Internal	24	75	27	80	30	86	24 ±5	75 ±10	26	79	29	84
F-Channel Battery, Internal	23	73	27	80	29	84	--	--	--	--	29	84
P-Channel Battery, External	23	73	26	79	29	84	--	--	--	--	29	84
F-Channel Battery, External	23	73	27	30	29	84	--	--	--	--	29	84
F_a Camera Lens Housing	28	82	28	82	28	82	16 ±5	61 ±10	18	64	24	75
Camera Mounting Bracket	27	80	27	80	27	80	--	--	--	--	28	82
Camera Electronics	29	84	37	98	39	102	19 ±5	66 ±10	21	70	27	80
Thermal Shroud Hat (-Y)	21	70	24	75	24	75	27 ±5	80 ±10	29	84	29	84
Thermal Shroud Lower (-Y)	25	77	32	89	35	95	24 ±5	75 ±10	26	79	33	91
Thermal Shroud Lower (+Y)	25	77	30	86	33	91	--	--	--	--	34	93
Bulkhead Near P-Channel P.A.	26	79	48	118	54	129	--	--	--	--	50	122
Bulkhead Near F-Channel P.A.	27	80	52	125	56	133	--	--	--	--	52	125
Deck 5 (-X, -Y)	21	70	27	80	30	86	--	--	--	--	34	93
Deck 4 (+Y)	25	77	32	89	35	95	--	--	--	--	36	97
Deck 4 (-Y)	26	79	35	95	33	102	--	--	--	--	38	100

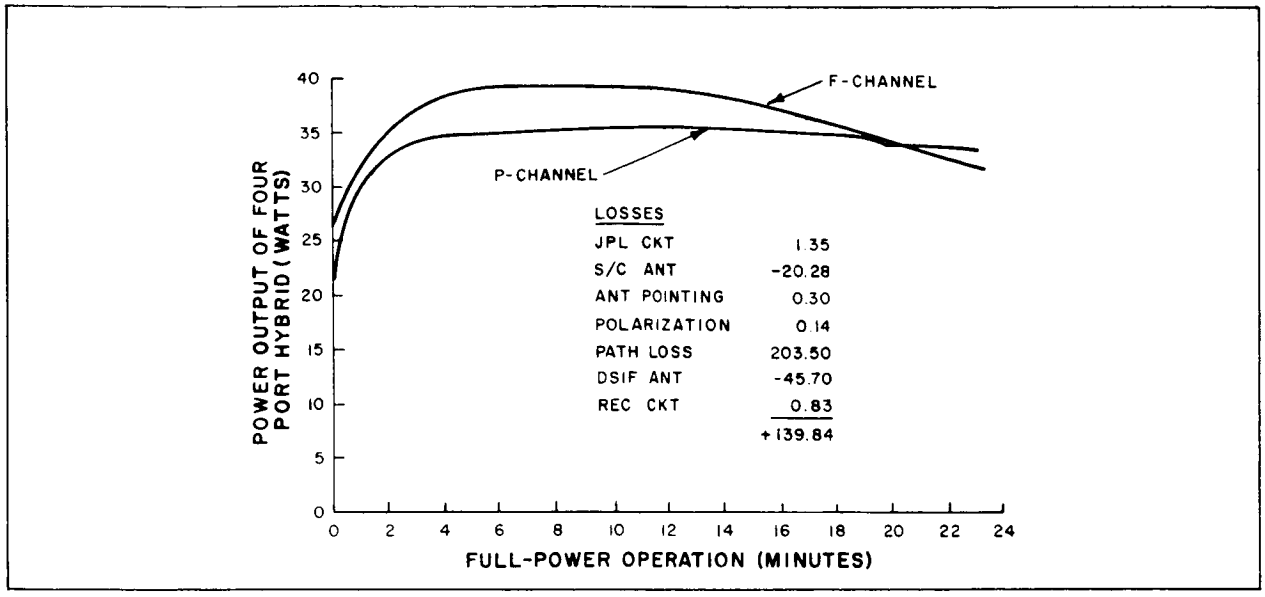

Figure 60. Ranger VIII F- and P-Channel Power Profile Throughout Terminal Mode

oscillator (VCO) was 3000 ± 1 cps, and had a deviation of approximately 95 cps. All 15-point telemetry data were normal and free of noise.

(2) Terminal Mode

The center frequencies of the F- and P-Channel 225-kc VCO's were 0.5 to 1.0 kc higher than nominal. However, the frequencies were within the linear range of the 225-kc discriminators in the ground station. The 15- and 90-point telemetry data received from the F- and P-Channel Transmitters were accurate and free of noise.

5. Controls Group

a. SATISFACTION OF MISSION REQUIREMENTS

Operation of Controls Group during the Ranger VIII mission was normal. TV Subsystem turn-on was accomplished by a CC&S warm-up command (TV-2) from the spacecraft Bus as part of the terminal-maneuver sequence. Full-power operation of the TV Subsystem was initiated by outputs from the F- and P-Channel 80-second timers in the Sequencer Assembly. No irregular or anomalous operation of the Controls Group was observed throughout the mission.

Some functions of the Controls Group, such as F- and P-Channel turn-off by RTC-5 command, and initiation of Subsystem warmup mode by Clock output or by RTC-7 command, were not exercised. Thus, no statement concerning the performance of these functions can be made.

b. EVALUATION OF PERFORMANCE

(1) Electronic Clock

The performance of the Electronic Clock during the Ranger VIII mission was satisfactory. The 64-1/4 hour count by the Clock was initiated by the closure of a microswitch in the spacecraft Bus at Agena-booster separation (S + 0).

All telemetry pulses from the Clock, up to and including the 64-hour pulse, occurred

TABLE 25
F- AND P-CHANNEL POWER OUTPUT DURING TERMINAL MODE

Minutes of Full-Power Operation	F-Channel Power Output		P-Channel Power Output	
	DBM	Watts	DBM	Watts
0	43.89	24.4	43.39	21.8
1	45.59	36.1	44.89	30.9
2	45.59	36.1	45.14	32.6
3	45.79	38.0	45.39	34.6
4	45.79	38.0	45.39	34.6
5	45.79	38.0	45.39	34.6
6	45.79	38.0	45.39	34.6
7	45.89	39.0	45.39	34.6
8	46.09	40.6	45.51	35.6
9	45.79	38.0	45.39	34.6
10	45.79	38.0	45.51	35.6
11	45.89	39.0	45.51	35.6
12	45.89	39.0	45.51	35.6
13	45.79	38.0	45.51	35.6
14	45.79	38.0	45.39	34.6
15	45.79	38.0	45.39	34.6
16	45.59	36.2	45.39	34.6
17	45.59	36.2	45.39	34.6
18	45.59	36.2	45.39	34.6
19	45.39	34.5	45.39	34.6
20	45.29	33.8	45.27	33.6
21	45.29	33.8	45.27	33.6
22	45.19	33.0	45.27	33.6
23	45.09	32.3	45.27	33.6

well within the specified time limits. Since TV Subsystem turn-on was not accomplished by the Clock output pulse, no positive indication of Clock turn-on was available.

Table 26 lists the predicted and actual elapsed time to each Clock telemetry pulse, beginning with Clock start at Agena booster separation.

The time for the Clock output pulse, determined by extrapolation, was assumed to have occurred after an elapsed time of 64 hours 16 minutes 15 seconds, or 75 seconds later than nominal, but well within the 5-minute tolerance.

A comparison of flight versus test performance of the Clock is presented in Table 27.

TABLE 26
PREDICTED AND ACTUAL ELAPSED TIMES[1] OF CLOCK TELEMETRY PULSES

Clock Telemetry Pulse	Time (GMT)	Elapsed Time from Clock Start(s)	
		Actual	Predicted
Start [2]	Day 48 - 17:30:14	S + 0	S + 0
1	Day 49 - 01:30:2	S + 7 h 59 m 58 s	S + 8 hrs.
2	Day 49 - 09:30:36	S + 16 h 0 m 24 s	S + 16 hrs.
3	Day 49 - 17:30:48	S + 24 h 0 m 34 s	S + 24 hrs.
4	Day 50 - 1:30:38	S + 32 h 0 m 38 s	S + 32 hrs.
5	Day 50 - 17:31:08	S + 48 h 0 m 54 s	S + 48 hrs.
6	Day 51 - 09:31:39	S + 64 h 1 m 15 s	S + 64 hrs.

[1] *Measurement accuracy is +0, −15 seconds.*

[2] *Time of Agena-booster separation. No telemetry is available for this event due to lack of ground-station visibility.*

TABLE 27
COMPARISON OF FLIGHT AND TEST PERFORMANCES OF ELECTRONIC CLOCK

Test	Operating Temperature (°F)	Performance*
Unit Flight Acceptance Test	32	64-1/4 hours - 33 sec
	131	64-1/4 hours + 86 sec
Clock Time Test on TV Subsystem	72	64-1/4 hours + 62 sec
Mission	71	64-1/4 hours + 75 sec

**Measurement accuracy is + 0, −15 seconds.*

(2) 80-Second Timer Circuits

The F- and P-Channel 80-second timers in the Sequencer Assembly performed satisfactorily during the mission to initiate full-power transmission.

The count of the 80-second timers was initiated by the CC&S warmup command from the Spacecraft Bus as part of the terminal-maneuver sequence. Timer periods observed during the mission are given in Table 28. The accuracy of the individual observations is within ±0.100 seconds, resulting in a maximum error of 0.200 for the nominal timer period. Comparison of flight and test performances for the 80-second timers is presented in Table 29.

(3) Command Control Unit (CCU)

Operation of the Command Control Unit was normal during the Ranger VIII mission. Cruise-mode turn-on was accomplished 15 minutes prior to launch through the "Cruise on Test" umbilical line to the Command Control Unit.

Clock turn-on was also performed through the CCU by means of a microswitch closure on the Clock-start input line at Agena-booster separation.

(4) Distribution Control Unit (DCU)

All command and control functions of the Distribution Control Unit, which were exercised, were performed satisfactorily during the mission.

TABLE 28
80-SECOND TIMER PERIODS DURING RA-8 MISSION

	Start Warmup (GMT)	Start Full Power (GMT)	Timer Period (seconds)
P-Channel Timer	09:33:09	09:34:28	79.0
F-Channel Timer	09:33:09	09:34:31	82.0

TABLE 29
COMPARISON OF FLIGHT AND TEST PERFORMANCES OF F- AND P-CHANNEL 80-SECOND TIMERS

	Temperature (°F)	P-Channel	F-Channel
Unit Flight Acceptance Test	32	78.83	81.86
	131	80.15	81.77
RA-8 Mission Test*	95	79.0	82.0
RA-8 Actual Mission*		79.0	82.0

* *Measurement accuracy is ± 1.0 second.*

(5) HCVR Control Module

All portions of the HCVR control module, which were exercised, performed satisfactorily. The turn-on fail-safe features incorporated in this module functioned in a proper manner.

6. Power Group

The Power Group of the Ranger VIII TV Subsystem consisted of the F- and P-Channel Batteries, the F- and P-Channel High-Current Voltage Regulators (HCVR), and the Low-Current Voltage Regulator (LCVR). The performance of all assemblies of the Power Group was normal during the Ranger VIII mission.

a. BATTERIES

The F- and P-Channel Batteries performed normally throughout the mission. Figure 61 shows the budgeted and expended power capacities of the F- and P-Channel Batteries for each phase of the Ranger VIII mission. A capacity of 29.1 ampere-hours was budgeted for the F-Channel Battery. Of that amount, a total of 13.3 ampere-hours was expended during the mission. The cruise-mode output voltages of the F- and P-Channel Batteries are shown in Figure 62. Under the no-load conditions at launch, the F-Channel Battery voltage was 35.5 volts. From Clock start (L + 23 minutes) until F-Channel turn-on, the F-Battery supplied 40 milliamperes of current to operate the TV Subsystem Clock. There was not a sharp drop in the F-Battery voltage at Clock start, but the voltage did decrease gradually throughout cruise mode. The Battery reached a plateau voltage of 34.9 volts at launch plus 11 hours and remained at that level until warm-up mode. At initiation of F-Channel warm-up, the F-Battery output dropped to 33.3 volts at a current drain of 8.0 amperes; and during full-power operation, the output dropped to 32.5 volts at a current drain of 13 amperes. The output-voltage profiles for the F- and P-Channel Batteries are shown in Figures 62 and 63 for cruise and terminal mode, respectively.

For P-Channel, the budgeted Battery capacity was 34.5 ampere-hours, while 24.0 ampere-hours of that amount was actually expended during the mission. The prelaunch voltage of the P-Channel Battery was 37.9 volts. During

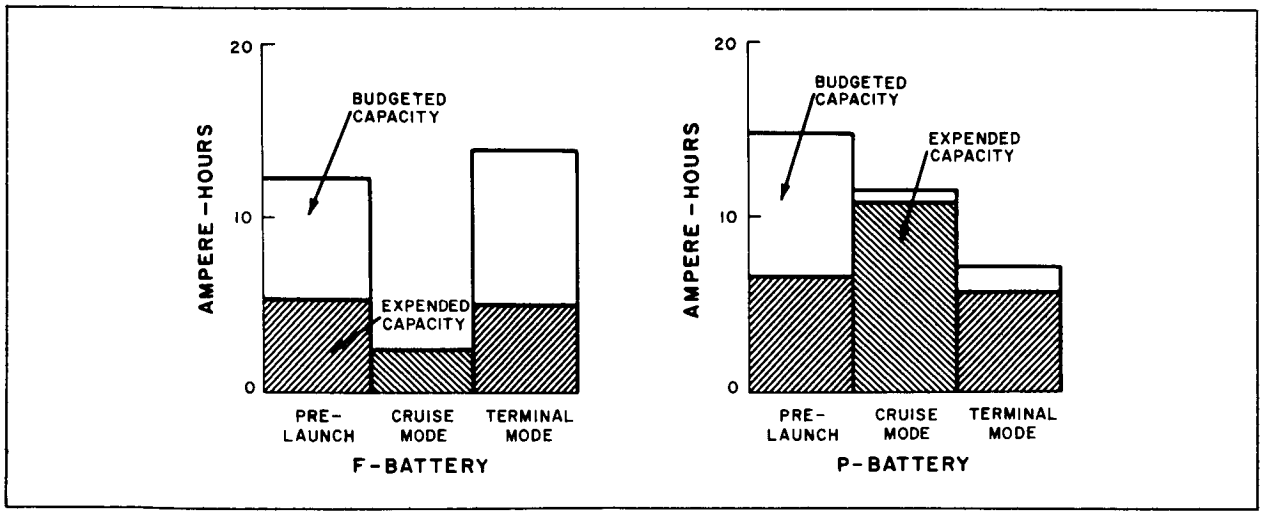

Figure 61. Ranger VIII F- and P-Channel Budgeted and Actual Battery Capacities

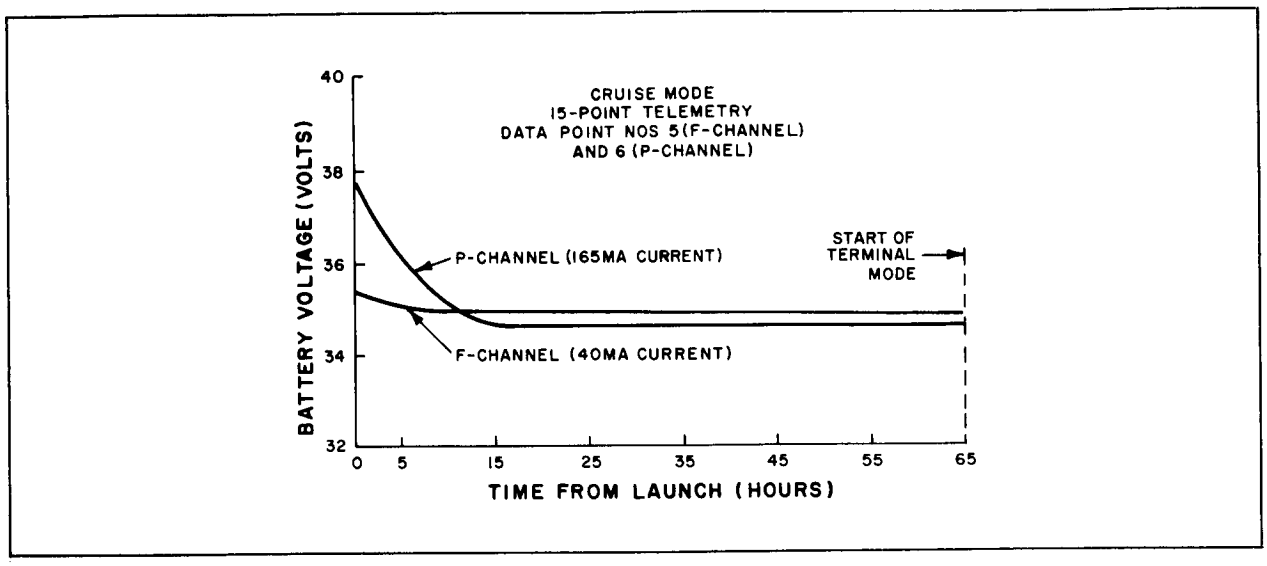

Figure 62. Ranger VIII F- and P-Battery Output Voltages During Cruise Mode

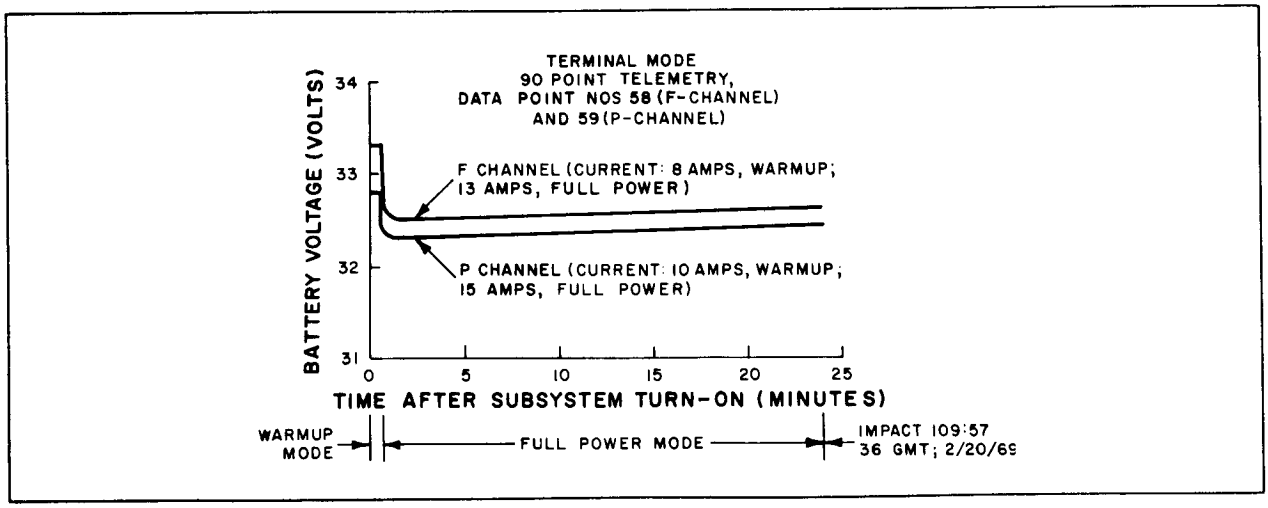

Figure 63. Ranger VIII F- and P-Battery Output Voltages During Terminal Mode

cruise mode, the P-Channel Battery provided the power to operate the cruise-mode telemetry circuitry, which provided a current drain of 165 milliamperes. At launch plus 16 hours, the P-Channel Battery had reached a plateau of 34.6 volts and remained at this level until P-Channel warm-up. At initiation of warm-up mode, the P-Battery output voltage dropped to 32.8 volts at a current drain of 10 amperes. At full-power operation of P-Channel, the P-Battery voltage decreased to an output of 32.3 volts at a current drain of 15 amperes.

b. VOLTAGE REGULATORS

The outputs of the Low-Current Voltage Regulator (LCVR) and the F- and P-Channel High-Current Voltage Regulators (HCVR) were

constant during their respective periods of operation. The output of the Low-Current Voltage Regulator was -27.4 volts throughout the mission. The F- and P-Channel High-Current Voltage Regulators each provided an output of -27.65 volts during full-power operation. These outputs were well within the specified output of -27.5 ± 0.5 volts.

The performance of the High-Current Voltage Regulators during the Ranger VIII mission was consistent with the performance observed during prelaunch testing. Table 30 presents a comparison of the mission and prelaunch test performances. The differences observed in the outputs of the regulated voltages are probably due to reading accuracy.

TABLE 30
COMPARISON OF PERFORMANCE OF HIGH-CURRENT VOLTAGE REGULATORS DURING PRELAUNCH TESTING AND RA-8 MISSION

	Environment		Voltage	
	Pressure (mm Hg)	Temperature (°F)	Unregulated Input (volts)	Regulated Output (volts)
F-Channel High-Current Voltage Regulator				
Unit Test	10^{-5}	32	-33.0 -30.5	-27.69 -27.20
	10^{-5}	131	-33.0 -30.5	-27.61 -27.09
Mission Verification Test Number 3 (No wires test)	10^{-5}	75	-32.08	-27.5
Mission	Space		-32.5	-27.65
P-Channel High-Current Voltage Regulator				
Unit Test	10^{-5}	32	-33.0 -30.5	-27.6 -27.6
	10^{-5}	131	-33.0 -30.5	-27.79 -27.77
Mission Verification Test Number 3 (No wires test)	10^{-5}	75	-31.85	-27.45
Mission	Space		-32.4	-27.45

Section V
Ranger IX Mission Evaluation

A. SUMMARY OF RANGER IX MISSION

1. Prelaunch

Approximately 3 hours before launch, the TV Subsystem was turned on in the reduced power mode for a final system check. Telemetry and video indications were normal except for one telemetry temperature sensor, which was recalibrated at this time. The countdown continued; at launch minus 25 minutes, cruise-mode telemetry was turned on. The telemetry data, evaluated by both the ETR launch team and the TV Subsystem analysis group, indicated that all assemblies of the TV Subsystem were functioning normally.

2. Launch

The Ranger IX Spacecraft was successfully launched from the ETR at 21:37:02 GMT on March 21, 1965 (Day 80). The launch was accomplished by an Atlas-Agena launch vehicle. The complete Ranger IX mission events list is presented in Table 31. At launch, the umbilical cable was disconnected from the launch vehicle, removing the full-power-inhibit circuit, which permitted only a reduced-power Subsystem output of approximately 125 milliwatts. The TV Subsystem telemetry data received by the analysis group from the ETR during launch confirmed that the TV Subsystem parameters were normal during the entire launch phase. The tracking station at Johannesburg acquired the spacecraft approximately 22 minutes after launch and started sending telemetry data to SDAT. The spacecraft entered the Earth's shadow at approximately the time of Johannesburg acquisition and remained in the shadow for 33 minutes. The temperature sensors located on the external shrouds of the TV Subsystem indicated the resulting decrease in temperature during this time.

3. Cruise Mode

Agena-booster separation occurred at launch (L) plus 15.4 minutes and generated a command to the TV Subsystem Clock to start its 63.5-hour count. Clock turn-on was verified on cruise-mode telemetry. Agena-booster separation also provided a backup for the removal of the full-power-inhibit circuit, and started a mechanical timer that provided backup functions for the spacecraft. One of these functions was to enable the silicon-controlled rectifier (SCR) gates in the TV Subsystem High-Current Voltage Regulators at separation (S) plus 30 minutes. Approximately 15 minutes after separation, the spacecraft solar panels were deployed and activated a microswitch which provided a backup circuit to enable the SCR gates. At L+70 minutes, spacecraft acquisition of the Sun was accomplished, and 2 hours and 24 minutes later, Earth acquisition occurred. Thus, the spacecraft was oriented in its normal cruise-mode position, with the z-axis pointing toward the Sun and high-gain antenna pointing toward the Earth. The 15-point telemetry continued to indicate normal performance with the 8- and 16-hour Clock telemetry steps occurring at the predicted times. Midcourse maneuver was initiated at approximately L+40 hours. The 15-point telemetry data from the TV Subsystem were interrupted for 10 minutes and 43 seconds during midcourse maneuver so that propulsion and attitude-control information could be transmitted over Channel 8. The midcourse maneuver consisted of a roll turn of 27.4° and then a pitch turn of +127.9°. Thus, the -y shroud and top hat surfaces were oriented toward the Sun and rose to a peak temperature of 98 and 124° F respectively

TABLE 31
RANGER IX MISSION EVENTS LIST

Mission Event	Event Time (GMT)		Nominal Mission Time
	Predicted	Actual	
Day 80			
Prelaunch Test On		17:56:00	T-221 min
Prelaunch Test Off		18:01:01	-
Cruise-Mode Telemetry On	-	20:41:31	T-55.5 min
Spacecraft on Internal Power	21:32:00	21:32:03	T-5 min
CC&S Uninhibit	21:35:00	21:35:00	T-2 min
CC&S Clear	21:36:00	21:36:00	T-1 min
Launch (L)	21:37:01	21:37:02	T = L = 0
Enter Earth's Shadow	-	21:50:22	-
Spacecraft/Agena Separation (S)	21:52:30	21:52:26	-
TV Clock Start	21:52:30	21:52:26	S = 0
DSIF-51 View Period Start	-	21:59:33	-
Transmitter Power Up	22:00:00	-	L+23
Leave Earth's Shadow	-	22:24:01	-
Solar Panels Extend Command	22:37:00	22:37:01	L+60 min
Solar Panels Extended	22:37:47	22:37:51	-
Sun Acquisition Command	22:40:00	22:40:01	L+63 min
Sun Acquisition Complete	-	22:47:30	-
DSIF-41 View Period Start	-	22:56:45	-
Day 81			
DSIF-41 View Period End	-	00:57-56	-
Earth Acquisition Command	01:08:00	01:08:02	L+211 min
Earth Acquisition Complete	-	01:11:50	-
TV Clock 8-Hour Pulse	05:52:33	05:52:36	S+8 hours
DSIF-12 View Period Start	-	08:28:39	-
DSIF-51 View Period End	-	09:41:49	-
DSIF-41 View Period Start	-	13:34:48	-
TV Clock 16-Hour Pulse	13:52:39	13:52:47	S+16 hours
DSIF-12 View Period End	-	17:35:44	-
DSIF-51 View Period Start	-	21:02:44	-
TV Clock 24-Hour Pulse	21:52:55	21:52:54	S+24 hours
Day 82			
DSIF-41 View Period End	-	02:59:55	-
TV Clock 32-Hour Pulse	05:53:01	05:53:01	S+32 hours

TABLE 31
RANGER IX MISSION EVENTS LIST (Continued)

Mission Event	Event Time (GMT)		Nominal Mission Time
	Predicted	Actual	
Day 82 (Cont'd)			
DSIF-12 View Period Start	-	08:51:09	-
DSIF-51 View Period End	-	10:22:48	-
Midcourse Maneuver Start (M)	12:03:39	12:03:40	M = 0
Roll Correction Start	12:03:44	12:03:46	M+5 sec
Roll Correction End	12:05:52	12:05:52	-
Pitch Correction Start	12:13:10	12:13:09	M+9.5 min
Pitch Correction End	12:22:57	12:22:57	-
Midcourse Motor Ignition	12:30:10	12:30:09	M+26.5 min
Midcourse Motor Turn-off	12:30:40	12:30:40	-
Sun Reacquisition Command	12:33:40	12:33:40	M+30 min
Sun Reacquisition Complete	12:42:40	12:42:20	-
Earth Reacquisition Command	13:01:40	13:01:40	M+58 min
Earth Reacquisition Complete	13:41:40	13:02:40	-
DSIF-41 View Period Start	-	13:57:45	-
DSIF-12 View Period End	-	18:06:10	-
DSIF-51 View Period Start	-	21:17:41	-
TV Clock 24-Hour Pulse	21:53:15	21:53:28	S+24 hours
Day 83			
DSIF-41 View Period End	-	03:14:40	-
DSIF-12 View Period Start	-	08:55:27	-
DSIF-51 View Period End	-	10:33:01	-
RTC-6 Command Sent	-	13:02:34	T-40 sec
Terminal Maneuver Start (T)	13:03:13	13:03:15	T = 0
Pitch Correction No. 1 Start	13:03:20	13:03:20	T+5 sec
Pitch Correction No. 1 Complete	13:03:44	13:03:44	-
Yaw Correction Start	13:12:44	13:12:44	T+9.5 min
Yaw Correction Complete	13:13:59	13:13:59	-
RTC-5 Command Start	13:17:00	13:17:00	-
TV Clock Off	-	13:17:38	-
Pitch Correction No. 2 Start	13:29:44	13:29:44	T+26.5 min
Pitch Correction No. 2 Complete	13:31:18	13:31:17	-
CC&S TV Turn-on (Warm-up)	13:48:14	13:48:13	T+45 min
TV Full-Power On	13:49:34	13:49:34	-
RTC-7 Command (Not Used)	13:53:14	-	T+50 min
DSIF-41 View Period Start	-	14:03:01	-
Impact	14:08:20	14:08:20*	I

*This time is actual impact time (1.3 seconds transmitting time was subtracted from end of data time)

during the pitch turn. At the end of midcourse maneuver, the spacecraft was reoriented in its normal cruise-mode position, and 1 hour later, the temperatures of the TV Subsystem had returned to the pre-midcourse values.

The 24- and 32-hour Clock telemetry steps occurred on time. At the time of the 32-hour step, the Clock also provided an output signal, which removed the Clock-output inhibit and the RTC-5 Clock turn-off inhibit. Forty-five hours after launch, the TV Subsystem temperatures stabilized at the following values:

- F_a Camera Lens Housing 65° F
- P-Channel Battery 78° F
- Top Hat (shroud) 79° F
- Lower Shroud 77° F
- F_b Camera Electronics 70° F

The 48-hour Clock telemetry signal occurred 62 (+0, -15) seconds late. This indicated that the Clock was running slow but well within the 5-minute overall tolerance.

4. Terminal Mode

The following information was used to determine the sequence of terminal events:

- The experimenters reported that pictures taken before approximately 18 minutes to impact would be no better than earth-based photographs.
- The spacecraft was functioning normally and could be expected to perform a normal terminal maneuver.
- The TV Subsystem was functioning normally. Analysis of the battery capacities and Subsystem temperatures indicated that the F- and P-Channels could operate in the full power mode for 60 and 30 minutes, respectively. However, it was noted that for these times, the final transmitter temperatures would be 5 to 10 degrees F higher than any temperatures seen during Ranger IX testing but not higher than temperatures on the PTM and QTM units during testing.

Based on the above, it was decided that the clock would be turned off after proper operation of the CC&S had been verified during spacecraft terminal maneuver, so that the CC&S could be relied on to turn on the TV Subsystem. If there were any doubt about the command link or the operation of the CC&S unit, the RTC-5 command was not to be sent. In order to send the RTC-5 command between the end of the yaw turn and the predicted Clock turn-on, the terminal maneuver was started at I-65 minutes instead of I-60 minutes.

The RTC-6 command was sent at 13:02:34 to start the spacecraft CC&S counter which supplies the terminal-maneuver commands to the attitude control system, and the warm-up (turn-on) and backup full-power commands to the TV Subsystem. The RTC-5 command was sent at 13:17:00 to turn off the TV Subsystem Clock. Upon receipt of the RTC-5 command by the spacecraft, the Clock and F-Channel Battery current telemetry readings went to 0 and the F-Channel Battery voltage increased approximately 0.5 volt indicating that the Clock had been turned off. At the predicted time of 13:48:13, the spacecraft CC&S commanded the F- and P-Channels into warm-up mode, and, 80 seconds later, each channel was switched into full power by the associated Camera Sequencer. For the next 19 minutes, both channels transmitted video pictures of the lunar surface.

B. EVALUATION OF REAL-TIME DATA

1. General

The 15- and 90-point telemetry formats are identical to those of Ranger VIII. As with the preceding successful flights, 15-point telemetry was used during the cruise portion

of the flight, and the computer was programmed for the 90-point diagnostic telemetry data at about one minute before TV Subsystem turn-on for entry into the terminal mode.

2. SDAT Data Accuracy

Cruise-mode telemetry data from Woomera, Goldstone, and Johannesburg tracking stations were plotted as minimum and maximum values sampled every hour, as in the preceding flights. The telemetry points plotted, to provide calibration of the various data stations, were the clock pulse (15-9), the LCVR (15-2), and the lower-shroud temperature (15-8). All stations varied no more than 0.1 volt from the nominal value. A comparison of the electronic clock telemetry readings between S+32 and S+48 hours is given in Table 32.

3. Comparison of 15- and 90-point Telemetry

When the TV Subsystem was placed into warm-up, the 90-point telemetry data were transmitted over the spacecraft Channel 8. Since these ninety points include values for some of the same data points as sampled by the 15-point telemetry during cruise mode, a basis of comparison was provided for ensuring the accuracy of the telemetry analysis. A strip-chart recording of analog telemetry, transmitted over F-Channel and Channel 8, was made at the Goldstone tracking station on day 83, starting at 13:56:56 (approximately 10 minutes before impact) and just prior to impact. It was examined for changes in telemetry units. The results of this comparison are presented in Table 33 and are well within expected limits.

4. Telemetry Evaluation of TV Subsystem Performance

The cruise-mode telemetry was employed to monitor TV Subsystem temperatures and power supply operation. The actual temperatures of the TV Subsystem assemblies during cruise and terminal modes were almost exactly as predicted in preflight calculations.

The TV Subsystem power supply consisted of a Battery and a High-Current Voltage Regulator (HCVR) for each of the F- and P-Channels, and a Low-Current Voltage Regulator (LCVR) on the P-Channel only. The power supply units functioned nominally throughout the mission.

At the start of F-Channel warm-up, the 90-point telemetry data were switched onto Channel 8. The signal profile from the full-power command data points Nos. 55 and 60 indicated that both channels went into warm-up mode for 80 seconds and then each channel was turned

TABLE 32
COMPARISON OF TELEMETRY READINGS FOR THE ELECTRONIC CLOCK

Station	High	Low	Average
Woomera (DSIF-41)	4.1	4.0	4.09
Goldstone (DSIF-12)	4.1	4.05	4.09
Johannesburg (DSIF-51)	4.2	4.0	4.11
CCC-6 (Computer)	4.3	4.0	4.12

TABLE 33
COMPARISON OF 15-POINT AND 90-POINT TELEMETRY READOUTS DURING TERMINAL MODE

Parameter Monitored / Telemetry Channel	Frame Started at 13:56:56 GMT			Frame Started at 14:07:00 GMT			Last Frame Started at 14:07:32 GMT		
	15 pt F Ch (Volts)	90 pt Ch 8 (Volts)	90 pt P Ch (Volts)	15 pt F Ch (Volts)	90 pt Ch 8 (Volts)	90 pt P Ch (Volts)	15 pt F Ch (Volts)	90 pt Ch 8 (Volts)	90 pt P Ch (Volts)
F_a Camera Lens Housing	2.5	2.5	-	2.6	2.55	2.55	2.6	2.6	2.55
P-Battery Current	4.3	4.3	4.3	4.4	4.4	4.4	4.4	4.3	4.4
F-Battery Terminal Voltage	3.6	3.6	3.6	3.6	3.6	3.7	3.6	3.6	3.62
P-Battery Terminal Voltage	3.45	3.5	3.45	3.5	3.45	3.5	3.5	3.5	3.45
F-Battery Current	4.3	4.3	4.3	4.3	4.3	4.3	4.3	4.3	4.35
F_b Camera Electronics	2.6	2.6	2.6	2.8	2.75	2.75	2.8	2.75	2.75
F-Transmitter IPA Cathode Current	-	1.5	1.5	-	1.4	1.5	-	1.5	1.5
F-Transmitter PA Cathode Current	-	1.3	1.3	-	1.3	1.35	-	1.3	1.3
P-Transmitter IPA Cathode Current	-	1.5	1.5	-	1.35	1.4	-	1.35	1.35
P-Transmitter PA Cathode Current	-	2.3	2.2	-	2.25	2.3	-	2.3	2.25
P-Transmitter PA Heat Sink	-	1.7	1.7	-	2.1	2.2	-	2.15	2.2
F-Transmitter PA Heat Sink	-	1.9	1.9	-	2.5	2.5	-	2.45	2.5

on into full-power operation by the associated Camera Sequencer. The telemetry data indicated normal supply voltages and operating temperatures for both channels. The Power Amplifier cathode-current profiles for the transmitters were almost identical to prelaunch full-power tests, confirming a high-power output for both channels. All telemetry indications for the TV camera equipment were normal.

The telemetry data for the F-Channel Video Combiner output indicated that the video output was greater than expected. This data point, No. 74 of the 90-point telemetry, measures the amplitude of the composite video signal, which has a range of 1.5 volts from sync tip to peak white for each camera, at the video combiner output and indicates that a video signal is being applied to the modulator input. Its use to establish scene luminance is limited, because it monitors two cameras that have a four-to-one difference in their dynamic ranges and the data sample had not been calibrated with the cameras.

The performance of the TV Subsystem telemetry was nominal throughout the mission. The 90-point commutator stopped on data point 69 at the end of the prelaunch test, and started on the same point at terminal mode, signifying no movement of the commutator during cruise mode.

During the terminal mode there was a momentary interruption of the JPL-provided Channel-8 analog telemetry for 13 seconds (day 83, 13:58:06 to 13:58:19 GMT); F- and P-Channel telemetry were uninterrupted.

It can be stated that, during the 64 hours 31 minutes 18 seconds of the Ranger IX lunar mission, the Ranger TV Subsystem performance, was normal. All operating parameters were within design specifications, and all cameras and systems exceeded specification requirements.

C. FLIGHT MODEL III-4 (RANGER IX) EQUIPMENT PERFORMANCE

1. General

Every aspect of the performance of the Flight Model III-4 TV Subsystem during the Ranger IX mission achieved or exceeded specification requirements. The countdown, launch, and cruise phases of the mission, as evaluated from the 15-point telemetry, very closely followed the predicted levels of operation. The terminal phase of the mission, from the initiation of warm-up until impact, produced results which exceeded all expectations. A terminal maneuver was performed which aligned the common optical axis of the cameras with the spacecraft velocity vector, thereby allowing excellent picture nesting and almost eliminating image smear. The Electronic Clock was reset by means of a RTC-5 command to allow for the initiation of warm-up of the TV Subsystem by means of a CC&S command at a time which was essentially ideal to provide area identification and also ensure continuing operation until impact.

The performance of the Camera equipment, as well as that of the transmission link to Earth, was evaluated from the mission film and magnetic-tape records. The received picture quality far exceeded all expectations.

The thermal profile during the mission closely approximated the predicted values. No abnormalities were experienced. It was noted that temperature changes were experienced during the terminal maneuver of the spacecraft. Since this is the first mission to employ a terminal maneuver, no prior mission data of this nature has been previously available. The evaluation of thermal control is based on the received telemetry.

The communications equipment performance, evaluated by picture quality, video signal levels, and signal strength as measured during the mission, was excellent.

The command and control equipment operated flawlessly throughout the Ranger IX mission.

The power equipment including the batteries and the associated regulators performed equally well during the Ranger IX mission. No shortcomings in performance were detected.

2. Camera Group

The mission requirements of high-resolution pictures of the lunar surface and of picture nesting were achieved by the Ranger IX Spacecraft.

The TV Subsystem sent back 5,866 pictures during the approximate 19-minute terminal-mode operation: 5,422 pictures were taken by the partial-scan cameras, and 444 pictures by the full-scan cameras. The images on the F_b and P3 Cameras were being scanned at impact. Figures 64 through 68 show the extent of information that was received from these cameras before impact. The minimum resolvable crater size in these pictures is given in Table 34. The minimum resolvable crater size in the last pictures taken by all of the cameras is given in Table 35.

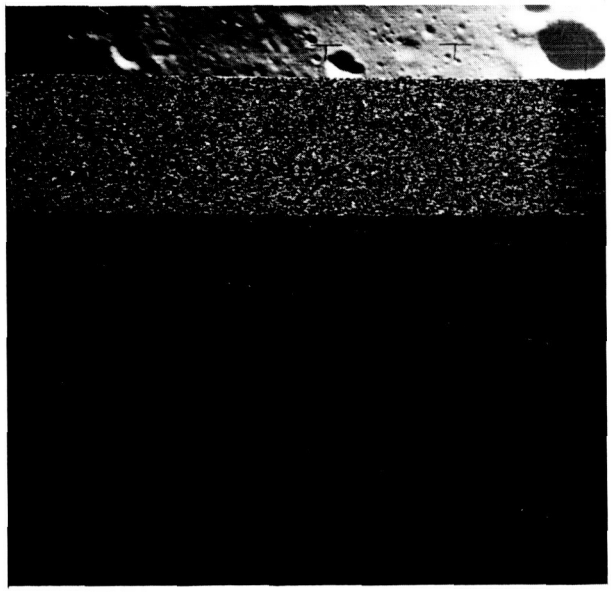

Figure 64. Ranger IX Final Pl- and P3- Camera Pictures

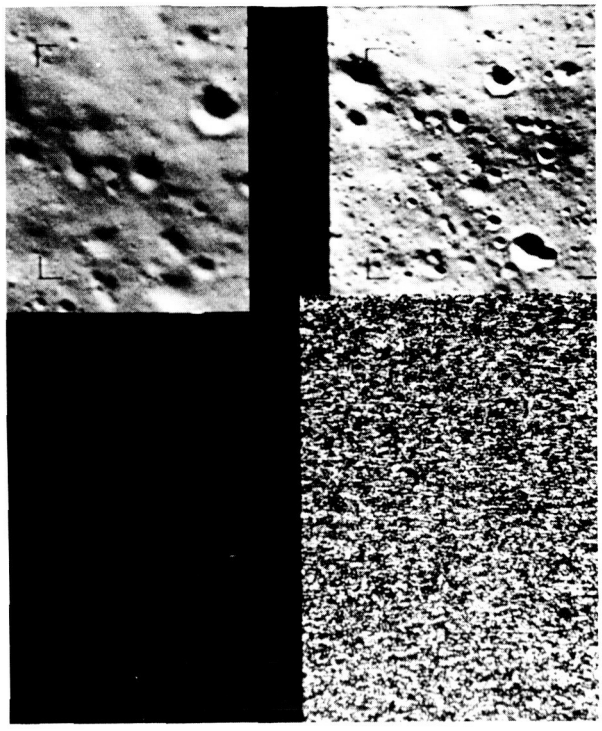

Figure 65. Ranger IX Final F_b-Camera Picture

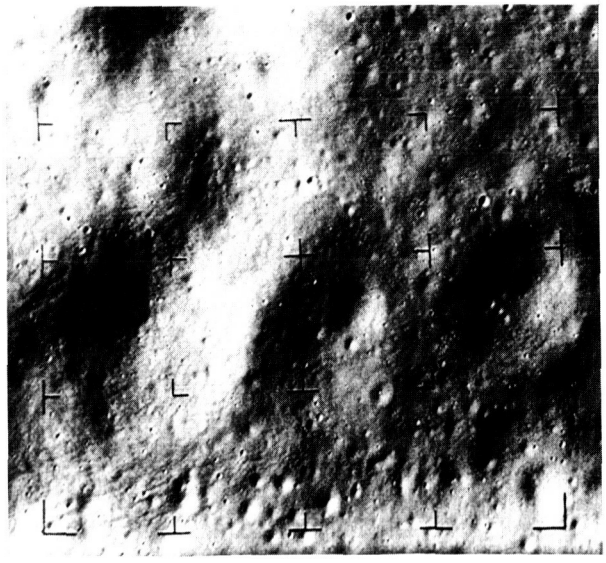

Figure 66. Ranger IX Final Complete F_b-Camera Picture Taken 5.5 Seconds Before Impact (8.3 miles altitude)

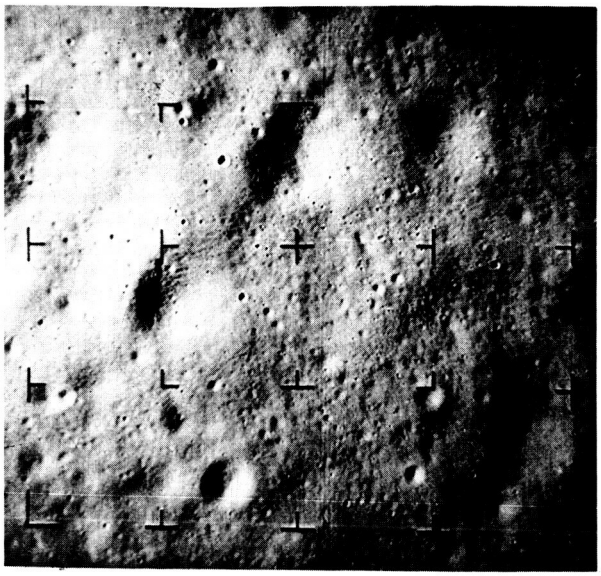

Figure 67. Ranger IX Final F_a-Camera Picture Taken 2.97 Seconds Before Impact (4.5 miles altitude)

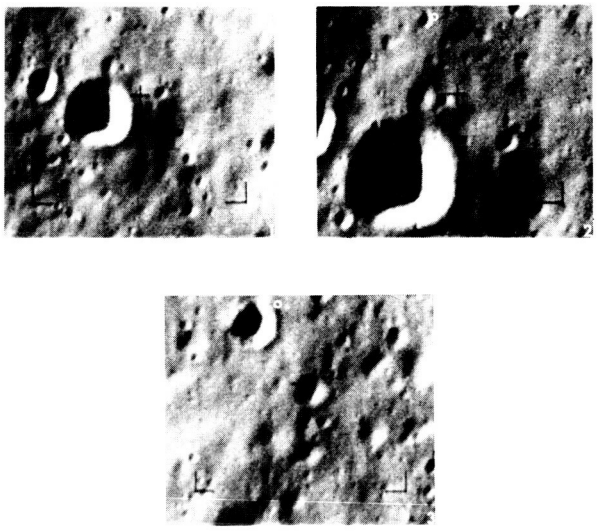

Figure 68. Ranger IX Final Three PI Camera Pictures (No. 3 Taken 0.453 Second Before Impact)

TABLE 34
MINIMUM RESOLVABLE CRATER SIZE IN FINAL F_b AND P3 CAMERA PICTURES

Camera	Time Before Impact (seconds)	Altitude (feet)	Approximate Area Covered at Exposure (sq. ft.)	Approximate Minimum Crater Diameter (feet)
F_b	0.411	3267	640 x 550	1.4
P3	0.253	2000	250 x 225	2.5

The terminal maneuver aligned the common optical axis of the TV cameras along the spacecraft velocity vector, providing excellent camera nesting. An example of F_b Camera nesting is shown in Figure 69.

In general, the performance of the cameras during the mission was similar to that experienced during tests. During the overall Ranger IX test cycle, shutter noise bursts were very prominent in the P1 and P2 Cameras and were to a much lesser extent in the P3 and P4 Camera. These bursts appear as short white segments in a particular line when they occur during the scan of video information. When a burst occurs during the clamp portion of a horizontal scan line, the video output for that line is driven to the black clip level and the entire line appears as a black line resulting in a loss of information. Throughout the Ranger IX mission, the total effect of these shutter-induced noise bursts was negligible.

The Ranger IX Cameras maintained excellent resolution throughout the test cycle. An example of this performance is shown in Table 36. This table shows limiting resolution as

TABLE 35
MINIMUM RESOLVABLE CRATER SIZE IN LAST COMPLETE PICTURES

Camera	Time Before Impact (seconds)	Altitude (miles)	Approximate Area Covered	Approximate Minimum Crater Diameter (feet)
P1	0.453	0.785	155 x 115 ft.	1.7
P2	0.893	1.35	310 x 275 ft.	3.5
P3	1.06	1.65	1100 x 1000 ft.	11.5
P4	0.693	1.1	725 x 625 ft.	8.0
F_a	2.97	4.5	2.1 x 1.9 mi.	25
F_b	5.53	8.3	1.6 x 1.4 mi.	20

determined from the camera response to RETMA patterns, viewed via 35-mm film. These tests were performed at JPL. The results of the thermal-vacuum test were selected as an example since the thermal-vacuum test is the most severe of all tests performed on the cameras.

During the mission, the camera performance was equally outstanding. Examples of this performance are shown in Figures 70 through 75. These pictures have A-scope presentations of a single horizontal line of video information, corresponding to the intensified scan line on the scene picture. Adjacent to the pictures of the oscilloscope traces are indicated the approximate values of the scene illumination. These values were determined from the transfer characteristics obtained during camera calibration. Vertical scale of these pictures is equal to 250 mv/cm.

The excellent transient response of the cameras can be seen in the steep, black-to-white video transitions, as the strobe line passes through a shadowed crater in many of the pictures. The camera gains were set for almost optimum lunar brightness as indicated by the high-contrast pictures. At no time did saturation occur.

Some performance defects, present during testing, either did not occur during the mission or were so infrequent that they were considered negligible. These were as follows.

- Shutter-Induced Noise Bursts: Noise pulses, which appeared primarily in the P1 and P2 Cameras, caused by an electrostatic discharge from the camera shutter blade;
- Mask Leakage: The P2-Camera mask was not completely opaque, causing a light leakage of approximately 2.5 percent of scene luminance;
- Nuvistor Microphonic Increase: The increase in the nuvistor microphonics occurring in the P1 Camera during the latter test phases;
- Chopper Spikes in the F_a Camera Video Signal: Power-supply chopper spikes, which were traced to the ground of the 1000-volt mesh filter, occurring in the F_a-Camera video signal;
- Vidicon Microphonics: Vidicon microphonics induced in the F_a and P2 Cameras by the P4-Camera shutter;

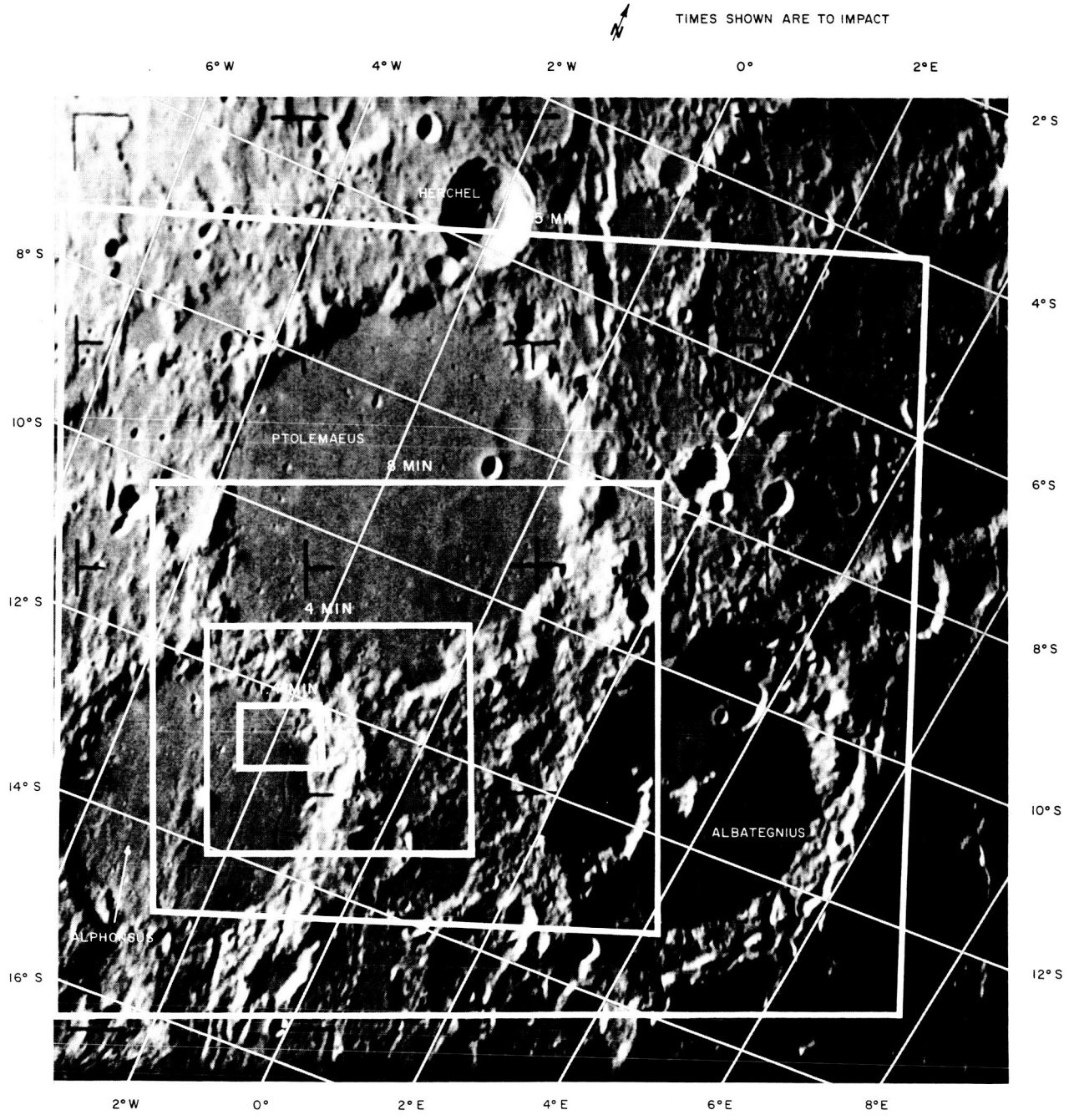

Figure 69. Picture Nesting Achieved by Ranger IX F_b-Camera

- First frame of the F_a Camera not exposed: The noise transient occurring at full-power turn-on would occasionally cause the trigger pulse to be applied to the shutter-drive multivibrator when it was in the wrong state.

TABLE 36 CAMERA RESOLUTION DURING THERMAL-VACUUM TESTING			
Camera	Door Test (Ambient) (TVL)	Thermal-Vacuum Test	
		13° C (53° F) (TVL)	36° C (98°F) (TVL)
P1	200	200	200+
P2	225	225	220
P3	245	210	245
P4	260	210	245
F_a	750	725	775+
F_b	775	750	775+

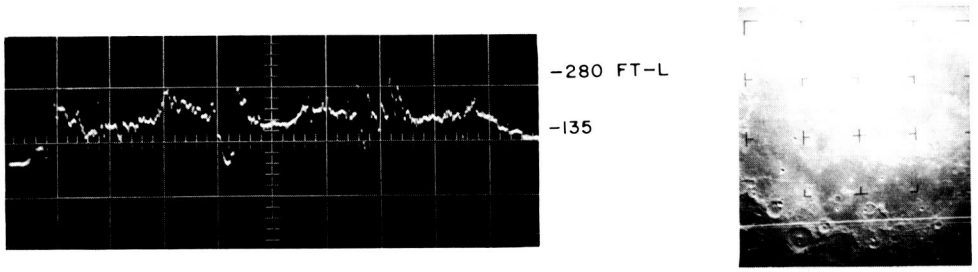

Figure 70. Selected Line of Ranger IX F_a-Camera Video 15 Minutes Before Impact

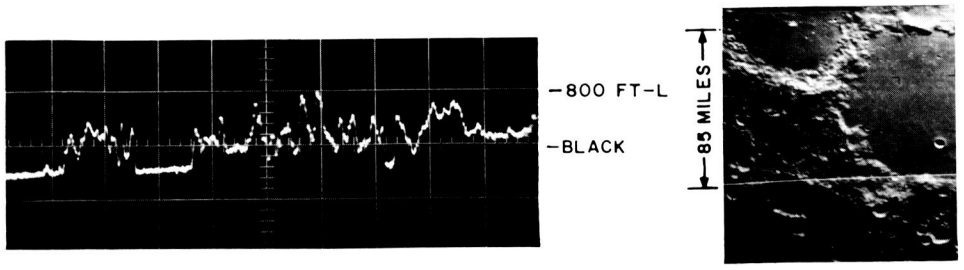

Figure 71. Selected Line of Ranger IX F_b-Camera Video 10 Minutes Before Impact

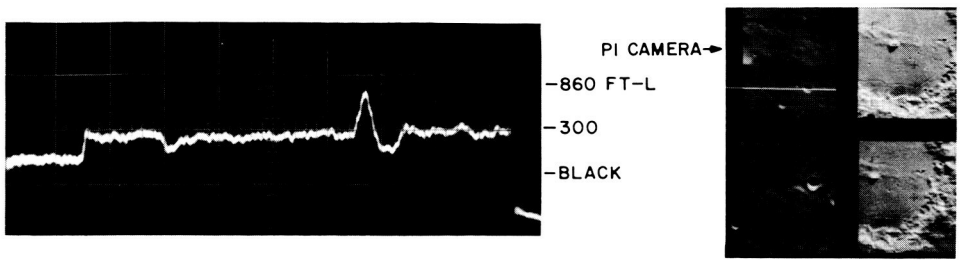

Figure 72. Selected Line of Ranger IX PI-Camera Video 5 Minutes Before Impact

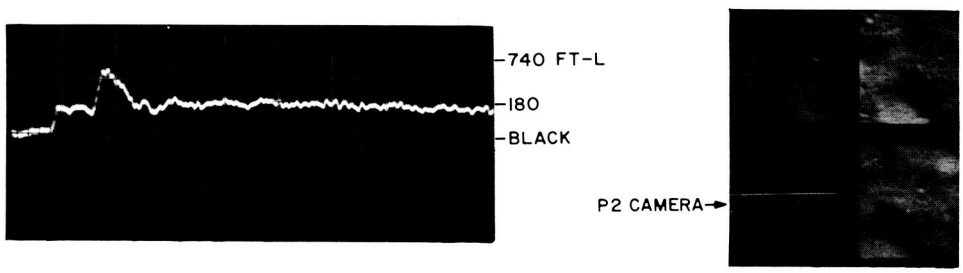

Figure 73. Selected Line of Ranger IX P2-Camera Video 7 Seconds Before Impact

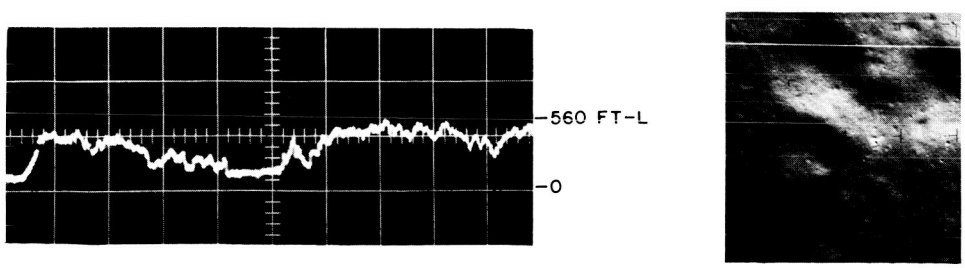

Figure 74. Selected Line of Ranger IX F_b-Camera Video 5.53 Seconds Before Impact

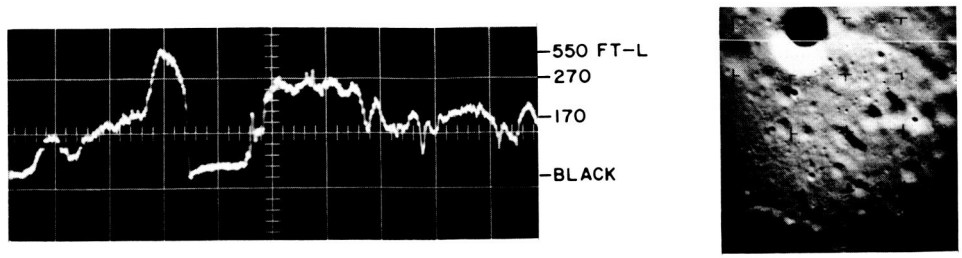

Figure 75. Selected Line of Ranger IX F_a-Camera Video 2.97 Seconds Before Impact

The erase characteristics of the Ranger IX Cameras were as follows:

Camera	Percent Erase
P1 and F_b	98
P2, P3, and P4	97
F_a	95.5

The pictures obtained during the Ranger IX mission revealed no evidence of residual information.

Transfer characteristics for the six flight cameras are shown in Figures 76 and 77.

Some significant improvements in the performance of Flight Model III-4 over previous flight models were as follows:

- 15-kc cross talk: In previous TV Subsystems, cross talk was between 50 and 80 millivolts; in Flight Model III-4, it was less than 10 millivolts. This was achieved through experience gained in the grounding and harnessing in the previous flight models;
- Mesh: Five of the six vidicons of Flight Model III-4 were equipped with the 1500-line mesh electrode. Modulation of the read beam by the mesh was almost negligible. An improved signal-to-noise ratio was realized. The excellent signal-to-noise ratios for the Flight Model III-4 cameras were:

Camera	Signal-to-Noise Ratio (db)
P1	36
P2	30.5
P3 and F_a	35.5
P4	35.6
F_b	34

- Reduction of low-frequency video amplifier noise: Low-frequency noise sources, such as zener diodes, were selected for minimum noise contribution.

Although performance of the TV Subsystem during the Ranger IX mission was excellent, the following characteristics on Flight Model III-4 were somewhat objectionable.

- Differences in shutter exposure times: The P3 and P4 cameras had timing differences in the in-out shutter strokes. During calibration of these cameras, the difference in video output was found to be approximately 80 millivolts. During the mission, the P3 Camera had approximately a 60-mv difference, and the P4 Camera had approximately a 50-mv difference in video amplitude due to shutter speed variations.
- Shading: The nonuniform electrical charge distribution over the target area (shading) has been a persistent camera

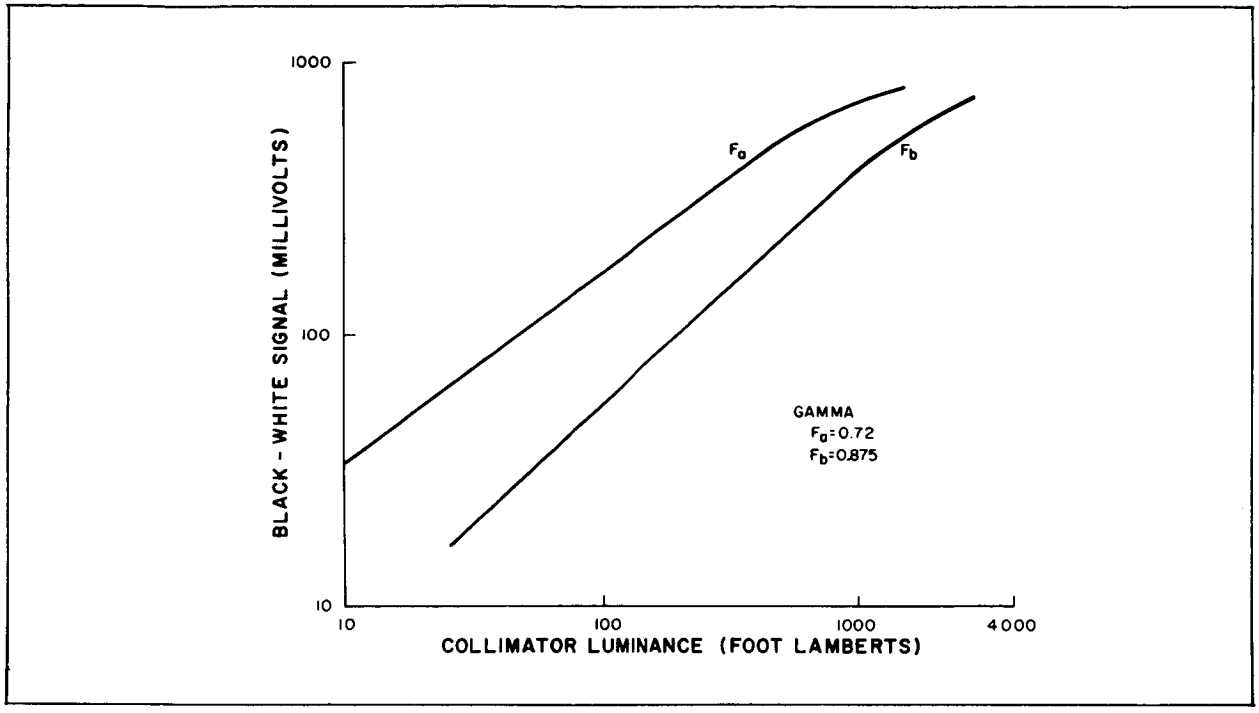

Figure 76. Light-Transfer Characteristics Curves for the Ranger IX Full-Scan Cameras

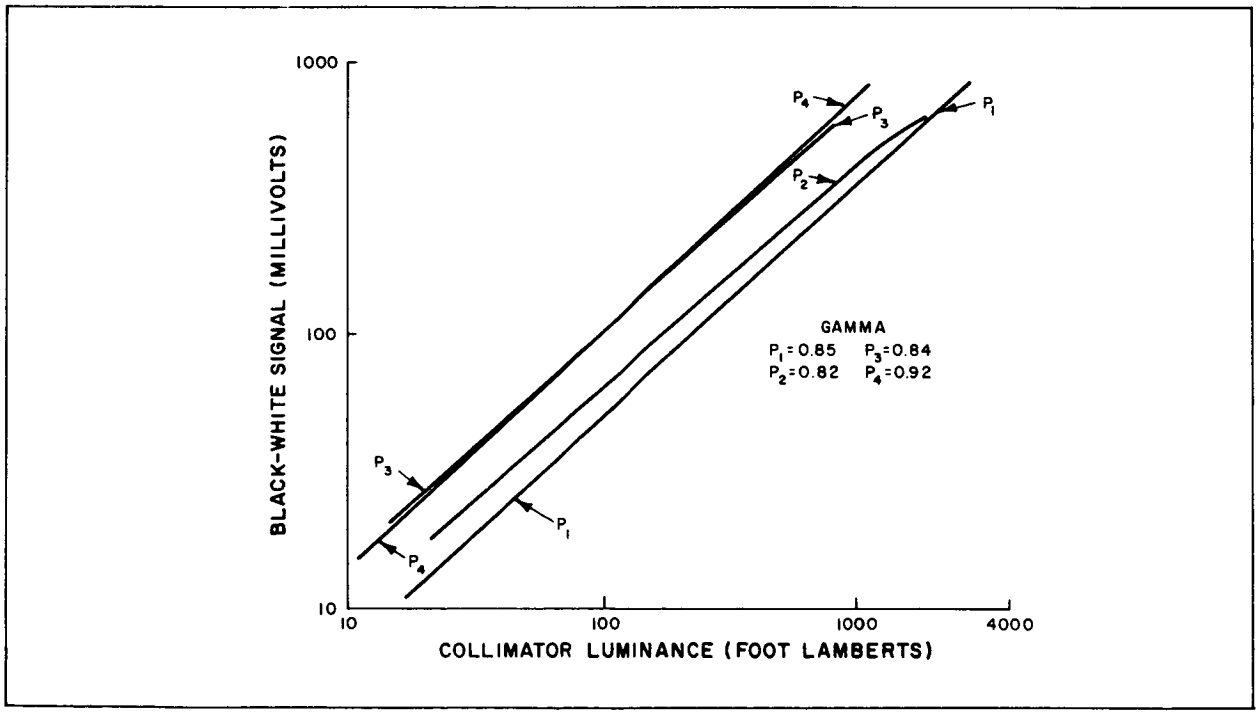

Figure 77. Light-Transfer Characteristics Curves for the Ranger IX Partial-Scan Cameras

problem which recently has been greatly improved by modifying the vidicon construction and optimizing the location of the vidicon in relation to the yoke.

3. Thermal Control Group

a. FLIGHT TEMPERATURE PREDICTIONS

The thermal configuration of the Ranger IX TV Subsystem is identical to that of the preceding Ranger Subsystems. The same methods were used to predict the flight temperatures of major parts of the Subsystem. Predicted and telemetered results are summarized in Table 37.

b. THERMAL-CONTROL PAINTS APPLIED TO RANGER IX

The paints used on the fins of the Ranger IX TV Subsystem were a mixture of PV-100 white paint and MIL-E-5557 type III black paint and are identified as light gray (RCA Drawing 1758619-29) and dark gray (RCA Drawing 1758619-30), respectively. Mixtures of the gray paints were prepared in November 1964 for use on the Ranger IX TV Subsystem. In an effort to obtain the same flight temperatures on Ranger IX as occurred on Ranger VII, the solar absorptivities of the paints were decreased. This decrease allowed for the increased solar constant at the time of the anticipated March launch. The desired values of solar absorptivity for the Ranger IX paints were 0.48 and 0.67 as compared with 0.51 and 0.71 for Ranger VII. Samples of the paint were sent to JPL for measurement at STL. The spectral-measurement history of these paints, which were used in the final finishing of the thermal shroud, is given in Table 38.

Measurements of absorptivity at ETR on the Ranger IX thermal shroud fins were obtained using the Lion Model 25A portable reflectometer and the RCA calibration standards. The accuracy of this reflectometer is estimated to be ±5 percent.

Measurements indicated that an area of Fin B, on the -Y side of the shroud had absorptivity readings as low as 0.37 (below standard). The predicted temperatures for the fin indicated a decrease in cruise mode temperature of less than 1° F when the substandard area was taken into consideration. Repainting (at ETR) was not considered necessary since the Ranger VIII flight temperatures were approximately 5° F higher than nominal. Therefore, because of the difference in the solar constants in February and March the Ranger IX fin temperatures were expected to be 3 to 4° F higher than nominal.

c. SUMMARY

Temperatures of the five points monitored during cruise mode were all within 6° F of the midpoint of the predicted range of stabilized cruise-mode temperatures. Thus, the temperatures of the spacecraft were within the range of desirable temperatures for the initiation of terminal operation as verified during a number of tests at this same level. A comparison of test temperatures and flight temperatures for the same period of operation are listed in Table 39.

4. Telecommunications Group

Evaluation of telecommunications performance during the Ranger IX mission is based on the RF power transmitted by the F- and P-Channel transmitters. The data obtained during the Ranger IX mission indicated that communications performance compared closely with the results of prelaunch system tests, which were nominal.

This section describes the techniques that were employed to measure the RF power received at the ground station for each channel and the methods employed to infer the level of the power that was transmitted from the TV Subsystem Four-Port Hybrid. The results of the different power-measuring techniques vary by ±1 db; however, this is of no consequence, since the received RF signal level was 10 db

TABLE 37
CRUISE-MODE EQUILIBRIUM TEMPERATURE PREDICTIONS FOR FLIGHT MODEL III-4

Location on TV Subsystem	Temperature Calculated by RCA Absorptivity		Temperature Calculated by JPL/STL Absorptivity		Actual Flight Temperature (Telemetry, RA-9)	
	°C	°F	°C	°F	°C	°F
Thermal Shroud, Hat, -Y side	22	72	25	77	26	79
Camera Lens Housing	12	54	15	59	17	63
Thermal Shroud, -Y side, Below Fin A	19	66	22	72	25	76
Battery, Internal, Ch. P.	18	64	21	70	26	78
Camera Electronics, -Y side	19	66	22	72	21	70
Power Amplifier, -X side, Cavity End, Ch. F	19	66	22	72		
Power Amplifier, +X side, Cavity End, Ch. P	19	66	22	72		
Camera Mounting Bracket	20	68	22	72		
High-Current Voltage Regulator, +Y side, Ch. P	15	59	18	64		
Transmitter Power Supply, +X side, Ch. P	16	61	19	66		
Temperature Control Plate (Fin F)	30	86	32	90		
Thermal Shroud, +Y side, Below Fin A	18	64	21	70		
Thermal Shroud, -Y side, Between Fins B & C	24	75	27	81		
Deck No. 3 -Y side	22	72	25	77		
Deck No. 4 -Y side	18	64	21	70		
Deck No. 5. -Y side	15	59	18	64		

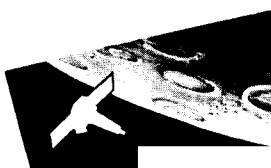

TABLE 38
SPECTRAL-MEASUREMENT HISTORY

Paint Description	Absorptivity Measured By	Design Absorptivity Values Desired	Samples Painted at RCA (Nov. 1964)	Samples Painted During Painting of RA-9 Fins at JPL	RA-9 Fins Measured with Portable Reflectometer at ETR
Light Gray RCA 1758619-29	RCA	0.48	0.49	0.49	0.49
	JPL/STL	0.51	--	0.52	--
Dark Gray RCA 1758619-30	RCA	0.67	0.65	0.65	0.65
	JPL/STL	0.71	--	0.69	--

above receiver threshold. At such a strong signal level, the peak-to-peak signal-to-rms noise ratio was approximately 40 db, and no degradation of picture quality would have occurred as the result of a 2-db decrease in the received signal level.

a. RF POWER OUTPUT DURING TERMINAL MODE

Three techniques were used to measure the RF power output of the F- and P-Channel transmitters during the terminal mode of the Ranger IX mission. RCA used two techniques: one employing a spectrum analyzer, and the other employing a diode detector. The third technique, used by JPL, employed a filter system.

(1) Spectrum Analyzer

One of the outputs of the 30-megacycle isolation amplifiers at the Pioneer site was connected through a directional coupler to a spectrum analyzer as shown in Figure 78. A signal generator was connected to the output of the directional coupler so that the signal generator input to the spectrum analyzer was reduced 17 db. The highly directional characteristics of the coupler and the degree of isolation of the amplifier were sufficient so that the generator signal did not interfere with the JPL or the RCA receivers. This technique, which was used in all system tests and produced results within ±0.5 db, depends on the scope persistence to allow the determination of peak amplitude. This exists only when there is no video. The F-Channel peak amplitude is easier to read than the P-Channel amplitude since it is modulated at a much slower rate than P-Channel. P-Channel peak amplitude is usually read 1 db below normal when the P-Cameras are fully modulated. The calculated power profile is given in Table 40. The power output of the Four-Port Hybrid was calculated by measuring the relative peak level of the F- or P-Channel signal with respect to the peak amplitude of the JPL beacon, and adding this to the known JPL RF level at the output of CASE II (telemetry address 56) and to the known loss from the Four-Port Hybrid to the output of CASE II (0.99 db). The maximum power of 27.1 watts for F-Channel during the mission was equal to the F-Channel power obtained during camera calibration with both channels operating. The calibration data used for comparison was taken during the prelaunch test. During tests, the F-Channel power has consistently maintained a maximum level for

TABLE 39
RA-9 TEST TEMPERATURES vs FLIGHT TEMPERATURES

Telemetry Point Location	III-4 Test, Cruise Mode		III-4 Test, 19 Min Full Power		III-4 Test, 30 Min Full Power		RA-9 Flight, Stabilized Cruise Mode Prediction		RA-9 Actual Flight, Stabilized Cruise Mode		RA-9 Impact, 19 Min Full Power	
	°C	°F	°C	°F	°C	°F	°C	°F	°C	°F	°C	°F
P-Channel Battery, Internal	26	79	28	82	30	86	22 +5	72 +10	26	78	28	83
F-Channel Battery, Internal	26	79	28	82	30	86	--	--	--	--	28	82
P-Channel Battery, External	24	75	27	80	30	86	--	--	--	--	--	--
F-Channel Battery, External	24	75	27	80	30	86	--	--	--	--	29	84
F_a-Camera Lens Housing	24	75	24	75	24	75	15 +5	58 +10	17	63	22	72
Camera Mounting Brkt.	23	73	23*	73*	21*	70*	--	--	--	--	27	80
Camera Electronics	27	80	32	89	36	97	18 +5	64 +10	21	70	25	77
Thermal Shroud Hat (-Y)	22	71	16*	61*	13*	55*	25 +5	77 +10	26	79	24	76
Thermal Shroud Lower (-Y)	26	79	25*	77*	28*	82*	21 +5	70 +10	25	76	28	83
Thermal Shroud Lower (+Y)	27	80	22*	71*	26*	79*	--	--	--	--	42	108
Bulkhead Near P-Channel PA	27	80	40	104	49	120	--	--	--	--	41	106
Bulkhead Near P-Channel PA	27	80	46	115	46	133	--	--	--	--	50	122
Deck 5(-X, -Y)	22	71	25*	77*	30*	86*	--	--	--	--	35	95
Deck 4 (+Y)	28	82	26*	79*	31*	88*	--	--	--	--	39	102
Deck 4 (-Y)	28	82	27*	80*	32*	89*	--	--	--	--	30	85

*Input heaters turned off during full-power operation negates true readings in the area.

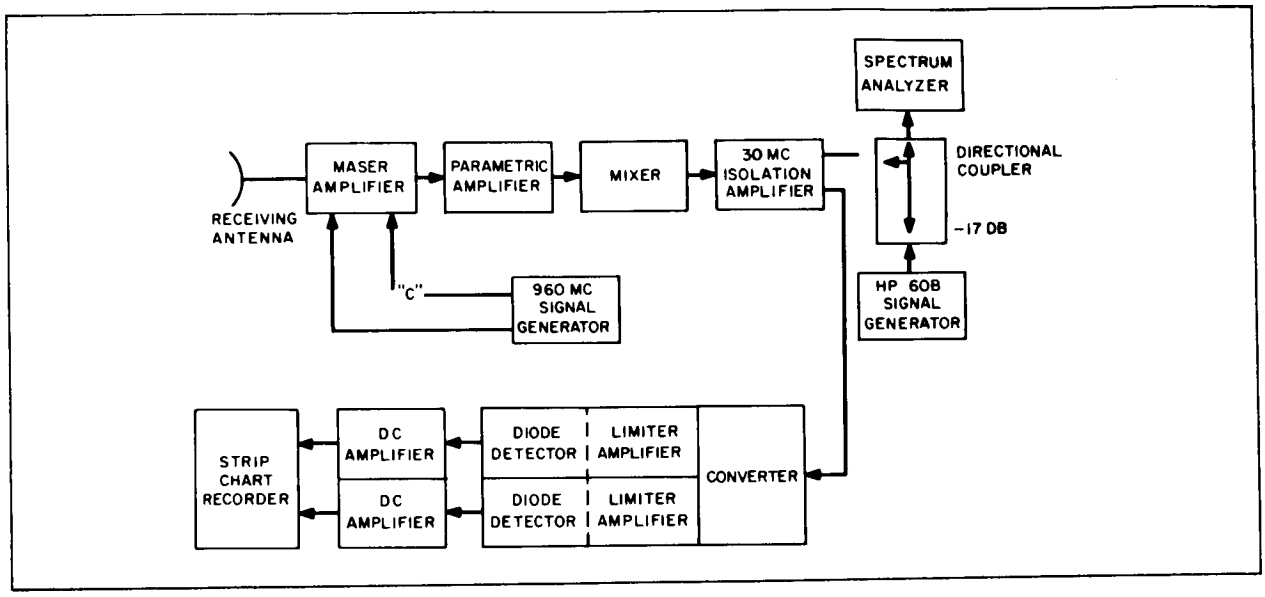

Figure 78. Diode-Detector Technique of Terminal-Mode Power Measurement

20 minutes. Therefore, the decrease in power to 22.6 watts at impact minus 5 minutes appeared to be due to a change in maser passband. The postimpact calibration indicated that the F-Channel output was down 1.86 db relative to the JPL beacon. The preimpact calibration was down 0.45 db.

A maximum power output of 20.9 watts for P-Channel was 0.9 db lower than the 25.6 watts expected because of reading P-Channel 1 db lower than normal. The premission calibration indicated that P-Channel was down 0.2 db from the JPL beacon; the post-impact calibration was down 0.45 db.

(2) Diode-Detector Power Monitor Technique

This technique measured and recorded the signal levels from the F- and P-Channel transmitters on the spacecraft as referred to the maser input. It was thought that this technique would be an accurate means of calibration; however, the varying passband and gain of the maser amplifier reduced its accuracy. The strip-chart recordings show a smooth power profile for both transmitters for the entire 19 minutes of full-power operation. The only small variations recorded occurred when the Echo ground transmitter stopped transmission and when a gradual frequency change occurred at impact minus ten minutes because the power recording is a function of frequency.

A block diagram of the diode detector technique is shown in Figure 78. The detector was connected as shown in Figure 79. Two of these detectors were physically incorporated in the Dual Channel Limited Amplifier.

The DC output from the detector varies as a function of RF signal strength since no limiting occurs before the point at which the RF signal is detected. The DC signal is amplified in a Sanborn Model 150-1000A Amplifier which actuates a pen on the Sanborn Model 154-100B Recorder. A readout is obtained for each channel.

Calibration was accomplished by feeding the output of a signal generator (set to the center frequency of the appropriate channel) through the path marked "C" in Figure 78. The loss through the path from the maser to the RCA

TABLE 40
RA-9 POWER OUTPUT PROFILE

Time (Minutes)	F-Channel				JPL HP608 Setting (dbm)	P-Channel			
	HP608 Setting (dbm)	Relative to JPL (db)	(1) Relative to JPL Corrected (db)	(3) Four-Port Hybrid Power Output (watts)		HP608 Setting (dbm)	Relative to JPL (db)	(2) Relative to JPL Corrected (db)	(3) Four-Port Hybrid Power Output (watts)
I-78	-34.7				-51.0	-34.6			
I-18' 47"	-33.0	+18.0	+18.45	22.6		-34.2	+16.8	+17.0	16.2
I-18	-32.8	+18.2	+18.65	23.7		-33.8	+17.2	+17.4	17.8
I-17	-32.7	+18.3	+18.75	24.3		-33.3	+17.7	+17.9	20.0
I-16	-32.2	+18.8	+19.25	27.1		-33.1	+17.9	+18.1	20.9
I-14	-32.2	+18.8	+19.25	27.1	-51.0	-33.2	+17.8	+18.0	20.4
I-12	-32.2	+18.8	+19.25	27.1		-33.1	+17.9	+18.1	20.9
I-10	-32.5	+18.5	+18.95	25.4		-33.1	+17.9	+18.1	20.9
I-7	-32.5	+18.5	+18.95	25.4		-33.2	+17.8	+18.0	20.4
I-5	-33.0	+18.0	+18.45	22.6		-	-	-	-
I-4	-33.0	+18.0	+18.45	22.6	-51.0	-	-	-	-
I-2	-33.0	+18.0	+18.45	22.6		-33.3	+17.7	+17.9	20.0
I-1	-33.0	+18.0	+18.45	22.6		-33.3	+17.7	+17.9	20.0
I+9	-33.8					-32.2			

(1) Using I-83' Passband correction factor of +0.45 DB

(2) Using I-83' Passband correction factor of +0.2 DB

(3) 4 Port Hybrid Power Output = (Signal level relative to JPL) + (correction Factor) + 0.99 + 24.10)

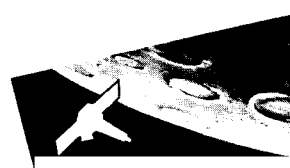

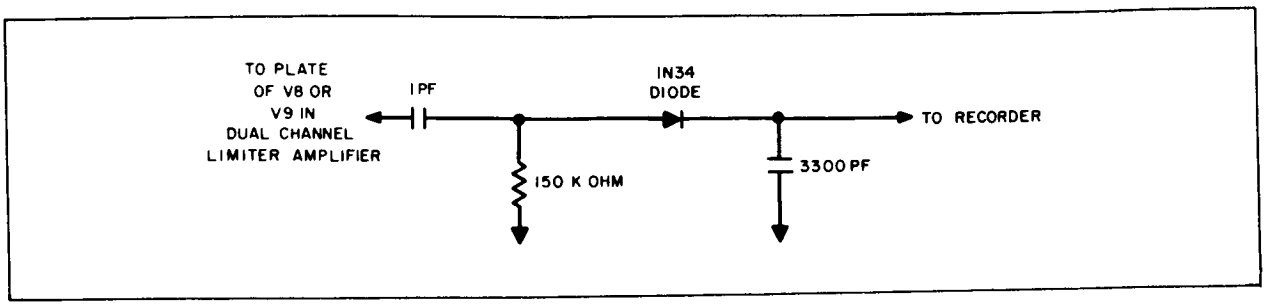

Figure 79. Diode-Detector Circuit

OSE was supplied by JPL. Based on an expected nominal mission level of -96.5 dbm, the required signal generator output level setting was obtained as follows:

Loss, maser to RCA OSE	44.51 db
Loss, signal generator cable	1.00 db
Total loss	45.51 db
Nominal mission signal level at maser	-96.5 dbm
Signal generator setting for nominal signal	-51.0 dbm

The gains of the DC amplifiers were adjusted to provide a readout at about 3/4 scale on the recorder chart for a -96.5 dbm input level to the maser. The recorder was also calibrated in 1 db intervals for ±3 db. A calibration of the measuring equipment was performed just prior to ground-station acquisition of the spacecraft (warm-up minus 1.0 hour) and within 9 minutes after impact.

Coincident with the above calibrations, the bandwidth of the input to the maser and the maser gain were checked by JPL personnel. The input to the maser bandpass curve changed radically from preacquisition to postimpact. Since the vertical scale of the spectrum analyzer was calibrated from the same source, the observed RF signal relative to the JPL beacon signal was 2.5 db lower than expected. Therefore, when both F- and P-Channels appeared to be above nominal, it was an expected result. F-Channel reached a maximum of nominal plus 2.5 db and P-Channel, nominal plus 1.83 db. It was realized that a discrepancy did exist. However, since this calibration was performed close to the time of TV Subsystem turn-on, it was decided not to recalibrate.

(3) Telemetry Verification

The telemetry indicated that both F- and P-Channels achieved nominal power output. F- and P-Channel IPA cathode currents were also normal.

b. TRANSMITTERS

(1) Center Frequency

The center frequencies obtained during the mission, given in Table 41, are very close to those obtained on launch day. For approximately 30 seconds at Impact minus 10 minutes, there were variations of ±15 kc as the operator manually tuned the ground local oscillator, which was performed after the ground transmitter stopped transmission because of an overloaded circuit breaker. The final local oscillator setting was approximately 12 kc below nominal.

(2) Frequency Stability

The frequency of the F-Channel carrier signal drifted 5 kc during the 19-minute full-power mode, as expected. The center frequency

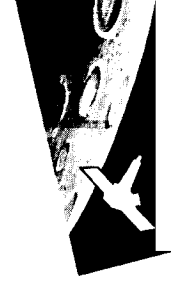

TABLE 41
CENTER FREQUENCIES OBTAINED DURING THE RA-9 MISSION

Time		Sync Tip (volts)	Center Frequency Drift (±kc)	Sync Tip (volts)	Center Frequency Drift (± kc)
T-0 *	I-20**				
T+1'20	FP+0	-0.904	-10.1	-0.880	+50.8
T+2'20"	FP+1	-0.886	+40.1	-0.880	+50.8
3'20"	FP+2	-0.886	+40.1	-0.880	+50.8
4'20"	FP+3	-0.892	+20.3	-0.871	+80.4
5'20"	FP+4	-0.893	+20.0	-0.868	+90.3
6'20"	FP+5	-0.895	+10.4	-0.864	+100.4
7'20"	FP+6	-0.896	+10.2	-0.856	+120.8
8'20"	FP+7	-0.896	+10.2	-0.852	+14
8'50"	FP+7.5	-0.894	+10.7	-0.852	+14
9'50"	FP+8.5	-0.896	+10.2	-0.850	+15
(1)		40 mv	+12	+49 mv	+14
	FP+11 I-8	-0.855	+13	-0.801	+29
	I-7	-0.855	+13	-0.795	+30
	I-6	-0.855	+13	-0.791	+32
	I-5	-0.855	+13	-0.787	+33
	I-4	-0.851	+14	-0.785	+33
	I-3	-0.849	+15	-0.780	+35
	I-2	-0.851	+14	-0.775	+36
	I-1	-0.850	+14	-0.771	+37
	I	-0.850	+14	-0.766	+39

*T= Warm-up = 134h 8m 13s after launch

**I = Impact

(1) Ground Transmitter shut off due to circuit breaker at I-10 minutes.

of the P-Channel carrier signal was 20 kc above nominal, as expected.

(3) Deviation

Deviation of the F- and P-Channel carriers was normal.

(4) Frequency Response

The F- and P-Channel frequency responses were normal.

c. TELEMETRY ASSEMBLY

(1) Cruise Mode

All telemetry components performed nominally during cruise mode. The 15-point telemetry contained some noise due to interchannel modulation; however, it did not introduce an error exceeding one percent.

(2) Terminal Mode

The frequency of the F- and P-Channel 225-kc VCO's were within the linear range of 225-kc discriminators in the ground station. The 15- and 90-point telemetry data, as received from the F- and P-Channel transmitters, were accurate and free of noise. The maximum difference between functions that were common to the telemetry broadcast over the 15-point F-Channel 225-kc VCO and the telemetry broadcast over the 90-point P-Channel 225-kc VCO (or Channel 8 JPL beacon) was one percent, which is excellent for a system that was designed to operate within ±5 percent.

5. Controls Group

a. SATISFACTION OF MISSION REQUIREMENTS

The operation of the TV Subsystem command and control circuitry was normal during the Ranger IX mission. The TV Subsystem Clock was inhibited by an RTC-5 command after the start of the terminal maneuver. The TV Subsystem turn-on was then initiated by the CC&S (TV-2) command. Full-power operation was initiated by outputs from the F- and P-Channel 80-second timers in the Sequencer Assembly. No irregular or anomalous operation of the Controls Group was observed throughout the mission.

Some functions of TV command and control, such as F- and P-Channel turn-off by RTC-5, TV warm-up via command RTC-7, and the free-run capability of the P1 Camera, were not exercised, and no statement can be made concerning performance in these areas.

b. CLOCK INHIBIT PHILOSOPHY

The performance of the midcourse maneuver was delayed to allow for more accurate correction of the spacecraft trajectory. As a result of this delay, the TV Subsystem Clock would have turned on F-Channel earlier than desired. The decision to send an RTC-5 command and turn off the Clock was made by SDAT as a result of the following considerations:

- Little, if any useful information could be obtained from an early F-Channel turn-on via the Clock.
- Ranger VIII had a noisy P-Camera, during a 23-minute full-power mission, which was attributed in part to the length of operation of the cameras and, consequently, to the higher operating temperature.
- F-Channel full-power operation for 43 minutes could have resulted in a higher temperature than experienced during any Ranger IX testing for the F-Channel IPA. However, this higher temperature would have been within the designed capability of the transmitter.
- Optimum picture quality was desired. It was felt that the cameras would probably perform satisfactory during a 43-minute

F-Channel and 10-minute P-Channel full-power mission with little degradation, but a shorter mission was preferred.

With no real benefit of an early F-Channel turn-on and the possibility of minor degradation with the longer mission, an RTC-5 command was sent to inhibit the Clock.

c. EVALUATION OF PERFORMANCE

(1) Electronic Clock

The performance of the Clock during the Ranger IX mission was satisfactory. The Clock was started by a microswitch closure that occurred when the spacecraft separated from the Agena.

All Clock telemetry pulses up to an including the 48-hour pulse occurred within the specified time limits. The Clock was turned off by an RTC-5 command after the start of the terminal maneuver. Telemetry confirmation of Clock turn-off occurred after RTC-5 verification by JPL.

The nominal and actual elapsed time of each Clock telemetry pulse is given in Table 42. If an RTC-5 command had not been sent, Clock turn-on, determined by extrapolation, would have occurred at 63 hours 31 minutes 13 seconds elapsed time (or 73 seconds later than nominal), which is within the allowable 5-minute tolerance.

Comparison of flight and test performance of the Clock is given in Table 43.

(2) Sequencer 80-Second Timer Circuits

The F- and P-Channel 80-second timers in the Sequencer Assembly operated properly during the mission. The timers were started at TV Subsystem warm-up upon receipt of the warm-up command from the Spacecraft Bus as part of the terminal maneuver sequence. Timer periods observed during the mission are given in Table 44.

Comparison of flight and test performances for the F- and P-Channel 80-second timers is given in Table 45.

TABLE 42
PREDICTED AND ACTUAL ELAPSED TIME OF CLOCK TELEMETRY PULSES

Telemetry Pulse	GMT	Elapsed Time from Clock Start	
		Actual*	Nominal
Start (Agena Separation)	21:52:26	S+0	S+0
1	05:52:36	S+8 hr 10 sec	S+8 hr
2	13:52:47	S+16 hr 21 sec	S+16 hr
3	21:52:54	S+24 hr 28 sec	S+24 hr
4	05:53:01	S+32 hr 35 sec	S+32 hr
5	21:53:28	S+48 hr 1 min 2 sec	S+48 hr

*Measurement accuracy is plus 0, minus 15 seconds.

TABLE 43
COMPARISON OF FLIGHT AND TEST PERFORMANCES OF ELECTRONIC CLOCK

Test	Temperature	Date	Performance*
AED Simulated Mission Test (Thermal-Vacuum)	59° F to 95° F	11-27-65	63.5 hr + 56 sec
JPL Mission Test No. 1 (Thermal-Vacuum)	98° F	1-22-65	63.5 hr - 10.5 sec
ETR Clock Test	78° F	2-26-65	63.5 hr + 36 sec
Mission	70° F	3-24-65	63.5 hr + 73 sec**

*Measurement accuracy is plus 0, minus 15 seconds.

**Extrapolated with an accuracy of ±10 seconds.

TABLE 44
80-SECOND TIMER PERIODS DURING RA-9 MISSION

Timer	Start Warm-up (GMT)	Start Full Power (GMT)	Timer Period (seconds)
P-Channel	13:48:13.5	13:49:33.8	80.3
F-Channel	13:48:13.5	13:49:34.8	81.3

TABLE 45
COMPARISON OF FLIGHT AND TEST PERFORMANCES OF F- AND P-CHANNEL 80-SECOND TIMER

Test	Temperature (°F)	Date	Timer Period (seconds)	
			P-Channel	F-Channel
Flight Acceptance Test	31	5-1-64	79.1	81.3
	132	5-1-64	80.3	80.9
RA-9 Actual Mission	85*	3-24-65	80.3	81.3

*Accuracy is ±5° F

(3) Command Control Unit (CCU)

Operation of the CCU was normal during the mission. Cruise-mode turn-on was initiated prior to the launch by a Cruise-On Test command through the umbilical connector.

The operation of the Clock 32-hour enable relay circuit was verified by the reset of the Clock during the terminal maneuver sequence through the use of an RTC-5 command.

(4) Distribution Control Unit (DCU)

The DCU operated satisfactorily during the mission. The Clock power relay circuit functioned normally. Since the TV Subsystem performance was without failure, the fuses in the DCU that could have protected portion of the Subsystem in the event of a failure were not needed.

(5) High-Current Voltage Regulator (HCVR) Control Module

All portions of the control module in the F- and P-Channel HCVR's, which were exercised, performed normally. The fail-safe turn-on features incorporated in this module functioned properly.

6. Power Group

The Power Group of the Ranger IX TV Subsystem consisted of the F- and P-Channel Batteries, the F- and P-Channel High-Current Voltage Regulators (HCVR), and the Low-Current Voltage Regulator (LCVR). The performance of all assemblies of the Power Group was normal during the Ranger IX mission.

a. BATTERIES

The F- and P-Channel Batteries performed nominally throughout the mission. Figure 80 shows the budgeted and expended power capacities of the F- and P-Channel Batteries for each phase of the Ranger IX mission. Capacities of 29.1 ampere-hours and 34.2 ampere-hours were budgeted for the F- and P-Channel Batteries, respectively. Of that amount, 12.5 ampere-hours and 21.8 ampere-hours for the respective batteries were expended during the

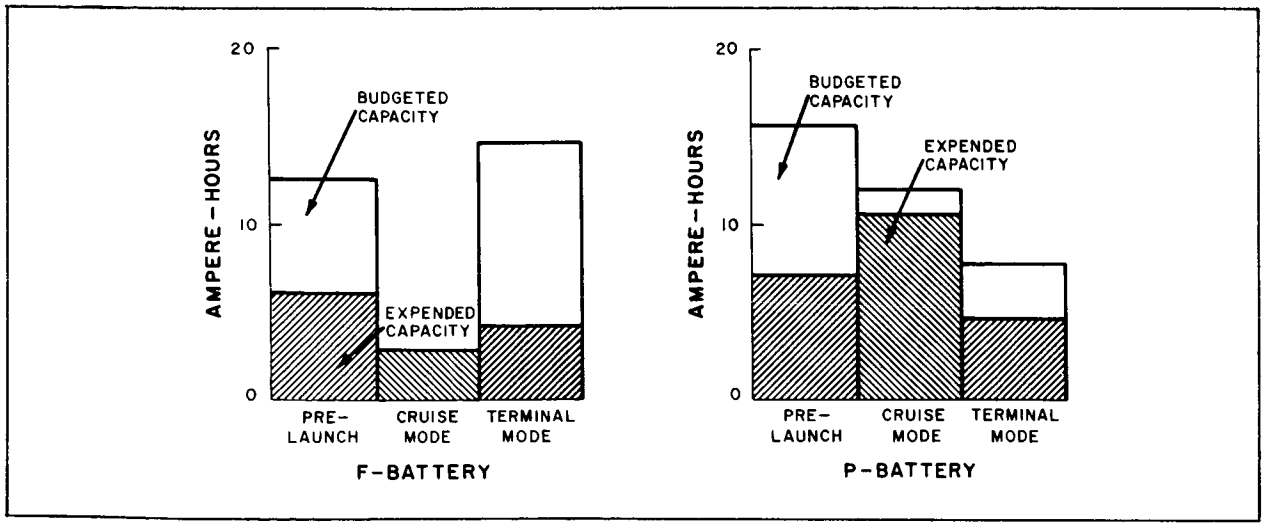

Figure 80. Ranger IX F- and P-Channel Budgeted and Actual Battery Capacities

mission. F-Battery temperatures were between 79 and 84° F throughout the mission. This range is within the specified limits and is the ideal operating temperature range for the batteries. P-Battery temperatures, as given by the 90-point telemetry during terminal mode, were between 87 and 96° F. However, this point was erratic prior to launch. From the results of the Ranger VII and Ranger VIII missions, it was found that all battery thermistors were within several degrees of one another. Since three of the four thermistors were within 2 degrees of each other and since the erratic thermistor varied from the group by 9 to 12° F, this reading was discredited.

F- and P-Battery voltages obtained during cruise mode by the 15-point telemetry are shown in Figure 81. The F-Battery voltage and current from the start of terminal maneuver to impact are shown in Figure 82. The portion of the mission from the start of terminal maneuver to TV Subsystem turn-on was obtained from 15-point telemetry; the portion from Subsystem turn-on to impact was obtained from 90-point telemetry. P-Battery terminal voltage and current are shown in Figure 83.

The F-Battery voltage was approximately 36 volts at launch, under a no-load condition. From Clock start, at launch plus 15 minutes, to TV Clock disable, at approximately 30 minutes before TV turn-on, the F-Battery supplied 0.040 ampere for Clock operation. Just prior to Clock disable, the F-Battery voltage was 34.8 volts. At Clock disable, the 0.040-ampere load was removed and the battery voltage increased to 35.3 volts. At warm-up, the current drain on the F-Battery was 7.8 amperes and the voltage was

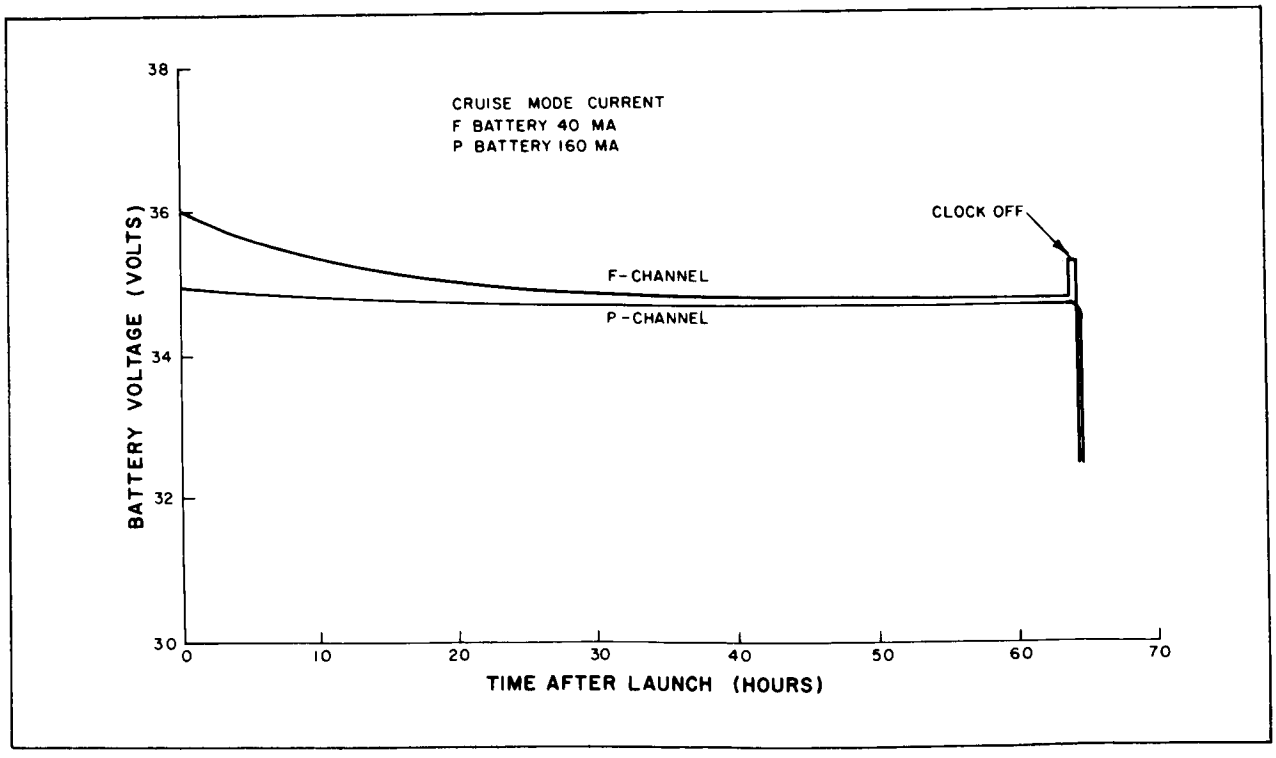

Figure 81. Ranger IX F- and P-Battery Output Voltage Profiles Obtained from 15-Point Telemetry

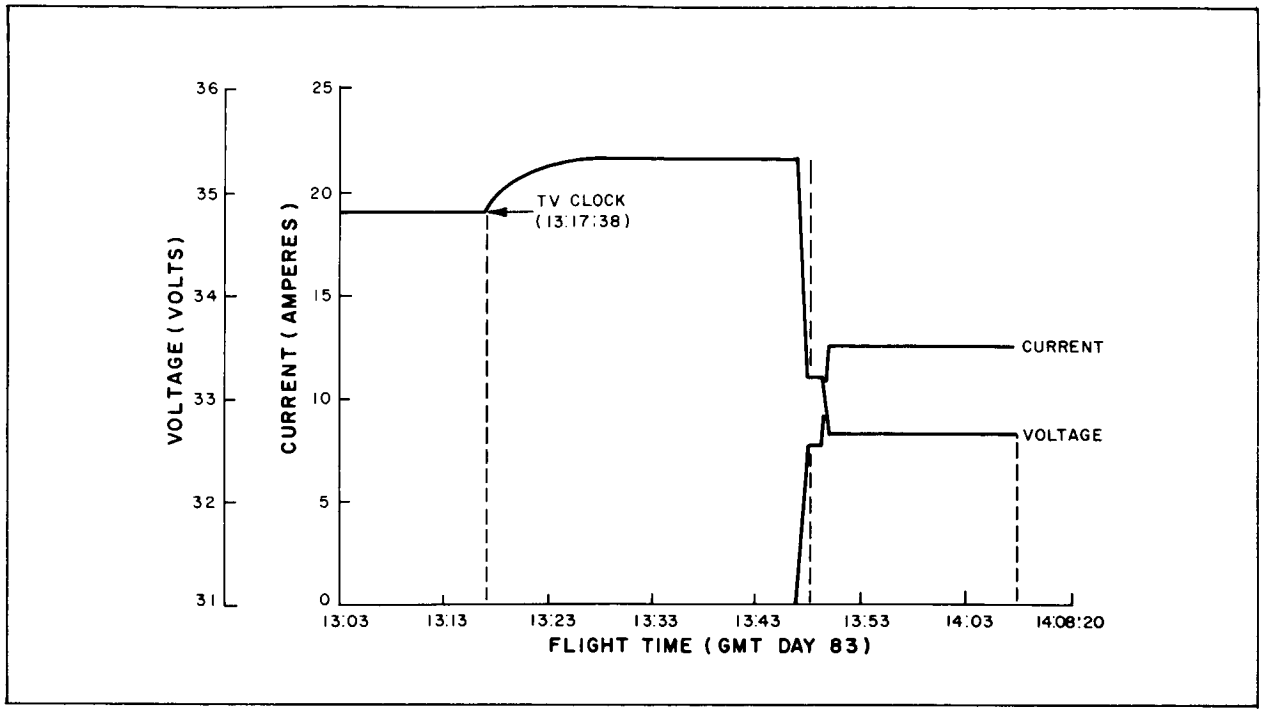

Figure 82. Ranger IX F-Battery Voltage and Current from Terminal Maneuver to Impact

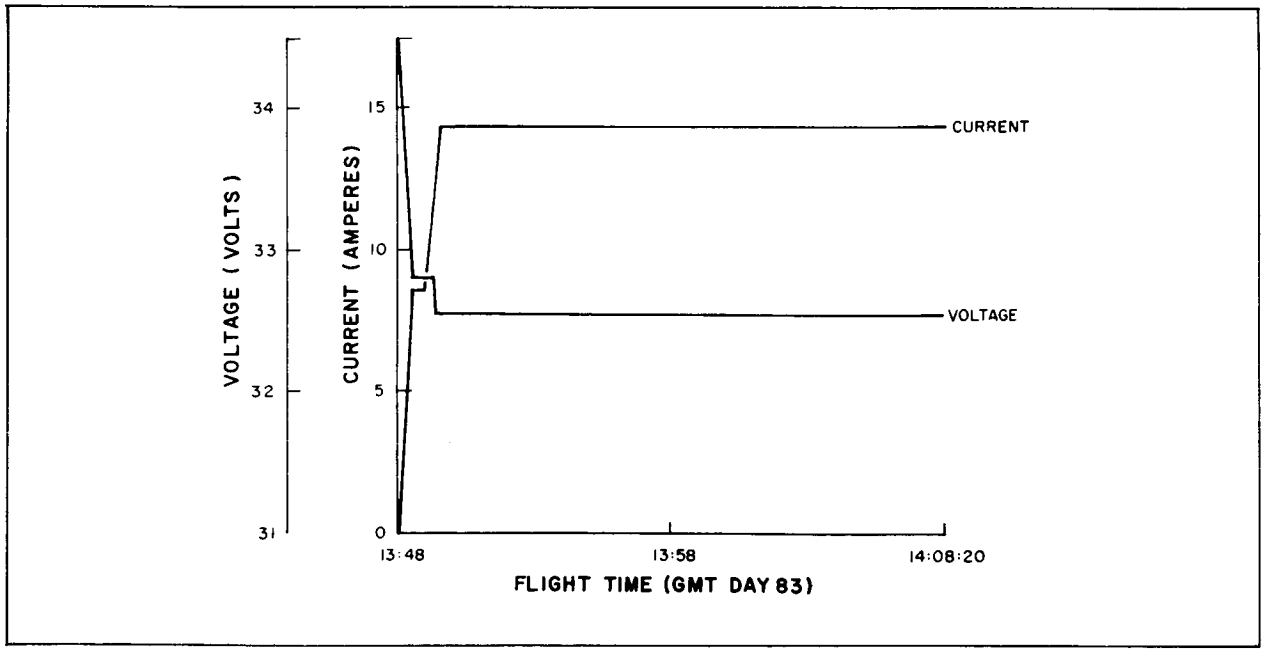

Figure 83. Ranger IX P-Battery Voltage and Current During Terminal Mode

33.2 volts. In full-power operation, the F-Battery current drain was 12.5 amperes and the voltage was 32.6 volts. P-Battery supplied 0.160 ampere for cruise-mode telemetry from launch minus 15 minutes, in the countdown, to Subsystem warm-up. P-Battery voltage at launch was 34.9 volts. Just prior to Subsystem warm-up, P-Battery voltage was 34.7 volts. At warm-up the current drain was 8.6 amperes and the voltage was 32.8 volts. At full power, the current drain was 14.3 amperes and the voltage was 32.5 volts. The battery specification is a minimum of 30.45 volts.

b. VOLTAGE REGULATORS

The output of the Low-Current Voltage Regulator (LCVR) was constant at 27.5 volts from launch to Subsystem turn-on. At turn-on, the voltage dropped to -27.4 volts because this regulator supplied part of the 90-point telemetry load. Design specifications for the Low-Current Voltage Regulator call for an output voltage of -27.5 ±0.5 volts. The output of the F- and P-Channel High-Current Voltage Regulators (HCVR) was -27.7 and -27.6 volts, respectively. Both regulators were within design specifications of -27.5 ±0.5 volts.

Section VI

Conclusions

The performance of the Ranger TV Subsystems equaled or exceeded all of the mission requirements imposed upon the design. A number of factors can be concluded as contributing to the success of the Ranger TV Subsystem missions. The following factors were primarily responsible for this outstanding scientific accomplishment:

- RCA Management Approach
- Institution of a Program of Test Models of the TV Subsystem
- Extensive Testing Program
- Redesign and Rework Program Following Ranger VI
- Reliability and Quality Assurance Programs
- Actual Operation of Flight Equipment

The Management Approach taken by RCA in establishing a Ranger TV Subsystem Project Office at the Astro-Electronics Division, Princeton, New Jersey, centralized the overall project-effort direction and responsibility. The Project Office defined the technical tasks to be performed, allocated and monitored the tasks given to the various skill groups within AED and other contributing RCA Divisions, provided all necessary liaison between the Project Office and the skill groups and the other RCA Divisions, and performed all required liaison with the Jet Propulsion Laboratory, Pasadena, California. Thus, the Project Office maintained a constant continuity of effort throughout the project. In addition, resident JPL personnel were established at RCA as were RCA personnel at JPL. This approach provided an efficient organization capable of performing the management tasks necessary for a project of this type.

The plans incorporated in the TV Subsystem project for the early assembly of test models of the Subsystem were proven to be well founded. These test models were as follows:

- 2 Mechanical Test Models (MTM);
- Engineering Test Model (ETM);
- Thermal Control Model (TCM);
- Life Test Model (LTM);
- Proof Test Model (PTM);

These models of the Subsystem were available early in the project and permitted the extensive testing and evaluation of the various designs at all stages of the project. These models permitted the early verification of the basic Subsystem design, and later provided a means of incorporating and testing modifications prior to their incorporation into the Flight Models. The availability of these models also permitted JPL to determine the procedures for integration of the TV Subsystem with the Ranger Spacecraft Bus in advance of the delivery of the actual Flight Models.

Following the failure of Ranger VI, the Proof Test Model was used to incorporate the design changes for the modified split-system configuration to determine modification compatibility and feasibility without use of the Flight Models. The modifications proven through testing could then be incorporated on the Flight Models with no attendent loss of time. The close liaison which existed between RCA and JPL personnel during the early portions of the project, and the continuity of effort and personnel, were responsible for facilitating the major redesign and rework portion of the project on the PTM. Almost all personnel participating in this project had a thorough understanding of the TV Subsystem design,

the Assemblies, and the problems that had been encountered. Thus, virtually no time was lost in indoctrinating the personnel at RCA and JPL to the design and the necessary modifications. The availability of JPL personnel at RCA, and the same availability by RCA personnel at JPL, permitted a smooth, rapid, and thorough rework of the various assemblies involved. Thus, the rework program was completed in a minimum amount of time.

The reliability and quality assurance programs which RCA instituted at the beginning of the TV Subsystem project were implemented at all stages of the project. Reliability models of the major assemblies and of the Subsystem were made and detailed parts analysis and failure mode and effects studies performed. The quality assurance program included an extensive effort in monitoring all subcontractors supplying equipment to RCA. Design integrity, mean time between failures, parts counts, parts selection, and assigned confidence levels, all were an integral part of the reliability and quality assurance programs.

The conclusion can therefore be drawn that the "text-book" performances of Ranger VII, VIII, and IX demonstrates that RCA's approach to and implementation of the Ranger TV Subsystem project was a complete and unqualified success.